EXPERIMENTAL EVALUATION OF FUNDAMENTAL FREQUENCIES OF BUILDINGS

by

Kuei-hua Rebecca Huang

May 2007

Department of Civil Engineering and Applied Mechanics

McGill University, Montreal, Canada

A thesis
Submitted to the Office of Graduate and Postdoctoral Studies
in partial fulfillment of the requirements
for the degree of Masters of Engineering
at McGill University

ABSTRACT

The application of dynamic testing to civil engineering structures provides a means to understanding a structure's dynamic properties. Such testing includes Forced Vibration Test (FVT), Earthquake Response Test, Ambient Vibration Testing (AVT), and Free Response Test. AVT has become a popular dynamic testing methodology due to its practical and economical advantages.

In this research, the feasibility of employing AVT to obtain reliable fundamental frequencies of buildings was studied by performing AVT inside the Burnside Hall building of McGill University. All measurements were taken by two pairs of CityShark II Microtremor Acquisition and velocimetres. Three system identification approaches, direct Fourier Transform, Power Spectrum Density, and Auto-Regressive-Moving-Average were studied and compared.

It is recommended to use both the direct Fourier Transform and the Auto-Regressive-Moving-Average to extract frequency contents from AVT data. Use of the Power Spectrum Density could easily filter out important frequency content because AVT signals typically have small amplitude.

The lowest translational frequency of the Burnside building was identified to be 1.4 Hz, and the lowest rotational frequency was identified to be 2.2 Hz. Translational modes were best obtained by placing sensors near the centre of rigidity, and rotational modes were best obtained by placing sensors at corners of the building. In addition, the amplitude of the modal peaks increased as the floor elevation increased. Strong wind amplified the fundamental modes, whereas mild wind excited all modes almost equally.

The fundamental periods calculated from the 1995 and 2005 NBCC were larger than that obtained from the experimental AVT period. This shows that non-structural components could contribute significantly to the stiffness of a building when the excitation is small.

SOMMAIRE

L'application des méthodes d'essai dynamiques aux structures de génie civil permet d'améliorer notre compréhension du comportement sismique des structures par une meilleure connaissance de leurs caractéristiques dynamiques. Des exemples de méthodes courantes de mesures expérimentales pour les bâtiments sont : la réponse en vibration forcée (FV), le monitorage sismique, la réponse aux vibrations ambiantes (AV) et la réponse transitoire en vibration libre. La méthode de mesure des vibrations ambiantes a gagné en popularité avec l'avancement des hautes technologies compte tenu de ses nombreux avantages pratiques et économiques.

Dans cette recherche, l'auteure étudie la faisabilité d'utiliser la méthode AV pour obtenir des valeurs fiables et réalistes de la période fondamentale des bâtiments. Des mesures de vibrations ambiantes ont été faites dans le bâtiment Burnside Hall du campus de l'Université McGill . Toutes les mesures ont été prises à l'aide de deux paires de vibromètres sensibles aux micro-mouvements et leur système d'acquisition CityShark II. Les données recueillies ont ensuite été traitées selon trois approches courantes d'identification des systèmes : la transformée de Fourier, la densité spectrale, et la méthode ARMA (*Auto-Regressive-Moving-Average*). Les résultats des différentes techniques d'analyse ont été comparés afin de recommander la meilleure approche possible pour une campagne de mesure exhaustive. En conclusion, l'auteure recommande d'utiliser ensemble la méthode de la transformée de Fourier et la méthode ARMA pour extraire les fréquences naturelles fondamentales. La méthode de la densité spectrale est douteuse dans cette application car elle peut facilement filtrer des signaux de fréquences critiques compte tenu de la faible amplitude typique des micro-mouvements ambiants.

Les résultats obtenus pour Burnside Hall ont permis d'identifier la période fondamentale à 1.4 Hz ainsi que deux modes rotationnels à 2.2 Hz. L'influence des modes translationnels est mieux captée en localisant les senseurs près du centre de rigidité des planchers alors que les modes torsionnels sont clairement identifiés en plaçant les paires de senseurs le plus près possible des coins du bâtiment (le plus loin du centre de torsion de l'étage) pour maximiser l'intensité des mouvements enregistrés. L'étude a vérifié que l'amplitude des crêtes de réponse associées aux modes de vibration de

l'ensemble du bâtiment augmente avec l'élévation des étages. Ainsi, dans les bâtiments multi-étagés la combinaison des mesures simultanées aux étages intermédiaires et supérieurs permet de valider le caractère dynamique d'ensemble de la structure. Les mesures par temps venteux sont également préférables aux mesures par temps calme, les vents forts ayant tendance à mobiliser davantage la réponse d'ensemble dominée par les modes fondamentaux alors que les micro-vibrations ambiantes mesurées par temps calme présentent un contenu en fréquence plus uniforme sur une large bande.

Les périodes naturelles calculées pour ce bâtiment selon les formules empiriques du Code national du bâtiment (versions 1995 et 2005) sont surestimées par rapport aux résultats extraits des mesures ambiantes. Ceci confirme notamment que les composants architecturaux des bâtiments ont une importante influence sur la rigidité des bâtiments en particulier quand les déformations sont faibles.

ACKNOWLEDGEMENTS

I wish to thank my supervisor, Professor Ghyslaine McClure, for her continuous guidance throughout this thesis research. She made herself available to discuss my measurement results and provided insightful discussions. She also proofread this thesis and provided valuable feedback.

The CityShark measuring instruments provided by the Civil Engineering and Applied Mechanics Department, McGill University, are gratefully appreciated. This research cannot be achieved without these instruments and the collaboration of Professor Luc Chouinard.

I would like to thank Damien Gilles, Arden Heerah, and Salman Saeed for their assistance with taking measurements and stimulating discussions. As well, I would like to thank Philippe Rosset for his guidance on taking measurement.

I especially wish to thank my family for their constant support and encouragement throughout my education.

TABLE OF CONTENTS

LIST OF FIGURES

CHAPTER ONE

INTRODUCTION

1.1 General

Dynamic testing of structures provides a means to understanding a structure's dynamic properties such as the fundamental frequencies, internal damping, and mode shapes. Such tests are routinely employed in the fields of mechanical engineering and aerospace engineering. The application of dynamic testing to civil engineering structures first appeared in the 1930s. With the advancement of computer technology, accurate measurement and improved analysis techniques have emerged. When the fundamental frequencies of a structure resonate with the frequencies of the external excitations, large motion can be detected, especially when the excitation has a large magnitude. The identification of dynamic properties of an object from dynamic testing is termed "system identification (SI)". Selection of the proper SI analysis approach depends strongly on the type of dynamic testing.

Ambient Vibration Testing (AVT) is a dynamic testing that directly measures a structure's response to ambient loads such as wind, traffic, tidal waves, pedestrians, or nearby operating machinery. Research has shown that there are several practical applications of AVT in structural engineering. These include:

- structural health monitoring (Wenzel 2005; Beck et al. 1994)
- validation of design codes (Hong and Hwang 2000; Karbassi 2002)
- validation of design numerical models (Brownjohn et al. 1998; Beck et al. 1995)

- comparison of structural properties between undamaged, damaged, and repaired buildings (Beck et al. 1994; Udwadia and Trifunac 1974; McVerry 1979)
- detection of local damage in structural members (Wenzel 2005; Ivanovic et al. 2000)
- observation of building response to different loading types (Marshall 1994; Brownjohn 1998; Udwadia and Trifunac 1974; Trifunac 1972; McVerry 1979)
- observation of nonlinear soil-structure interactions (Kircher 1976; Ivanovic et al. 2000)

The dynamic properties of a structure undergo change from their initial value as buildings age or are subjected to unusually large forces that alter their stiffness. Buildings in particular may also undergo changes in their mass distribution contributed by operational and functional components (Hiramtsu 1988, Drake 1995). Some architectural components may also be added or modified during the life of the building, which may also alter the effective stiffness of the building (Brownjohn 2003).

1.2 Research Objectives

The aim of this research is to conduct a preliminary study to establish a methodology of AVT testing and analysis for future studies. These include:

- Conduct a literature review on building dynamic testing methods;
- Study the feasibility of employing Ambient Vibration Testing (AVT) to obtain reliable values of the fundamental frequency of buildings;
- Compare and recommend optimum system identification techniques for extracting the fundamental frequency of buildings from AVT records.

1.3 Thesis Organization

Chapter Two presents a literature review on dynamic testing. This includes forced vibration testing, ambient vibration testing, free vibration response testing, and earthquake response test. With respect to each testing method, related research studies are presented to show their background and significant conclusions. The development of system identification is also introduced by means of related research studies.

Chapter Three gives a detailed description of the AVT experiments, including the geometry and structural system of the building, functions and capacity of the equipment, and rationale of the testing procedure.

Chapter Four presents theoretical background on system identification techniques that are used to extract the fundamental frequency. Concept and derivations on the Fourier transformation, periodogram power spectrum density, autoregressive-moving-average are introduced.

Chapter Five presents a discussion of the AVT measurements made in this study. A comparison of recommended identification methodologies from ambient vibration records is presented. In addition, the effect of measurements at different floor elevations, the influence of noise in ambient excitation, and the effect of sensor locations are discussed.

Chapter Six summarizes the thesis and its main conclusions.

Chapter Seven presents some recommendations for future studies on AVT. These recommendations address the testing procedure, the identification methodology, and the limitations of this research.

CHAPTER TWO

LITERATURE REVIEW

A literature review on the existing dynamic test methodologies in buildings is presented, including Forced Vibration Test, Earthquake Response Test, Ambient Vibration Test, and Free Vibration Response Test. The advantages and disadvantages of each testing method are specified. As well, a review on the development of companion analysis techniques is also included in this chapter.

2.1 Techniques of Vibration Testing for Buildings

Historically, Forced Vibration Test (FVT) has been performed by exerting artificial loads at single or multiple locations in a building. Jennings et al. (1971, 1972) identified the dynamic properties of the 22-storey steel-frame Gas and Electric Company in San Diego. The building was excited by placing on the 20^{th} floor two eccentric-mass vibration generators from which sinusoidal excitation was produced by eccentric masses that rotated about a vertical axis. Force level and frequencies were adjusted by changing the eccentric weights and pulley systems. Figure 2.1 shows the general view and cross-section layout of a vibration generator (Hudson 1962). The above-mentioned FVT were conducted on weekends for two months to minimize disturbance to the occupants.

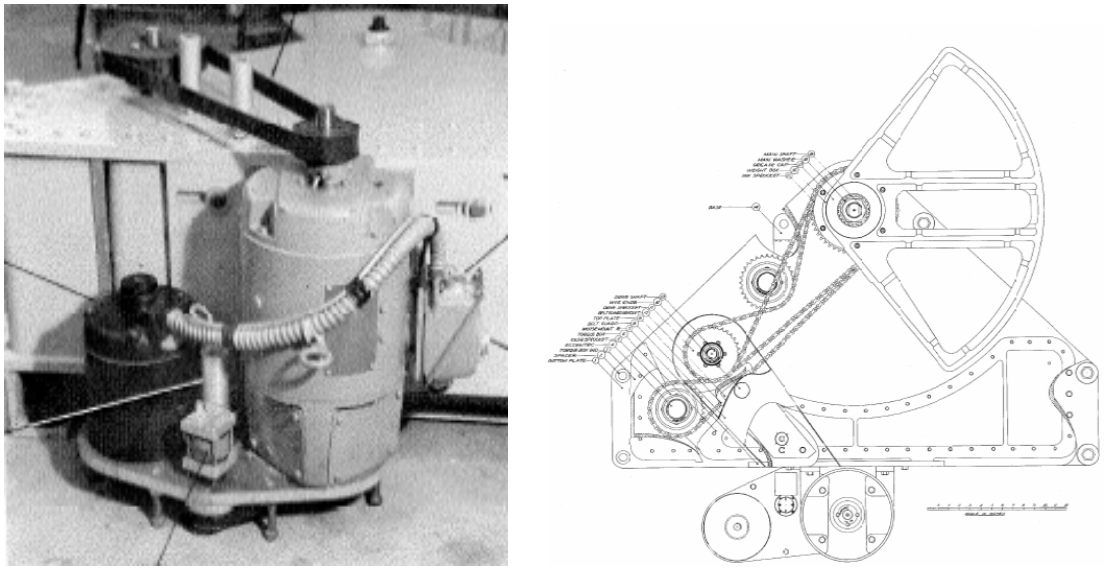

Figure 2.1 General view (left) and cross-section layout (right) of an eccentric-mass vibration generator (after Hudson 1962)

The main advantage of FVT is that precise input excitation is controlled and measured. However, FVT causes disturbance to the building occupants. As well, the forced excitation may not have enough energy to transmit to the entire building to trigger a global response.

Earthquake Response Test (ERT) was not popular before the 1970s due to the scarcity of earthquake time-history data. The source of excitation, earthquakes, produces random and large-amplitude signals that can be measured at the ground floor. These signals are comparatively larger in magnitude than the signals of Ambient Vibration Test. Nevertheless, the identification techniques developed in analysing ERT data have provided important theoretical background in analysing Ambient Vibration Test signals.

Beck (1978) studied the response to the 1971 San Fernando earthquake from the 42-storey steel-frame Union Bank building in Los Angeles and from the 9-storey steel-frame JPL Building 180 in Pasadena. He concluded that the distribution of earthquake

forces cannot be reliably estimated from a limited number of response records. However, the earthquake responses of undamaged buildings can be reliably reproduced from time-invariant linear models.

McVerry (1979) confirmed Beck's conclusion that reproduction of earthquake response of undamaged structures is possible. Furthermore, McVerry showed that the periods of ten steel and reinforced concrete buildings in California were progressively lengthened at the beginning of an earthquake and remained stable after the strongest shake. The lateral stiffness degraded due to permanent damage to the lateral load resisting system. This effect is illustrated in Figure 2.2, which is the response of the Robert Millikan Library to the San Fernando earthquake.

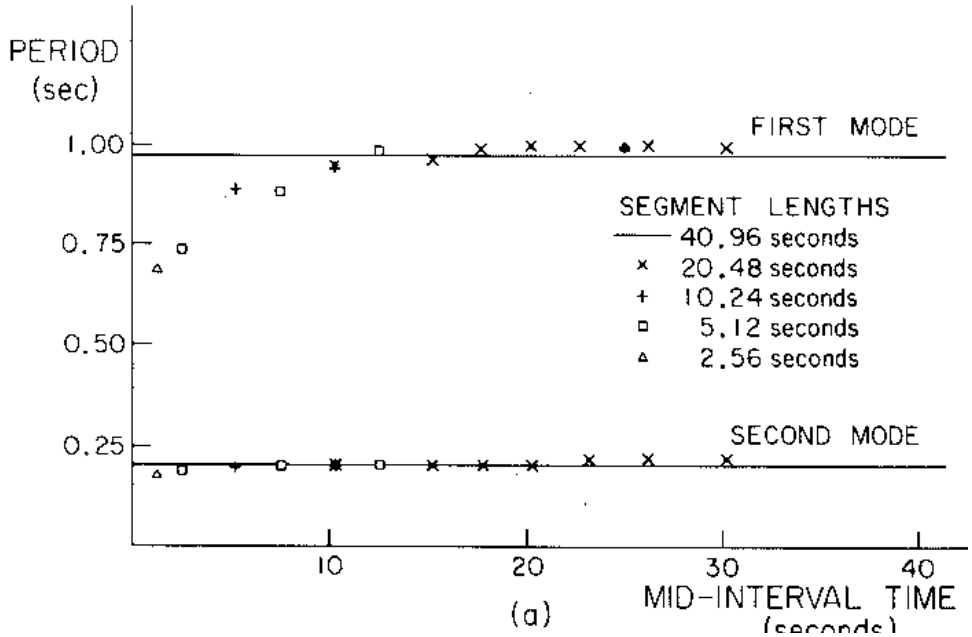

Figure 2.2 Illustration of typical period lengthening occurred in earthquake response measurement (after McVerry 1979)

McVerry also demonstrated that buildings behaved very differently to earthquakes of different magnitudes. The periods identified from less than 0.03g peak

ground excitation earthquakes matched closely to the periods extracted from vibration tests (ambient and forced testing pre- and post-earthquake), whereas the periods identified from above 0.20g peak ground excitations were significantly longer than the periods obtained from vibration tests. Clearly, stronger excitations triggered structural softening.

Recently, more earthquake responses of extensively instrumented buildings in seismically active areas have been studied: Naeim (2000) studied 20 buildings in Los Angeles from the 1994 Northridge earthquake responses; Çelebi et al. (1992) studied the 1989 Loma Prieta earthquake response of the 30-storey Park Plaza Building (moment-resistant reinforced-concrete frame) in Emeryville, California; Assi (2005) identified the fundamental periods and recommended rooftop acceleration amplification factors based on seismic responses of 11 buildings that experienced the 1999 Chi-Chi earthquake in Taiwan.

In addition, seismic research on operational and functional components of buildings has become increasingly important. Hiramatsu et al. (1988) studied the responses of telecommunication towers and antennas to six earthquakes in Japan; McClure et al. (2004) and Assi (2006) performed seismic analysis of steel lattice telecommunication towers on building rooftops generated in 3-D numerical models in Canada and Taiwan.

The advantage of earthquake response monitoring is that earthquakes initiate a global response instead of localized response. However, this testing method requires extensive permanent instrumentation and relies on the occurrence of earthquakes.

The concept of Ambient Vibration Testing was first introduced in the early 1930s by the US Coast and Geodetic Survey (Carder 1936) and became feasible with the introduction of computers. Unlike FVT, free response or earthquake response test, the input force of AVT cannot be measured. Typically, AVT signals are small in amplitude and random. The use of AVT has become popular due to the following reasons:

- AVT neither interferes with the normal operation of the structure nor requires shakers to exert artificial forces. This is particularly important when conducting dynamic testing on large structures such as bridges.
- AVT measuring equipment is portable and light. This allows collecting data at several measuring points in a short period of time.
- The loads of AVT are usually distributed over the building and thus mobilize a global response instead of the localized sinusoidal excitation that is typically used in forced vibration testing.

In Crawford and Ward's study (1964), the natural periods of the three lowest frequency modes were extracted from random wind excitation from a 19-storey Federal Government building located at Ottawa, Canada. In the 1970s, AVT was performed globally on various structure types: about three-quarter of the studies were concentrated on buildings, dams, chimneys, and silos, and the remaining one-quarter of the studies focused on bridges (Ivanovic 2000).

Comparative studies of AVT and FVT were conducted in the 1970s and the 1980s to assess the effects of small and large amplitude excitations on structures. Trifunac (1972) compared the results of FVT and AVT on two buildings: the 22-storey steel-frame San Diego Gas and Electric Building, and the 9-storey reinforced concrete Robert

Millikan Library Building on the campus of the California Institute of Technology. This study showed that the frequencies of the six lowest frequency modes obtained from AVT were only slightly larger (by 10% maximum) than that obtained from FVT. Marshall et al. (1994) compared the dynamic properties extracted from FVT and AVT on five buildings in the San Francisco Bay area: the 13-storey reinforced concrete moment-frame California State University Administration Building, the 60-storey pyramid-shaped steel-frame Transamerica Building, the 6-storey precast and post-tensioned floor beam San Bruno Commercial Office Building, the 12-storey moment-resisting steel-frame Santa Clara County Office Building, and the 30-storey reinforced concrete moment-frame and shear-wall Pacific Park Plaza. The FVT used records of the Loma Prieta earthquake of October 17, 1989. It was found that the frequencies of the first translational mode from AVT were 10% to 30% higher than the frequencies obtained from FVT.

Comparative studies between AVT and numerical model responses were conducted. It should be noted that accurate computer modeling of buildings is extremely difficult – and AVT measurements can help improve these models. Experimental measurement provides important information on the state of the actual building. Beck et al. (1995) studied a 4-storey steel-frame and a 2-storey buildings on the campus of California State University, and an 11-storey steel-frame building in West Los Angeles; McVerry (1979) studied the 15-storey moment-resisting steel Kajima International Building in Los Angeles; and Brownjohn (1998) studied the 67-storey Republic Plaza in Singapore. According to Beck, large precast concrete spandrels may provide significant non-structural stiffness at low levels of excitation, thereby shortening the natural period of buildings from the design value of the bare structural frame.

AVT can also reflect the change of a building's stiffness pre- and post- an earthquake. Research by Udwadia and Trifunac (1974) reported that an important reduction in frequencies was observed in a 39-storey moment-resisting steel-frame building after the San Fernando Earthquake of February 9, 1971. The reduction was 19% in N-S mode, 15% in E-W mode, and 17% in torsional mode. A reduction of 13.8% and 9.3% in the 1st and 2nd E-W mode frequencies, and 4.75% in the stiffer N-S direction was also found in a 9-storey reinforced concrete building.

Research on free vibration response entails the development of time domain identification techniques. Ibrahim and Mikulcik (1973) presented the time domain theory by studying the free vibration response of a computer-generated uniform beam. They stated that identification of a distributed-loading system is possible, if the number of measurement stations equals to the number of modes excited in the test structure. Similarly, simulated free response of more complex systems, a numerical rectangular plate and a real space shuttle payload, was studied by Ibrahim and Pappa (1982). The practicality of applying Ibrahim's time domain technique was studied by Huang and Lin (2001). The free response of a three-span highway bridge in Taiwan was measured by dropping a 14-ton truck from 20-cm height at the mid span of the bridge. Details of the above-mentioned free response studies are discussed in section 2.2

Since 1990, different modal identification methodologies have been studied to improve, in particular, the accuracy of AVT measurement (Cooper 1992; Beck et al. 1995; Kadakal and Yuzugullu 1996; Hong and Hwang 2000; Huang 2001; Huang and Lin 2001; Hung and Ko 2002; Brownjohn 2003). The literature review of these developments is presented in section 2.2.

2.2 System Identification Techniques

2.2.1 Introduction

A "system" is an assemblage of components which receives input variables and produces observable output signals, as shown in Figure 2.3. In this research, a building is a rather complex system of interconnected structural components (the primary load-bearing system) and operational and functional components including architectural components and building contents, which are not intended to carry external loads imparted on the structure. Other common engineering systems are mechanical machines, aircrafts, satellites, and many electrical and biomedical devices. Each system has unique properties that reflect its function. The process of extracting information about a system is called "system identification", denoted as "SI." In this research, the purpose is to extract the fundamental frequencies of the Burnside Hall building from ambient vibration responses.

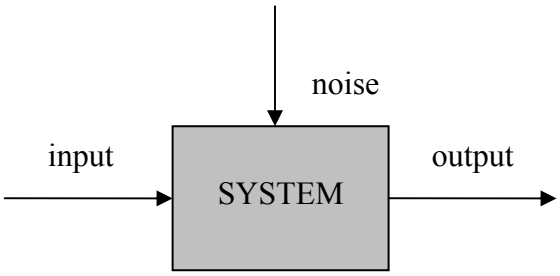

Figure 2.3 Conceptual illustration of a system

2.2.2 Frequency-Domain and Time-Domain Analysis

System identification techniques can be categorized into two groups according to the processing domain of the recorded time-history data: frequency-domain and time-

domain. Frequency-domain modal analysis is based on the Fourier transformation. Background theory is summarized in Chapter 4. Power spectrum density functions have been traditionally applied to the analysis of dynamic testing and are still predominant for vibration testing analysis. With the exception of FVT where periodic characteristics of the input can be controlled, the random excitation in AVT and Earthquake Response Test poses difficulty in obtaining accurate system modal information because the input function is unknown. This difficulty has lead to the development of numerous time-domain SI techniques. As well, frequency domain techniques are strictly valid only for linear systems, which is rare in practice.

Two main SI techniques, Ibrahim Time Domain (ITD) method and variations of the Auto-Regressive method (AR), have been used for processing AVT data (Huang 2001). ITD was first introduced in the field of rocket and spacecraft engineering in the 1970s (Ibrahim 1973). In Ibrahim (1982), ITD was used to identify modal parameters from the free vibration response of a computer-generated rectangular plate and a real space shuttle payload. The free response of the plate was simulated by assigning values to natural frequencies, damping, and response levels; and the free response of the space shuttle payload was measured from ground vibrations. A total of 225 measurement stations were placed on the plate and 142 stations on the space shuttle payload. In an ideal noise-free response record, the number of identified modes must match that of the excited modes of the testing object. In reality, however, the number of excited modes contributing to the response is unknown due to noise. Using as many as 300 degrees-of-freedom in analysis, Ibrahim concluded that an oversized model improved the accuracy and completeness of modal parameter identification: the oversized identification models

weakened the strength of the "noisy modes" and aided identification of higher modes. Although ITD works well with free-response data, it cannot be applied directly to process AVT or earthquake response. Instead, the Random Decrement Technique, which transforms AVT data into free-decay responses, needs to be applied before using the ITD technique (Huang 2001).

The auto-regressive (AR) methodology builds a mathematical model which is able to produce response data that are similar to the AVT response measurements. The concept was first proposed by astrophysicist Yule (1927) to simulate the time series of sunspots. Application of AR models to civil engineering structures has started to appear in the literature in 1970s (Gersch 1972).

Kadakal (1996) also used the AR method to identify the frequencies and damping of the Sabanci Centre in Istanbul, Turkey. The structure consists of two shear-wall reinforced concrete towers with 33 storeys and 28 storeys. In comparison to modal information obtained from frequency-domain power spectrum density functions, Kadakal concluded that AR could identify both the dominant frequencies and damping with greater accuracy.

Huang and Lin (2001) compared the fundamental frequencies of a three-span highway bridge in Taiwan using three different approaches: an AR model for traffic-induced vibration; the ITD method for an impulse load generated at the mid span of the bridge; and numerical results from the eigenvalue analysis of a linear finite element model (on SAP90) of the bridge. It was found that the frequencies obtained from the FEM were consistently lower than those identified using the AR and ITD methods. As well, excellent agreement was observed in the identified frequencies from the AR model

and ITD; it is noteworthy that the AR model was able to identify more modes than the ITD method.

Variations of the AR method include the Vector-Backward-Auto-Regressive model (VBAR) (Hung and Ko 2002; Cooper 1992), and the Auto-Regressive-Moving-Average model (ARMA) (Andersen 1997). Hung and Ko utilized the VBAR technique to study the free vibration response of a 3 degree-of-freedom numerical model and a uniform cantilever steel beam. This identification technique can process only output data.

The auto-regressive AR and ARMA models are based on the simplifying assumption that the observed response data form a *stationary process* (Huang 2001). In a stationary process, the mean value of all records at a specific time t_1, equals to the ensemble average of the product at two instantaneous times, t_1 and $t_1+\tau$.

Other time-domain identification methods include the Eigensystem Realization Algorithm (ERA) introduced for aerospace structures in the 1980s (Juang et al. 1984, 1986; Pappa et al. 1993), and the Subspace Algorithm introduced in the 1990s which greatly improved the accuracy of the modal parameters identified from noisy data (Viberg 1995; Huang et al. 2001). Both the ERA and the Subspace algorithm employ the technique of singular value decomposition (SVD) by specifying an oversized model order first, then selecting the meaningful (physical) models by reducing the models to an equivalent physical model (Andersen 1997, Hung and Ko 2002). However, the elimination process in SVD requires subjective judgement based on prior knowledge of the structure and is prone to erroneous results.

Overall, time-domain SI methodologies have the advantage of processing output-only data and greatly improve the accuracy of damping estimates. They are also useful in

identifying closely-spaced modes, and processing multi-channel measurements (Hung and Ko 2002). All these improved time-domain methods provide good complementary tools to frequency-domain analysis.

CHAPTER THREE

EXPERIMENTAL SETUP AND TESTING PROCEDURE

3.1 Building Description

Burnside Hall, shown in Figure 3.1, is a 14-storey building with 2-storey basement on the downtown campus of McGill University in Montreal. The 13th storey is a mechanical floor that is not accessible to the public. The basement is connected to the nearby Adams building and houses an underground parking that expands beyond the footprint of the building that is apparent from the outside.

The structural system consists of a combination of reinforced concrete beam and columns, a central core and shear walls. Constructed in 1970, the building is 51 m in height and has a rectangular plan with lengths of 30.5 m by 33.5 m.

Figure 3.1 Exterior view of Burnside Hall of McGill University, Montreal

3.2 Equipment

Two CityShark II Microtremor Acquisition Stations, each connected to a velocimetre as shown in Figure 3.2, were used to perform Ambient Vibration Tests. During recording, the velocity of building responses is measured in three directions: north-south, east-west, and vertical. The sampling frequency can be selected at specific values between 10 to 1000 Hz (10, 20, 25, 30, 40, 50, 60, 75, 80 100, 125, 150, 200, 250, 300, 400, 600, 750, 1000 Hz); the gain can be set between 2^0 to 2^{13}; and the recording duration can be set between 1 to 60 minutes. The CityShark station is operated by an internal 12V DC battery, and is capable of accommodating 6 channels of data acquisition. A flashcard is used to store data files. A remote control is available to start two recording stations simultaneously for synchronous measurements. However, the signal reception was unstable when it was used in a building. A pair of two-way radios was used to communicate between the two measuring stations.

Figure 3.2 CityShark acquisition stations (right) and velocimeter (left)

3.3 Procedure

The Burnside Hall building of McGill University was selected for ambient vibration testing due to its symmetric geometry and uniform structural system. Prior to measuring AVT in this building, preliminary testing was performed to study the effect of sensor locations and equipment setup in the Macdonald Engineering Building and the McConnell Engineering Building on the McGill downtown campus. A brief list of testing dates and weather condition is given in Table 3.1. A detailed list of each recording is shown in Appendix A. The wind direction and speed was measured at the Montreal Trudeau International Airport.

Table 3.1 Listing of AVT date, location and weather conditions

Date (year 2006)	**Site Name**	**Floor**	**Bldg Usage**	**Duration** (min)	**Wind Speed** (km/h)	**Wind Direction** (^{0})	**Weather Condition**	**Temp** (^{0}C)	**Air Humidity** (%)
01-Nov	Macdonald Building	F4, F3, F2, F0	Busy	10	20	230	Clear	8	51
03-Nov	Macdonald Building	F4, F3, F0	Busy	10	24	260	Clear	5	44
10-Nov	McConnell Building	F7, F5, F3, F1, F0	Busy	12	24-33	270	Cloudy	7	67
17-Nov	Burnside Building	F12, F9, F6, F2, F0	Busy	10	30	240	Cloudy	8.5	68
24-Nov	Burnside Building	F12, F9, F6, F3	Busy	10	9	60	Sunny	5	50
25-Nov	Burnside Building	F12, F9, F6, F3	Quiet	10	0-5	10	Sunny	0-3	70-84

Figure 3.3 provides the orientation and location of the recording equipments, numbered 1 to 5. The north arrow denotes the local north direction of the velocimeter.

Each sensor should be ideally placed at the floor's centre of rigidity or near the elevator cores to avoid the interference of torsional modes (Trifunac 1972). During experiments, translational modes were obtained at locations 1 and 2 near the centre of the building; and rotational modes were obtained at location 3 (outer perimeter), and locations 4 and 5 (corners of the building).

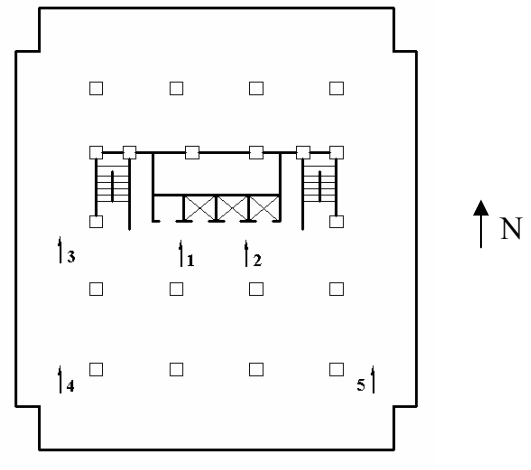

Figure 3.3 Instrumentation layout and direction of the CityShark recording system in Burnside Hall

The CityShark equipment is very sensitive to any ambient excitation. In order to distinguish noise from the real global building motion, AVT was performed at the same location on different days.

The record length was 10 minutes with a sampling rate of 100 Hz. Care should be taken to select a sampling rate. If the sampling rate is too low, the response above this rate cannot be measured and causes 'aliasing' error. To avoid this error, the Nyquist-Shannon sampling theorem states that the minimum sampling rate should be at least *twice* the signal frequency (Maia et al. 1997). If the frequencies of a building are unknown at

the time of sampling, it is recommended to test multiple sampling rates first. In addition, studies have shown that a record length of approximately *four times* the fundamental period provides adequate resolution for identification and reduces the error caused by noise in the data (McVerry 1979).

The CityShark data files contain a header of recording information, followed by three columns that correspond to the vertical, local north and local east components of the ambient motion. By default, the file name contains eight digits that represents the month, day, hour, and minute that a measurement was taken. An example of the data file is provided in Figure 3.4.

```
Original file name: 11251039.007
Transformed into: 061125_1039.007
ReadCity version: 3.2
Station serial number: 027
Station software version: 0623
Channel number: 3
Starting date: 25.11.2006
Starting time: 10:39:31.624
Ending date: 25.11.2006
Ending time: 10:49:31.614
Sample rate: 100 Hz
Sample number: 60000
Recording duration: 10 mn
Conversion factor: 52428.6
Gain: 128
Dynamic range: 5 V
Clipped samples: 0.74%
Latitude :   0  0.000
Longitude:   0  0.000
Altitude : 0 m
No. satellites: 0
Maximum amplitude: 131072 / 131072
-34486  -22542  -9118
-85895  -33815  27698
-56037  -24457  21124
-5738   -22635  -9795
56060   -35202  -15894
95964   -54899  -22130
7592    -41118  -13436
 …        …       …
```

Figure 3.4 An example of the CityShark data file

CHAPTER FOUR

THEORETICAL BACKGROUND

4.1 Introduction

Ambient forces in buildings are typically random with minor periodicity. Three assumptions are generally required to carry out system identification. Firstly, the system is linear so that the response to a linear combination of inputs is equivalent to the linear combination of each individual input. Hence, the ambient forces act on the system independently from each other. Secondly, the excitation is a "white noise", which is '*completely random, totally unpredictable, and not correlated with its earlier values'* (Ibrahim 1985). This implies that the energy content of the excitation is uniformly distributed at all frequencies. Thirdly, the response is ergodic; that is, any section of the time-history record resembles the average of a large ensemble of data. Mathematically, let *z(t)* be the time history record, the condition for ergodic data is (Clough 1993):

$$\lim_{n\to\infty}\frac{1}{n}\int_{-n/2}^{n/2} z(t)dt = \mathrm{E}\,[\mathrm{z(t)}] \tag{4.1}$$

4.2 Frequency Domain: Power Spectrum Analysis

Dynamic analysis in the frequency domain elaborates on the basis of Fourier transformation. However Fourier transformation cannot be applied directly because the random signal does not fulfill the Dirichlet condition (Maia et al. 1997; Ibrahim 1985), which requires:

$$\int_{-\infty}^{+\infty} | \; x(t) \; | \; dt \; < \; \infty \tag{4.2}$$

Instead, the output signal is processed using probability theory first. Let *w(t)* be the response measurement at time *t*. The average of the entire record is obtained by means of the auto-correlation function (Bendat 2000):

$$R_{ww}(\tau) = \lim_{T \to \infty} \frac{1}{T} \int_{-T/2}^{+T/2} [w(t)\, w(t + \tau)]\, dt \tag{4.3}$$

where τ represents a time shift from time *t*. The *auto-correlation function* measures the dependence of a signal on itself. Theoretically, the future signals of a random signal have little dependence on their present values. Hence, the greatest value of $R_{ww}(\tau)$ of a random signal occurs when $\tau = 0$, which is also the mean-square value of the signal. Similarly, the *cross-correlation function* calculates the average between two sets of responses, *w(t)* and *s(t)* (Bendat 2000):

$$R_{ws}(\tau) = \lim_{T \to \infty} \frac{1}{T} \int_{-T/2}^{+T/2} [w(t)\, s(t + \tau)]\, dt \tag{4.4}$$

Cross-correlation measures the dependence of one signal to another signal. The maximum $R_{ws}(\tau)$ is at $\tau = 0$. As τ increases, both the auto-correlation and cross-correlation approach zero. Hence both correlation functions fulfill the Dirichlet condition.

Beck (1994) and Ljung (1987) proved that in a classical dynamic system,

$$M\, \ddot{u}(t) + C\, \dot{u}(t) + k\, u(t) = f(t) \tag{4.5}$$

the cross-correlation of two signals is equivalent to the sum of their free vibration decay response under the assumptions that the system is stable and the excitations are Gaussian white noise. That is,

$$R_{ws}(\tau) = \sum_{-\infty}^{+\infty} [\Phi_{wr} A_{sr} e^{-\xi_r \omega_r \tau} \sin(\omega_d + \varphi_{jr})], \quad (4.6)$$

where Φ = the modal matrix, ξ_r, ω_r, ω_d are the damping ratio, natural frequency and damped natural frequency of the r^{th} mode, and A_{sr} and φ_{jr} are constants representing the amplitude and phase shift.

The frequency composition of the signal, $\Phi_{ww}(\omega)$, is found by performing the Fourier Transform on the auto-correlation function:

$$\Phi_{ww}(\omega) = \int_{-\infty}^{+\infty} R_{ww}(\tau) e^{-jw\tau} d\tau \quad (4.7)$$

Here, $\Phi_{ww}(\omega)$ is the *Power Spectrum Density (PSD)* of the signal. PSD originally refers to the power dissipated by an electrical component (Brook 1988), but here PSD refers to the energy content per unit frequency of a signal. In a lightly-damped system, which resembles most buildings, Clough (1993) proved that PSD had its peak values concentrated more at the natural frequencies of the system. It should be noted that the inverse Fourier Transform of PSD gives the auto-correlation function $R_{ww}(\tau)$:

$$R_{ww}(\tau) = \frac{1}{2\pi} \int_{-\infty}^{+\infty} \Phi_{ww}(\omega) e^{jw\tau} d\omega \quad (4.8)$$

Equations (4.7) and (4.8) form the Fourier transform pair, which is also known as the Weiner-Khintchine relationship.

In summary, the relationship between a random signal, its auto-correlation function, and its PSD is shown in Figure 4.1. It should be mentioned that the Fourier transform is a linear operation on the random variable. This makes the frequency spectrum an approximation of the true value if the system is nonlinear.

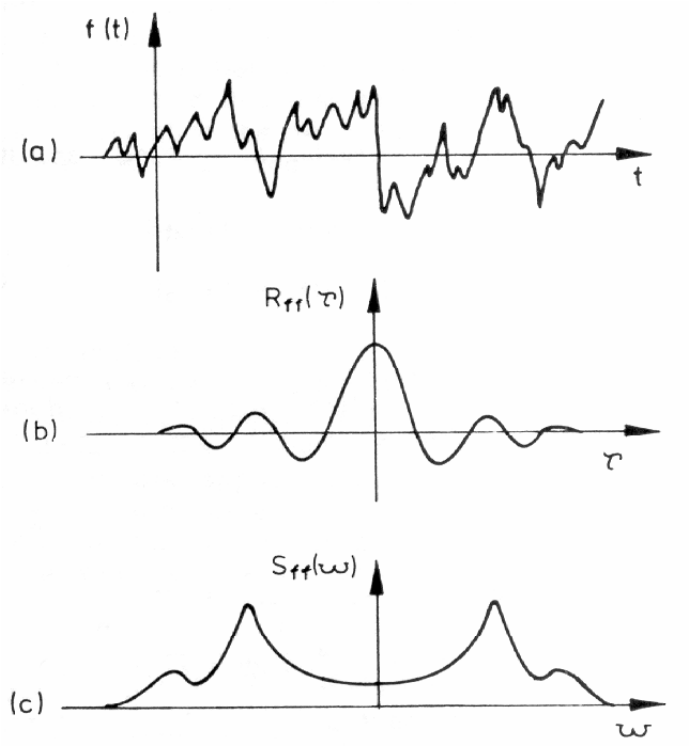

Figure 4.1 Ingredients of random signal (a) Time History; (b) Autocorrelation Function; (c) Power Spectral Density (after Ewins 2000)

4.3 Discrete Fourier Transform

During recording, the continuous real-time excitation is recorded digitally. This section discusses the equivalent digital processing of the theorem presented in section 4.1.

The frequency content of a continuous periodic signal of period T can be decomposed into sine and cosine components by the Fourier transform. The spectrum of the signal constitutes individual spectral lines at its frequencies.

The amplitude of any frequency component, n, is calculated by its Fourier coefficients, A_n and B_n as

$$C_n = (A_n^2 + B_n^2)^{1/2} \qquad \text{(Maia et al. 1997)} \qquad (4.9a)$$

where $A_n = \frac{1}{T}\int_0^T x(t)\cos\omega t\, dt$ (4.9b)

$B_n = \frac{1}{T}\int_0^T x(t)\sin\omega t\, dt$ (4.9c)

The Fourier coefficient of a random signal can be expressed as a complex combination of the sine and cosine components as

$X_n = A_n - i\,B_n$ (4.10a)

$= \frac{1}{T}\int_0^T x(t)\cos\omega t\, dt - i\,\frac{1}{T}\int_0^T x(t)\sin\omega t\, dt$ (4.10b)

$= \frac{1}{T}\int_0^T x(t)[\cos\omega t - i\sin\omega t]dt$ (4.10 c)

$= \frac{1}{T}\int_0^T x(t)\, e^{-iwt}\, dt$ (Maia et al. 1997) (4.10d)

In reality, a time-history record has limited length and is therefore non-periodic. Nevertheless, the assumption of a stationary signal implies that the signal repeats itself with a period, T, equal to the length of the record. Dividing T equally into N segments, each small segment resembles the sampling interval, $\Delta = T/N$. Let $t = k\Delta$, for k = 1, 2, … N, resemble the time elapsed from t = 0. Hence, equation (4.10d) can be expressed discretely as

$X_n = \frac{1}{N\Delta}\sum_{k=0}^{N-1} x(k)e^{-i\frac{2\pi n}{T}k\Delta}\Delta$ (4.11a)

$= \frac{1}{N}\sum_{k=0}^{N-1} x(k)e^{-i\frac{2\pi n}{N}k}$ (4.11b)

where *x(k)* is the signal amplitude at a sample interval *k*, and has the form

$x(k) = \sum_{k=0}^{N-1} X_n e^{i\frac{2\pi n}{N}k}$ (4.12)

This digital representation of the continuous Fourier transform is called *Discrete Fourier Transform* (DFT). The DFT operation requires N^2 multiply-and-add operations, which is a very cumbersome calculation when N is large. This problem, however, can be eased by implementing the well-known Cooley-Tukey Fast Fourier Transform (FFT) algorithm (1965).

It should be noted that the DFT coefficient in equation (4.12), X_n, is in fact the weighted discrete time-series of x(k). It contains both the real and imaginary solutions as shown in Figure 4.2.

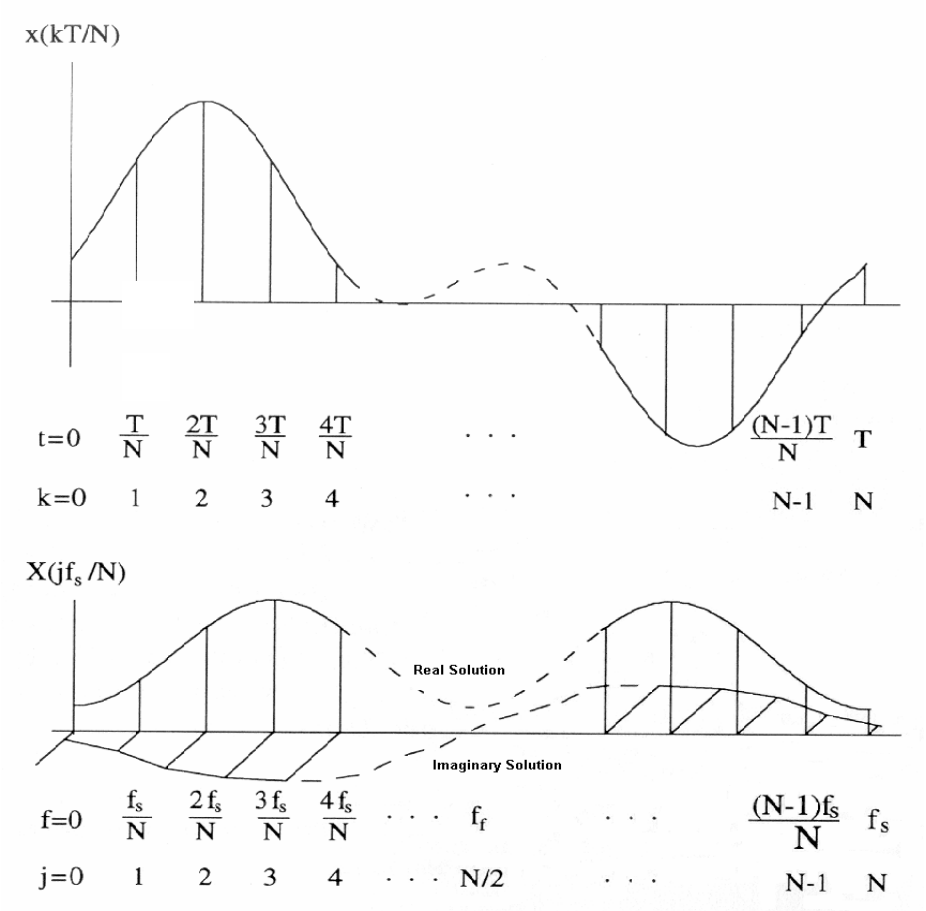

Figure 4.2 Composition of DFT coefficients (after Maia et al. 1997)

Let $\frac{f_s}{N}$ be the discrete frequency spacing. As can be seen in Figure 4.2, the real solution, denoted as x(j $\frac{f_s}{N}$), is an even function with symmetry at N/2. This real part of the solution is used to obtain the frequency content of the signal by its auto-correlation power spectrum as follows:

$$\Phi_{xx}(\,j\frac{f_s}{N}) = \frac{|\ x(\frac{jf_s}{N})\ |^2}{f_s N} \tag{4.13}$$

This power spectrum obtained from the real part of the DFT is also known as the *periodogram* (Maia et al. 1997; Ljung 1987). According to Naidu (1996), sharper peaks are obtained in the power spectrum of a random signal as the record length T → ∞, as shown in Figure 4.3. These peaks then form a continuous spectrum with different amplitude at each frequency of the signal.

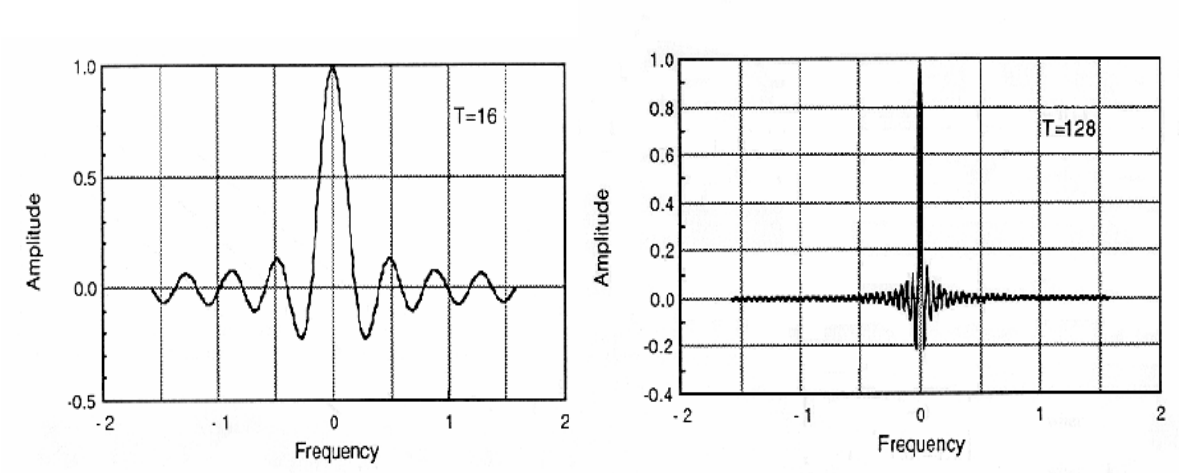

Figure 4.3 Spectra of a signal of different durations to show the effect of record length (after Naidu 1996)

4.4 Time Domain: Impulse Response Function

The impulse response function (also known as Dirac δ-function) is used in time-domain analysis. When a large force acts over a short period of time, the time integral is defined as the impulse of the force. The magnitude of the impulse, as illustrated by the shaded area in Figure 4.4, can be found as:

$$I = \int_{t}^{t+\varepsilon} f(t)dt \tag{4.14}$$

where τ is a very small time increment.

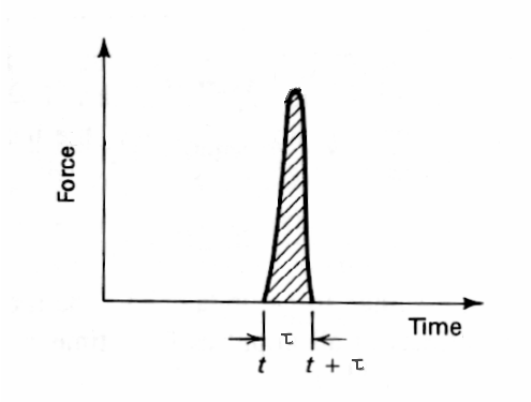

Figure 4.4 Impulse Response (after Humar 1990)

Consider an unit impulse, I = f(τ) τ =1. As τ approaches zero, the impulse becomes infinitely large. The corresponding response of the system to this impulse is termed the *impulse response function*, denoted as *h(τ)*. By mathematical manipulation, the response of a single-degree-of-freedom oscillator to an impulse function resembles its free vibration response. In an underdamped system which resembles most buildings not equipped with special external damping devices, the response, *x(t)* has the form (Maia et al. 1997):

$$x(t) = h(t-\tau) = e^{-\xi w_n (t-\tau)} \frac{1}{m\omega_d} \sin[\omega_d (t-\tau)] \tag{4.15}$$

where ξ is the damping ratio, ω_n the natural frequency, and ω_d the damped frequency. In a linear system, an arbitrary load function can be decomposed into a series of impulses using the principle of superposition. Let $f(\tau)\, d\tau$ be an instantaneous impulse. The response at a subsequent time t is obtained by adding the product of the impulse response function $h(t - \tau)$ and the magnitude of the pulse $f(\tau)\, d\tau$:

$$y(t) = \int_0^t f(\tau)\, h(t - \tau)\, d\tau \qquad \text{for } t > \tau \tag{4.16a}$$

$$= h(t) * f(t) \tag{4.16b}$$

This is the *convolution integral* or *Duhamel's integral*, where the symbol * represents the convolution operation. However, the mathematical expression for $h(t - \tau)$ is difficult to obtain. An equivalent expression of equation (4.16a) is

$$y(t) = \int_0^t f(t - \tau)\, h(\tau)\, d\tau \qquad \text{for } t > \tau \tag{4.17}$$

where the time shift is applied to the load function for computational simplicity. This expression provides the basis for the ARMA method used in this study.

4.5 Time-Domain: Auto-Regressive Moving Average

The Auto-Regressive-Moving-Average (ARMA) method is a time-domain system identification method. The central concept is to simulate the building as a mathematical model, which can generate responses that best resemble the measured time history record. The unknown ambient excitation used to create the ARMA model is assumed to be a white noise, denoted as *e(t)*. The ARMA model is assumed to be a linear system with a frequency response function H(f). The search of an adequate ARMA model involves utilizing the maximum likelihood method for estimation of the correlation coefficients and the non-linear

likelihood functions to achieve parameter optimization (Soderstrom 1989). The theory of ARMA presented next is summarized from Ljung (1987), Ibrahim (1985), Andersen (1997), and Bendat (2000).

Utilizing the concept of transfer function and auto-correlation function, the response of a system can be expressed as a summation of discrete impulse response functions as

$$y(t) = \sum_{k=1}^{\infty} h(k)\, e(t-k) \tag{4.18}$$

where the series *{h(k), 1 < k < ∞}* is the impulse response function of the system. The extraction of the frequency content requires further manipulation of h(k). First, let q^{-k} be the backward shift operator in relation to e(t) as

$$q^{-k}\, e(t) = e(t-k) \tag{4.19}$$

Consequently, from equation (4.18)

$$y(t) = \sum_{k=1}^{\infty} h(k)\, e(t-k)$$

$$= \sum_{k=1}^{\infty} h(k)\, q^{-k}\, e(t) \tag{4.20}$$

Let $$\sum_{k=1}^{\infty} h(k)\, q^{-k} = H(q) \tag{4.21}$$

then $$y(t) = H(q)\, e(t) \tag{4.22}$$

Here, H(q) is the *transfer function* or *transfer operator* of the linear system. It is also called the *unit harmonic response function*: the response of the system to a unit harmonic function $e^{i\omega}$. The frequency content of the system is therefore obtained by evaluating H(q) on a unit circle.

Let H(q) be a ratio of two parameters, A(q) and C(q), which allows flexibility during the identification process as will be shown later. The objective is to perform a numerical search for the most suitable parameters A(q) and C(q).

Let $$H(q) = \frac{C(q)}{A(q)} \quad (4.23)$$

where $$C(q) = \sum_{k=1}^{\infty} c(k)\, q^{-k} \quad (4.24a)$$

$$= c_0(0) + c_1(t-1) + c_2(t-2) + \ldots + c_n(t-n_c) \quad (4.24\,b)$$

The c_1, c_2 … c_n are the *correlation coefficients* between the state separated by n_c time period.

Likewise, $$A(q) = 1 + a_1(t-1) + a_2(t-2) + \ldots + a_n(t-n_a) \quad (4.24c)$$

From equation (4.22) and (4.23),

$$y(t)\, A(q) = e(t)\, C(q) \quad (4.25)$$

Now, substitute (4.24b) and (4.24c) to (4.25) returns

$$y(t) + a_1 y(t-1) + a_2 y(t-2) + \ldots + a_n y(t-n_a) =$$

$$e(t) + c_1 e(t-1) + c_2 e(t-2) + \ldots + c_n e(t-n_c) \quad (4.26)$$

Equation (4.26) is the ARMA model with order (n_a, n_c). In the case where the order $n_a = n_c = n$, Andersen (1997) proved that an ARMA (n,n) model can adequately account for the disturbance caused by non-linear structures and non-stationary measurement. There are many methods to select an appropriate ARMA model order. In this thesis, the order n is selected by comparing ARMA models with different orders. A large *n* permits more flexibility for a better fit; however, when *n* is too large, the ARMA model becomes too flexible and introduces erroneous frequencies at higher modes. A general rule of thumb to determine the order *n* is $m_s \leq n\, p$, where m_s is the state dimension of the true system and *p* is the number of sensors (Andersen 1997). When the state dimension of a system is not known,

spectral analysis can be performed to provide an estimate of m_s. In general, the state dimension is about twice the number of the resonance peaks from spectral analysis in an underdamped system (Andersen 1997). However, the actual state dimension will be larger due to the influence of non-white noise.

In addition, if the system is a symmetrical building, one set of response measurements (univariate ARMA model) is sufficient for system identification (Andersen 1997). However, asymmetrical buildings typically have closely-spaced modes, hence, multiple records from various locations (multivariate ARMA model) are necessary to reduce the bias involved in the model. A multivariate ARMA model is also required to evaluate damping and mode shapes.

Several variations of the ARMA model exist. When no flexibility is allowed in e(t) for identification, that is, $n_c = 0$ in equation (4.26), an *AutoRegressive model* is formed:

$$y(t) + a_1y(t-1) + a_2y(t-2) + ... + a_ny(t-n_a) = e(t). \quad (4.28)$$

Similarly, when no flexibility is allowed in y(t) for identification, that is, $n_a = 0$ in equation (4.26), a *Moving-Average model* is formed:

$$y(t) = e(t) + c_1e(t-1) + c_2e(t-2) + ... + c_ne(t-n_c). \quad (4.29)$$

As well, the ARMA can realize a system when the input record is available. In this case, equation (4.22) becomes

$$y(t) = G(q)u(t) + H(q)e(t), \quad (4.27)$$

where *u(t)* represents the input record, and *G(q)* represents the flexibility of the input in this identification equation.

CHAPTER FIVE

DISCUSSION OF RESULTS

The frequency spectra obtained from the ambient vibration measurement are presented and studied in this chapter. Aspects that will be addressed include comparison of the identification algorithms, effects of floor elevation, effects of ambient disturbance, and sensor locations. Comparison of the fundamental periods obtained from Ambient Vibration Tests and the National Building Code of Canada will be presented at the end of the chapter.

In order not to show repetitive information, only a limited number of spectra are shown in the discussion. Readers will be directed to view the relevant spectra listed in Appendix B.

5.1 Comparison of Analysis Methods

As introduced in Chapter 4, the methodologies include direct Fourier Transformation (FT), Power Spectrum Density (PSD), and Auto-Regressive-Moving-Average (ARMA). The purpose of this section is to compare and recommend identification methodologies for extracting the fundamental frequency of ambient vibration measurement of buildings.

AVT records typically are contaminated with noise (low signal-to-noise ratio). Thus, the ability to distinguish noise from real frequencies is an important consideration in AVT analysis. To illustrate this point, the identification algorithms are compared in two case studies, each representing a different recording environment.

Case One

This case study compares the effectiveness of using the FT, PSD, and ARMA algorithms to process measurements that are contaminated with significant noise. Measurements were obtained at location 2 during normal building operation hours on Friday, November 17, 2006. The average wind speed was 30 km/h. Significant noise is expected from pedestrian traffic, elevator usage, and the wind.

The spectra identified by FT, PSD, and ARMA on floor F2 (in front the administration office) are presented in Figure 5.1. Only NS direction spectra are presented here for demonstration. The corresponding EW direction spectra are listed in Appendix B3-4. As well, spectra of measurements taken on floors F6, F9, and F12 are listed in Appendix B5-10.

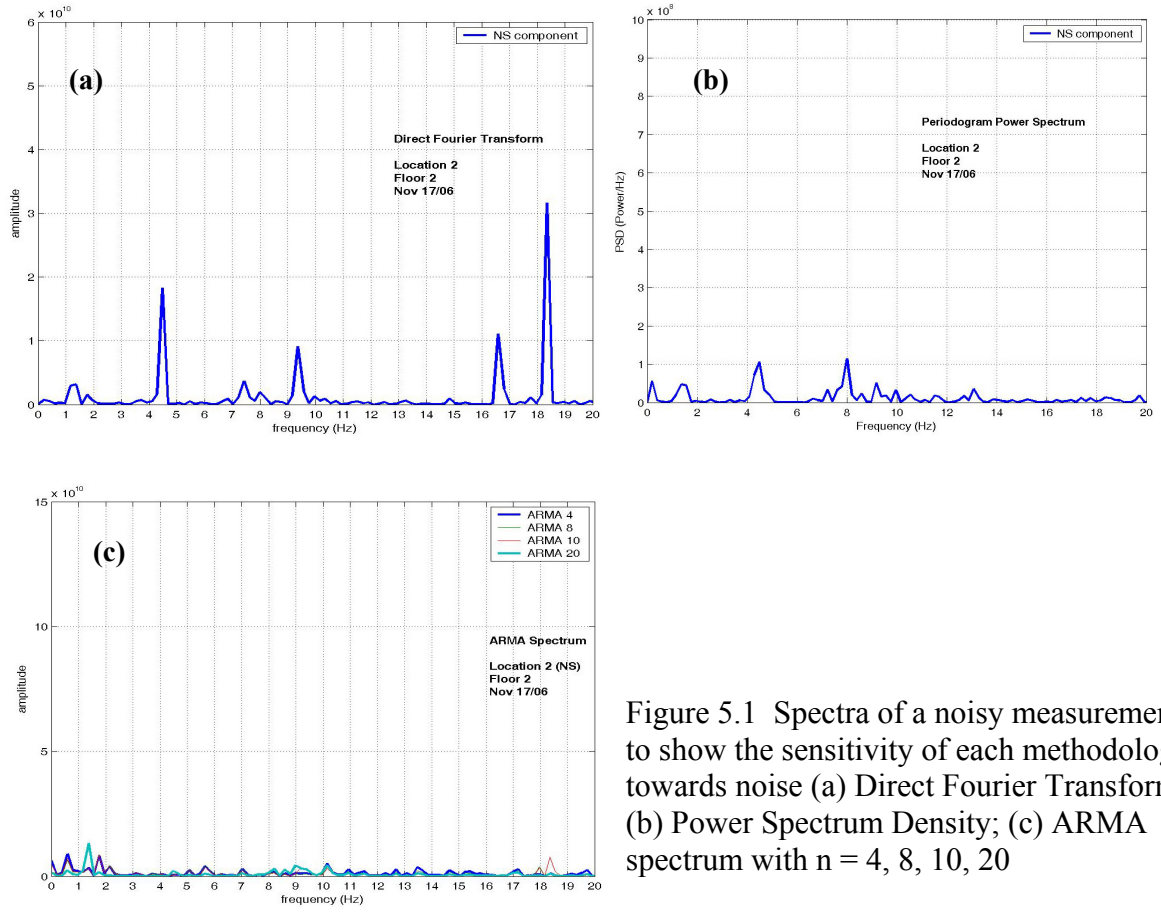

Figure 5.1 Spectra of a noisy measurement to show the sensitivity of each methodology towards noise (a) Direct Fourier Transform; (b) Power Spectrum Density; (c) ARMA spectrum with n = 4, 8, 10, 20

As shown in Figure 5.1, the fundamental sway frequency at about 1.4 Hz cannot be identified clearly in the FT and PSD spectra due to noise contamination. This mode, however, is identified clearly in the ARMA spectrum at the model of order n = 20. When n < 20, noise signals cannot be "diluted" substantially to reveal the fundamental frequency.

Attention should be drawn to the modal frequencies at 16.6 Hz and 18.3 Hz, which can be observed only in the FT and ARMA spectra, but not in the PSD spectrum. The explanation is that these two frequencies neither occur frequently nor have strong signal, thus are "filtered out" by the correlation functions of PSD.

These observations are consistent in the EW-direction spectra, as well as in the spectra obtained on floors F6, F9, and F12.

Case Two

The second case compares the effectiveness of applying the three identification algorithms to process measurement obtained in a low-disturbance recording environment. Measurements were taken at location 1 on floor F9 in the morning of Saturday, November 25, 2006. Access to the building was controlled and there was no pedestrian traffic to this floor during recording. The average wind speed was very low, 0-5 km/h.

The spectra identified by FT, PSD, and ARMA are presented in Figure 5.2. Only NS direction spectra are presented here for demonstration. The corresponding EW direction spectra are listed in Appendix B35-36. As well, spectra of measurements taken on floors F3, F6, F9, and F12 are listed in Appendix B31-38.

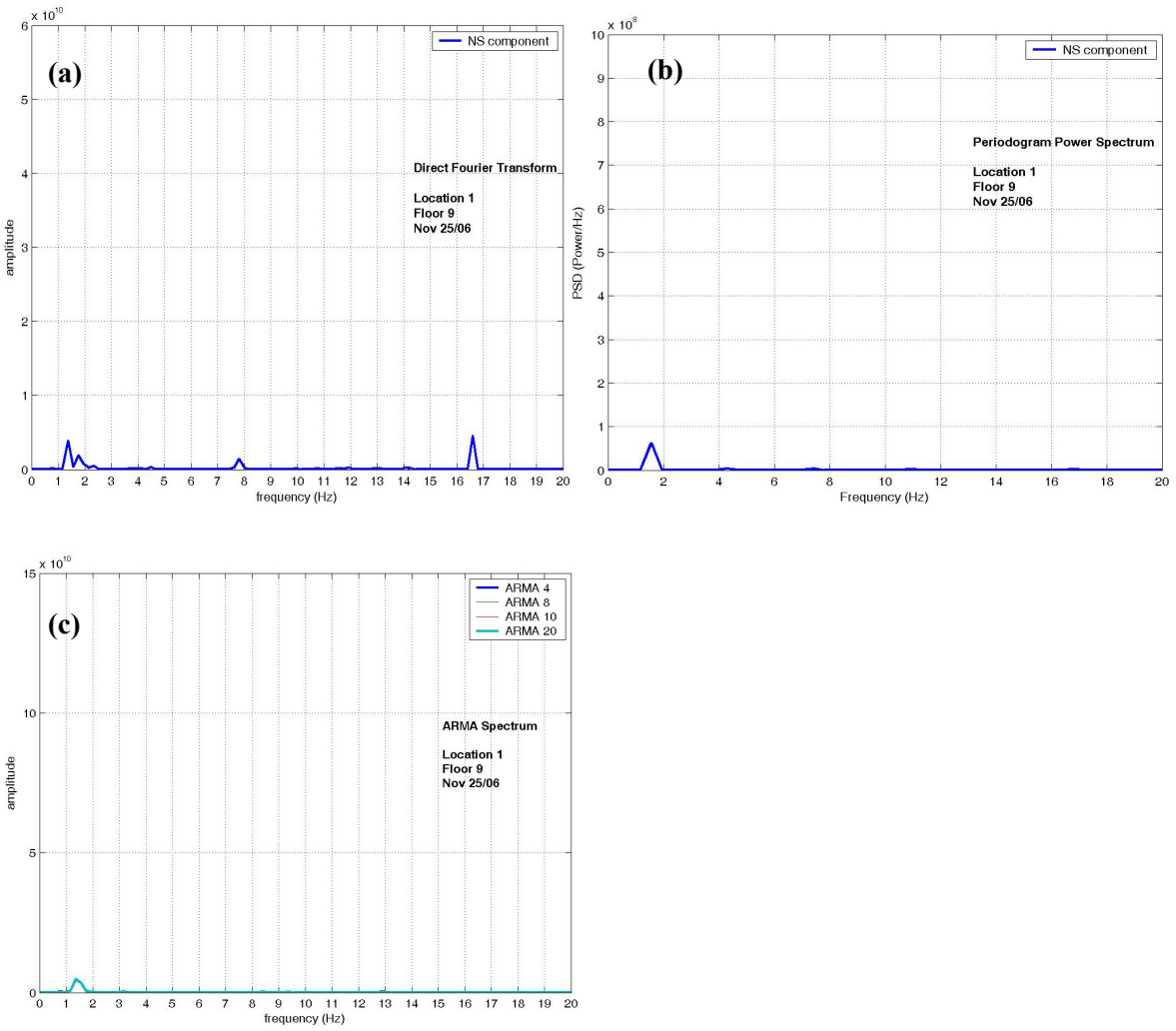

Figure 5.2 Spectra of a low-disturbance measurement to show the sensitivity of each methodology towards noise (a) Direct Fourier Transform; (b) Power Spectrum Density; (c) ARMA spectrum with n = 4, 8, 10, 20

In Figure 5.2, the fundamental sway frequency of 1.4 Hz can be extracted in all three spectra. However, the mode at 16.6 Hz is found only in the FT spectrum. Due to the low level of disturbance, the fundamental sway mode can be identified by the ARMA model at a low value of n = 4.

These observations are consistent in the EW-direction spectra, as well as in the spectra obtained on floors F3, F6, F9, and F12.

In conclusion, the FT and ARMA methods are preferred over PSD in a noisy and/or low-excitation situation, which is typical in AVT measurement. Loss of important yet weak signals could result from the correlation functions of PSD. Examples of such signals include those of higher modes and/or of lower storeys. However, when the signal-to-noise ratio is large, such as in Forced Vibration Testing, PSD is a preferred methodology and has been traditionally applied in structural identification analysis.

The ARMA analysis can effectively filter out noise and retain the fundamental frequencies in a noisy record. The ARMA technique is also known for extracting damping ratios with good accuracy; however, this aspect is not studied in this thesis. One drawback with ARMA is that the algorithm requires large computation power. Each ARMA analysis takes on average 2 minutes whereas FT and PSD analyses take less than 5 seconds. However, this is not a major concern as these processing times are easily manageable.

Thus, for the purpose of extracting building fundamental frequencies from AVT records, it is recommended to use both the direct FT and the ARMA model techniques. In particular, the FT method is very efficient and is able to retain the first two fundamental frequencies.

The FT spectra are used next to further examine the effects of floor elevation, ambient disturbance, and sensor locations.

5.2 Effects of Floor Elevation

The effect of floor elevation on modal frequencies is illustrated in Figure 5.3, which shows the FFT spectra of measurement taken on Friday, November 17, 2006. Sensors were placed at location 2 on floors F2, F6, F12, and basement. Three components, one vertical and two horizontal, are considered at the basement to observe the ground movement. Only

the NS and EW horizontal components are considered in F2, F6, and F12, because the vertical frequencies reflect the vertical motion of the floor slab instead of the overall building response.

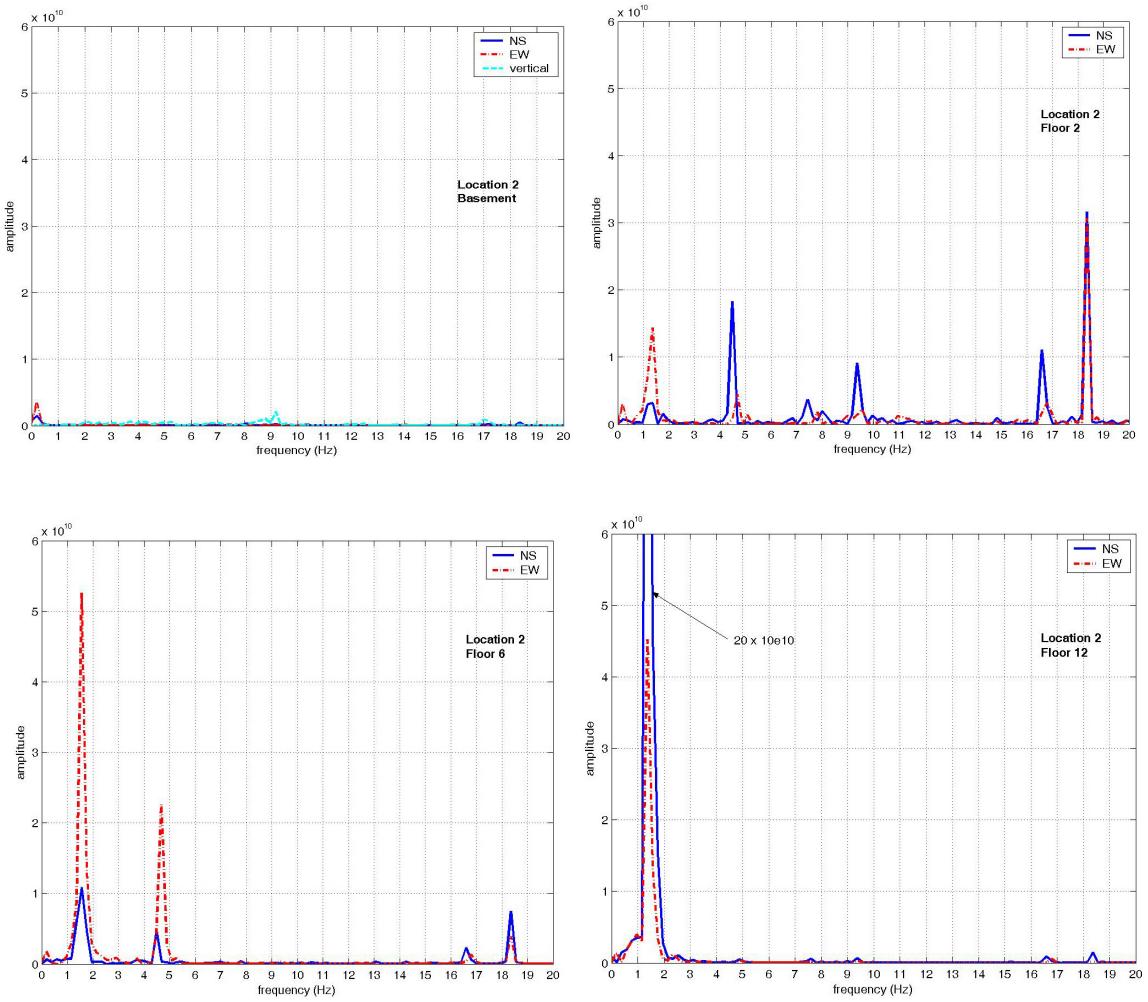

Figure 5.3 Fourier spectra at location 2 in Burnside Hall showing the effect of floor elevation

As shown in Figure 5.3, the fundamental sway frequency is around 1.4 Hz. As the storey level increases, the amplitude of this spectral peak also increases. This reflects that the overall flexibility of the building (essentially cantilevered structures) increases as

elevation increases. Very little activity is detected in the spectrum of the basement due to the rigidity of foundation.

In addition, higher modes of vibration found in the lower floors do not appear as clearly in the higher storeys. In Figure 5.3, frequencies at 1.4 Hz, 4.5 Hz, 7.8 Hz, 9.3 Hz, 16.6 Hz, and 18.2 Hz are found in F2; however, these higher frequencies are significantly smaller than the sway frequency in F6 and F12.

Measurements near the floor centre of the building are also available on November 24 and 25. The corresponding spectra are listed in Appendix B11-18 and B31-38. The effects of floor elevation are consistent in these spectra as well.

5.3 Effects of Ambient Disturbance

The effect of ambient disturbance (wind and building occupancy) is illustrated in Figure 5.4, which displays the FFT spectra of measurement on two different days. The left column displays measurement taken between 16:00-17:00 on Friday, November 17. The wind speed was 30 km/h and significant disturbance from building occupants was expected. On the contrary, the right column displays measurement taken between 9:00-12:00 on Saturday, November 25, 2006. The wind speed was 0 – 5 km/h and access to the building was controlled. Very minimal elevator usage was observed. The sensors were placed at location 2 on floors F6, F9, and F12.

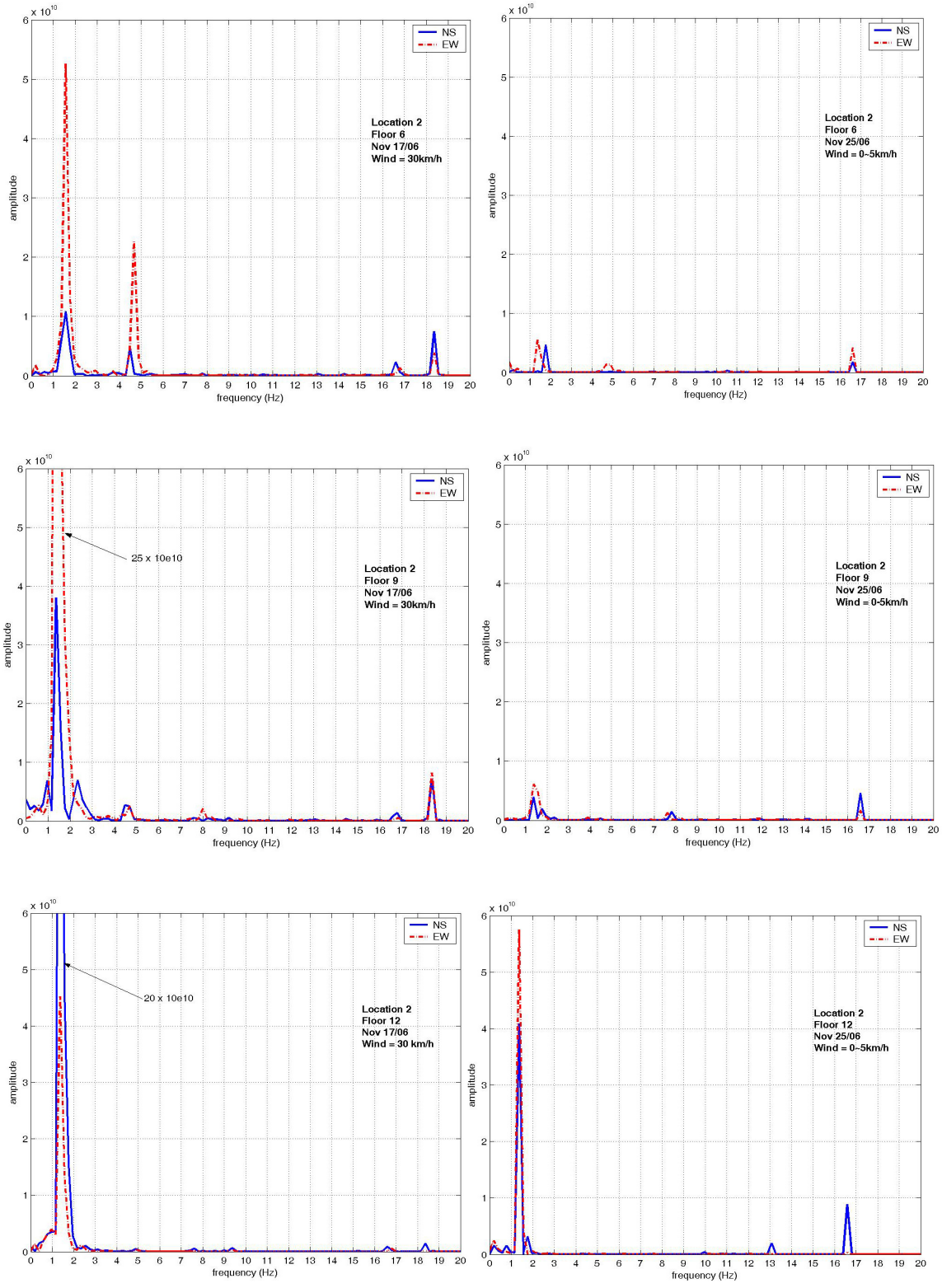

Figure 5.4 Fourier spectra at location 2 in Burnside Hall showing the effect of ambient noises

A comparison of Figure 5.4 shows that the spectra in the right column reflect a less-disturbed measuring environment. This is suggested by the fewer number of peaks and smaller peak magnitudes in these spectra. The fundamental frequency at 1.4 Hz can be observed in all spectra. However, the amplitude of the fundamental peak is significantly larger than the peaks of higher modes in the spectra at the left column (more disturbed environment), whereas the variation between peaks is smaller in the spectra at the right column.

As the effect of wind and building occupants are coupled, it is not distinguishable which factor excites the fundamental frequency more easily. However, a study by Crawford and Ward (1964) on the effect of wind gust concluded that strong winds excite mainly the fundamental modes, whereas lighter winds also excite the higher modes. The rationale is that as the winds increase in strength, the wind energy moves from a broad spectral peak toward the fundamental natural periods of the building; hence, the peak magnitude at the fundamental frequency is greater than the peak magnitude of other modes.

5.4 Effects of Sensor Location

The effect of sensor location is studied by comparing the FFT spectra obtained from two locations (locations 2 [centre] and 3 [side]) simultaneously on floor F12, where the peak amplitude is most amplified. For comparison purposes, the spectra from two days of measurement at the same locations are shown in Figure 5.5.

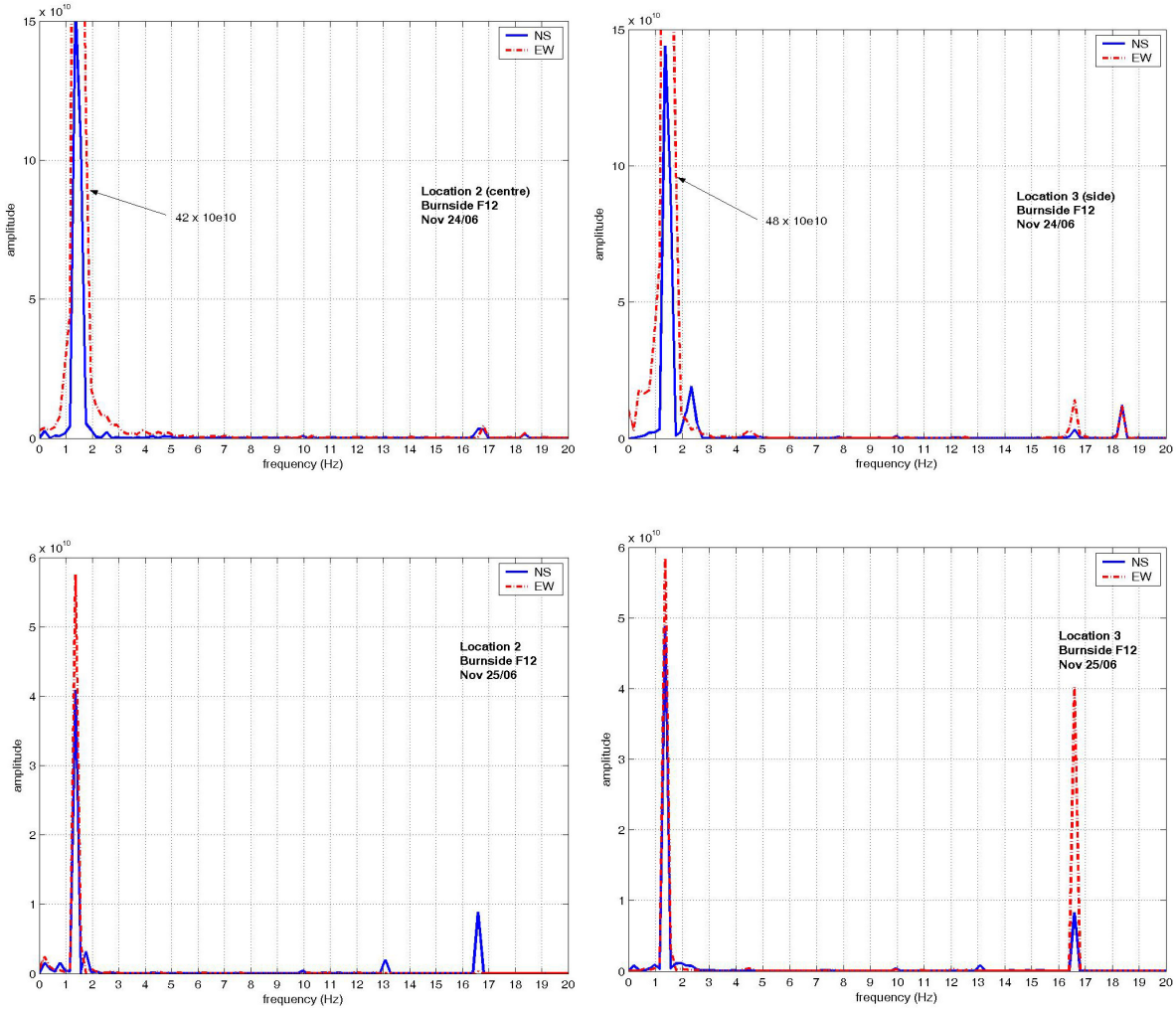

Figure 5.5 Fourier spectra of Burnside Hall showing the effect of sensor locations

Figure 5.5 shows that the fundamental frequency around 1.4 Hz occurs in all spectra. However, when sensors are placed at the side of the building plan (location 3), frequencies at 2.2 Hz and 16.5 Hz become stronger on November 24 and 25 respectively.

The effect of torsion is further studied by comparing the FFT spectra at corners (locations 4 and 5) on floor F12. The spectra from two days of measurement are shown in Figure 5.6. The spectrum at location 5 is not available on November 24. Readers may refer to Appendix B27 for spectra measured on floor F9 on November 24, and Appendix B47-54 for spectra measured on floor F9 on November 25.

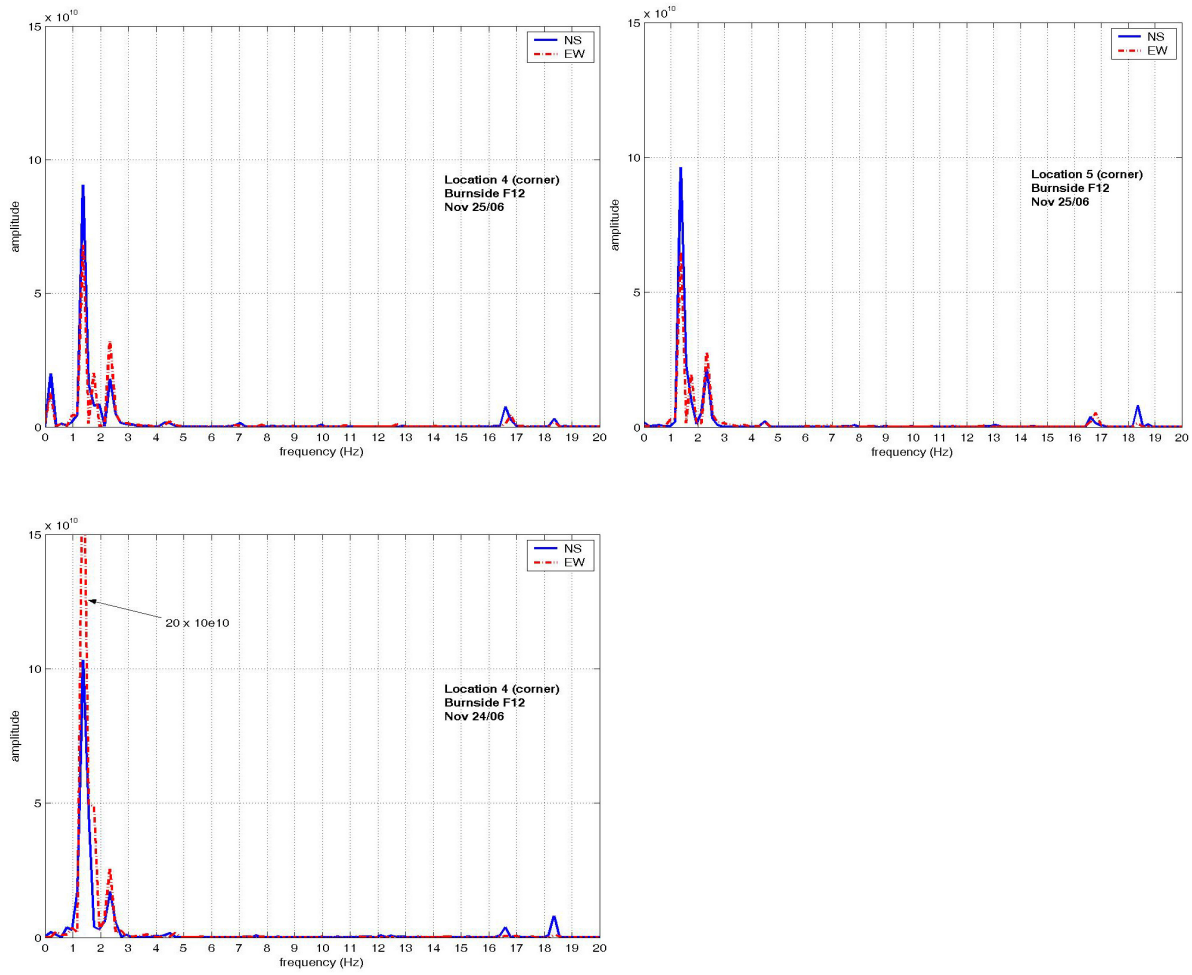

Figure 5.6 Fourier spectra of Burnside Hall showing the effect of sensor location at building corners

Observation of Figure 5.6 shows that the spectra at corners 4 and 5 have very similar spectral curves. This is an expected result because Burnside Hall has symmetrical floor layout and structural system (in two orthogonal directions), and these two corners have the same offset from the centre of the building. The peak at 2.2 Hz is consistently present in both the NS and EW directions. This is logical because the building experiences torsion in both components at the corners. This observation further proves the existence of the

fundamental torsional mode at 2.2 Hz that also exists at location 3 (side) in Figure 5.6, but only in the NS direction. Thus the first torsional mode is suggested to be at 2.2 Hz.

5.5 NBCC Code Comparison

The empirical formulae employed by the National Building Code of Canada (NRC/IRC 2005, NRC/IRC 1995) relate the fundamental period of buildings to the building's structural system, height, and floor dimensions. According to the 2005 NBCC 4.1.8.11 (3c), the fundamental lateral period of a shear-wall structure is:

$$T = 0.05\ h_n^{3/4}, \text{ where } h_n \text{ is the building height in metres.} \quad (5.1)$$

This yields a fundamental lateral period of 0.95 seconds, or a fundamental frequency of 1.05Hz. However, this building is a combination of shear-wall and reinforced concrete frame systems.

The 1995 NBCC does not have a specific formula for a shear-wall structure. For a concrete moment-resisting frame, the 1995 NBCC 4.1.9.1 (7a) specifies that the fundamental lateral period of is:

$$T = 0.075\ h_n^{3/4} \quad (5.2)$$

This yields a fundamental period of 1.43 seconds, or a fundamental frequency of 0.70 Hz.

It has been shown that the fundamental periods calculated from the 1995 and 2005 NBCC are larger than that obtained from experimental AVT (0.67 seconds). One possible factor to account for the differences in the fundamental periods could be due to non-structural components such as cladding, heavy mechanical equipments, and partitions, which add significant mass to the building.

These differences in the fundamental period obtained by AVT and NBCC also imply that the NBCC empirical formulae (eqs. 5.1 and 5.2) do not provide conservative estimates in

calculating the seismic base shears. It may be argued that at the design-level earthquake, the reactive mass and the effective lateral stiffness will have changed considerably and a comparison of inelastic response indicators would be necessary to assess whether the empirical formulae are conservative or not, which is beyond the scope of the present study.

CHAPTER SIX

CONCLUSIONS

The research conducted in this thesis has met the following objectives:

- Conduct a literature review on building dynamic testing methods, including Forced Vibration Test (FVT), Ambient Vibration Test (AVT), Free Vibration Response Test, and Earthquake Response Test (ERT).
- Study the feasibility of employing AVT to obtain reliable values of the fundamental frequency of buildings.
- Compare and recommend an optimum system identification technique for extracting the fundamental frequency of buildings using the AVT equipment available.

The following conclusions are drawn from the study:

Literature Review

- The lower frequencies of buildings evaluated with AVT are about 10% to 30% higher than those extracted from FVT.
- Architectural components (such as sheathings, partitions, ceilings, unreinforced masonry walls) contribute significantly to the lateral stiffness at low levels of excitation, thereby shortening the natural period of buildings.
- A reduction in a building's stiffness after a significant earthquake can be measured by AVT. This means that the significance of the damage incurred to the lateral load

resisting system can be assessed if a measure of the building's fundamental frequency is available prior to the earthquake.

- When a building is subjected to an earthquake, Earthquake Response Testing shows that the fundamental period is lengthened at the beginning of an earthquake (as damage gradually occurs) and remains stable after the strongest shake. The periods measured after light earthquakes (PGA < 0.03g) match closely those obtained with AVT and FVT, but the periods measured after strong earthquakes (PGA > 0.20g) were significantly longer than those obtained with AVT and FVT.
- Lighter winds excite the fundamental and higher modes almost equally; whereas stronger winds amplify the fundamental modes particularly.

Evaluation of Analysis Methodology

- The system identification techniques considered in this study include direct Fourier Transform (FT) and Power Spectrum Density (PSD) in the frequency domain, and Auto-Regressive-Moving-Average (ARMA) in the time domain.
- FT preserves the original testing data most effectively than PSD and ARMA approaches.
- PSD has been traditionally applied in FVT structural identification analysis. In an AVT record, however, higher modes are usually filtered out by PSD because their signals are too weak. Hence, it is not recommended to use PSD to process AVT data.
- an oversized-order ARMA model can most effectively filter out noise and retain the fundamental frequencies in a noisy record.
- An ARMA analysis took on average 2 minutes to perform, whereas FT and PSD took on average 5 seconds to perform. These running times are very manageable in practice.

- It is recommended to use both the FT and ARMA methods to analyze AVT records for extracting the fundamental frequencies of a building. The joint use of the two methods allows for validation of the results.

Feasibility of AVT Implementation

- AVT has shown to have the following important merits:
    - It does not interfere with the normal operation of structures.
    - The equipment is more portable and lighter than the equipment used in FVT.
    - It provides a realistic evaluation because loads are distributed over the building instead of being exerted from a localized location (as in FVT). These distributed loads mobilize a building's global response.
- The following results were obtained from three days of AVT measurements inside the Burnside Hall building of McGill University, Montreal. Five locations were selected for measurement. The sampling frequency and length were 100 Hz and 10 minutes respectively.
    - The fundamental frequency of 1.4 Hz was observed in both NS and EW directions in all spectra.
    - The first torsional mode was 2.2 Hz by placing sensors at the corners or on the perimeter of plan.
    - The amplitude of the fundamental modal peak increases as the floor elevation increases. This reflects that the overall flexibility of the building (essentially a cantilevered structure) increases as elevation increases.

- The higher modes of vibration found in the lower floors do not appear as clearly in the higher storeys. They may be essentially related to the building use and occupancy.
- The fundamental period obtained by AVT in Burnside Hall is consistently lower than the fundamental periods obtained by the 1995 and 2005 NBCC.

CHAPTER SEVEN

SUGGESTIONS FOR FUTURE WORK

Many interesting research projects can follow this work. The following topics are suggested for future studies:

- This thesis has shown that fundamental frequencies of buildings can be extracted from ambient vibration test (AVT). Future studies are recommended to evaluate the identification of internal damping and mode shapes with different system identification (SI) techniques.
- Extensive AVT measurement could be conducted on buildings with different lateral-load-resisting systems and/or different geometry (height, floor area, etc.) to observe their effects on the fundamental modes.
- Derivation of empirical formulas for calculating the fundamental period of buildings could be calibrated by means of statistical analysis when a large number of AVT records are accumulated. Such a study would provide realistic insights into the empirical formulas suggested in the NBCC and possibly contribute improved formulas.
- Long-term AVT monitoring of buildings provides continuous feedback on the structural health condition of buildings. This is important in earthquake-prone regions, as well as for post-disaster and highly important buildings.
- Non-structural operational and functional components in a building can substantially change the fundamental periods estimated for the structural framework. Such

influence could be examined by implementing AVT monitoring throughout the construction stage of a building.

- The SI theories presented in this thesis assume the linear behaviour of buildings. However, buildings enter the non-linear range of response as they become damaged. It is important to examine the effectiveness of AVT in such buildings. As well, various SI methodologies should be compared to examine their appropriateness in non-elastic situations. This would help establishing long-term AVT health monitoring on buildings in earthquake-prone regions.

REFERENCES

Andersen, P. (1997). "Identification of Civil Engineering Structures Using Vector ARMA Models," Aalborg University, Aalborg, Denmark.

Assi, R. (2006). "Seismic Analysis of Telecommunication Towers Mounted on Building Rooftops", Department of Civil Engineering and Applied Mechanics, McGill University, Montreal, Canada.

Beck, J. L. (1978). "Determining Models of Structures from Earthquake Records." *EERL 78-01*, California Institute of Technology, Pasadema, California.

Beck, J. L., May, B. S., and Polidori, D. C. (1994). "Determination of Modal Parameters from Ambient Vibration Data for Structural Health Monitoring." *First World Conference on Structural Control*, Los Angeles, California, USA.

Beck, J. L., May, B. S., Polidori, D. C., and Vanik, M. W. (1995). "Ambient Vibration Surveys of Three Steel-Frame Buildings Strongly Shaken by the 1994 Northridge Earthquake." *EERL 95-06*, California Institute of Technology, Pasadema, California.

Bendat, J. S., and Piersol, A. G. (2000). *Random Data Analysis and Measurement Procedures, 3rd ed*, John Wiley & Sons Inc., Toronto.

Bowerman, B. L., and O'Connell, R. T. (1993). *Forecasting and Time Series: An Applied Approach*, Wadsworth Inc., Belmont, California.

Brook, D., and Wynne, R. J. (1988). *Signal Processing Principles and Applications*, Edward Arnold, London, Great Britain.

Brownjohn, J. M. W. (2003). "Ambient Vibration Studies for System Identification of Tall Buildings." *Earthquake Engineering and Structural Dynamics*, 32, p. 71-95.

Brownjohn, J. M. W., Pan, T.-C., and H-K, C. (1998). "Dynamic Response of Republic Plaza, Singapore." *The Structural Engineer*, 76(11), p. 221-226.

Carder, D. S. (1936). "Vibration Observations, Chapter 5 in Earthquake Investigations in California 1934-1935." *Special Report No. 201*, US Dept. of Commerce, Coast and Geological Survey, Washington, D.C.

Celebi, M., and Safak, E. (1992). "Seismic Response of Pacific Park Plaza. I: Data and Preliminary Analysis." *Journal of Structural Engineering*, 118(6), p. 1547-1565.

Cooley, J. W., and Tukey, J. W. (1965). "An Algorithm for the Machine Computation of Complex Fourier Series." *Mathematics of Computation*, 19(90), p. 297-301.

Cooper, J. E. (1992). "The Use of Backwards Models for Structural Parameter Identification." *Mechanical Systems and Signal Processing*, 6(3), p. 217-228.

Crawford, R., and Ward, H. S. (1964). "Determination of the Natural Periods of Buildings." *Bulletin of the Seismological Society of American*, 54(6A), p. 1743-1756.

Drake, R. M., and Bachman, R. E. (1995). "Interpretation of Instrumented Building Seismic Data and Implications for Building Codes." *Proceedings of the 64th Annual Conference of the SEAOC*, Indian Wells, California, p. 333-344.

Dunand, F., Mehmet, C., Rodgers, J. E., Acosta, A. V., Salsman, M., and Bard, P.-Y. (2004). "Ambient Vibration and Earthquake Strong-Motion Data Sets for Selected USGS Extensively Instrumented Buildings." *Report 2004-1375*, USGS, Menlo Park, California.

Ellis, B. R., and Littler, J. D. (1988). "Dynamic Response of Nine Similar Tower Blocks." *Journal of Wind Engineering and Industrial Aerodynamics*, 28, p. 339-349.

Ewins, D. J. (2000). *Modal Testing: Theory, Practice and Application, 2ed*, Research Studies Press Ltd., London, England.

Gersch, W., and Luo, S. (1972). "Discrete Time Series Synthesis of Randomly Excited Structural System Response." *Journal of the Acoustical Society of America*, 51, p. 402-408.

Goel, R. K., and Chopra, A. K. (1997). "Period Formulas for Moment-Resisting Frame Buildings." *Journal of Structural Engineering*, p. 1454-1461.

Hans, S., Boutin, C., Ibraim, E., and Roussillon, P. (2005). "In Situ Experiments and Seismic Analysis of Existing Buildings. Part I: Experimental Investigations." *Earthquake Engineering & Structural Dynamics*, 34(12), p.1513-1529.

Hiramatsu, K., Sato, Y., Akagi, H., and Tomita, S. "Seismic Response Observation of Building Appendage." *Proceedings of 9th World Conference on Earthquake Engineering*, Tokyo-Kyoto, Japan, p. 237-243.

Hong, L. L., and Hwang, W.-L. (2000). "Empirical Formula for Fundamental Vibration Periods of Reinforced Concrete Buildings in Taiwan." *Journal of Earthquake Engineering and Structural Dynamics*, 29, p. 327-337.

Hsieh, K. H., Halling, M. W., and Barr, P. J. (2005) "Overview of System Identification and Case Studies Using Vibrational Techniques." *Proceedings of the 2005 Structures Congress and the 2005 Forensic Engineering Symposium*, New York, NY, p. 1-12.

Huang, C. S. (2001). "Structural Identification from Ambient Vibration Measurement

Using the Multivariate AR Model." *Journal of Sound and Vibration*, 241(3), p. 337-359.

Huang, C. S., and Lin, H. L. (2001). "Modal Identification of Structures from Ambient Vibration, Free Vibration, and Seismic Response Data via a Subspace Approach." *Earthquake Engineering & Structural Dynamics*, 30(12), p. 1857-1878.

Hudson, D. E. (1962). "Synchronized Vibration Generators for Dynamic Tests of Full-Scale Structures." California Institute of Technology, Pasadena, California.

Humar, J. (1990). *Dynamics of Structures*, Prentice-Hall Inc, Toronto.

Hung, C. F., and Ko, W. J. (2002). "Identification of Modal Parameters from Measured Output Data Using Vector Backward Autoregressive Model." *Journal of Sound and Vibration*, 256(2), p. 249-270.

Ibrahim, R. (1985). *Parametric Random Vibration*, John Wiley & Sons Inc, Toronto.

Ibrahim, S. R., and Mikulcik, E. C. (1973). "A Time Domain Vibration Test." *Shock and Vibration Bulletin*, 43.

Ibrahim, S. R., and Pappa, R. S. (1982). "Large Modal Survey Testing Using the Ibrahim Time Domain Identification Technique." *Journal of Spacecraft and Rockets*, 19(5), p. 459.

Ivanovic, S. S., Trifunac, M. D., and Todorovska, M. I. (2000). "Ambient Vibration Tests of Structures - A Review." *ISET Journal of Earthquake Technology*, 37(4), p. 165-197.

Jennings, P. C., Matthiesen, R. B., and Hoerner, J. B. (1971). "Forced Vibration of a 22-Storey Frame Building." *EERL 71-01*, California Institute of Technology, Pasadena and University of California, Los Angeles, California.

Jennings, P. C., Matthiesen, R. B., and Hoerner, J. B. (1972). "Forced Vibration of a Tall Steel Frame Building." *Journal of Earthquake Engineering and Structural Dynamics*, 1, p. 107-132.

Juang, J.-N. (1994). *Applied System Identification*, Prentice-Hall Inc., Toronto, Canada.

Juang, J.-N., and Pappa, R. S. (1984). "An Eigensystem Realization Algorithm for Modal Parameter Identification and Model Reduction." *AIAA Journal of Guidance*, 8(5), p. 620-627.

Juang, J.-N., and Pappa, R. S. (1986). "Effects of Noise on Modal Parameters Identified by the Eigensystem Realization Algorithm." *Journal of Guidance, Control, and Dynamics*, 9(3), p. 294.

Kadakal, U., and Yuzugullu, O. (1996). "A Comparative Study on the Identification

Methods for the Autoregressive Modelling from the Ambient Vibration Records." *Soil Dynamics and Earthquake Engineering,* (15), p. 45-49.

Karbassi, A., and Anvar, S. A. (2002). "Effective Use of Ambient Vibration Measurements for Evaluating Period Formulas for Steel and Reinforced Concrete Dual Systems." *Structural Engineering World Congress*, Yokohama, Japan, 2002.

Kircher, C. A., and Shah, H. C. (1976). "Ambient Vibration Study of Six Similar High-Rise Apartment Buildings: Comparison of the Dynamic Properties." *Proceedings of ASCE/EMD Specialty Conference on Dynamic Response of Structures: Instrumentation, Testing Methods, and System Identification*, Los Angeles, CA, p. 168-179.

Ljung, L. (1987). *System Identification: Theory for the User*, Prentice Hall, Englewood Cliffs, New Jersey.

Ljung, L. (1995). *Identification Toolbox. For Use with MATLAB*, The Mathworks Inc., Natick, MA.

Lutes, L. D., and Sarkani, S. (2004). *Random Vibrations - Analysis of Structural and Mechanical Systems*, Elsevier Inc., New York, USA.

Maia, N., Silva, J., He, J., Lieven, N., Lin, R.-M., Skingle, G., To, W.-M., and Urgueira, A. (1997). *Theoretical and Experimental Modal Analysis*, Research Studies Press Ltd., Baldock, Great Britain.

Marshall, R. D., Phan, L. T., and Celebi, M. (1994). "Full-scale Measurement of Building Response to Ambient Vibration and the Loma Prieta Earthquake." *Proceedings of the 5th U.S. National Conference on Earthquake Engineering*, Chicago, Il, p. 661-668.

MATLAB 6.5, Release 13. The MathWorks Inc Software.

McClellan, J., Burrus, C., Oppenheim, A., Parks, T., Schafer, R., and Schuessler, H. (1998). *Computer-Based Exercises for Signal Processing Using MATLAB 5*, Prentice-Hall Inc., New Jersey.

McClure, G., Georgi, L., and Assi, R. (2004). "Seismic Considerations for Telecommunication Towers Mounted on Building Rooftops." *13th World Conference on Earthquake Engineering*, Vancouver, B.C., Canada, 1-6 August, Paper No. 1988.

McVerry, G. H. (1979). "Frequency Domain Identification of Structural Models from Earthquake Records." *EERL 79-02*, California Institute of Technology, Pasadema, California.

Morgan, B., Larson, S., and Oesterle, R. (1987). "Field Measured Dynamic Characteristics of Buildings." *Proceedings of the sessions at Structures Congress*

'87 related to Buildings, Orlando, Florida.

Naeim, F. (1994). "Learning From Structural and Nonstructural Seismic Performance of 20 Extensively Instrumented Buildings." *Report OSMS 94-07*, CSMIP, Sacramento.

NRC/IRC. (1995). "National Building Code of Canada." National Research Council of Canada, Ottawa, Ontario.

NRC/IRC. (2005). "National Building Code of Canada." National Research Council of Canada, Ottawa, Ontario.

Pappa, R. S., and Elliott, K. B. (1993). "Consistent-Mode Indicator for the Eigensystem Realization Algorithm." *Journal of Guidance, Control, and Dynamics*, 16(5), p. 852-858.

Pardoen, G. C. (1983). "Ambient Vibration Test Results of the Imperial County Services Building." *Bulletin of the Seismological Society of America*, 73, p. 1895-1902.

Paz, M. (1991). *Structural Dynamics Theory and Computation, 3rd ed.*, Van Nostrand Reinhold, New York.

Pisarenko, V. F. (1973). "The Retrieval of Harmonics from a Covariance Function." *Geophysical Journal of the Royal Astronomical Society*, 33(3), p. 347.

Quek, S. T., Wang, W., and Koh, C. G. (1999). "System Identification of Linear MDOF Structures Under Ambient Excitation." *Earthquake Engineering & Structural Dynamics*, 28(1), 61-77.

Rahman, M. (2003). "Identification of Dynamic Characteristics of Linear Systems," Master Thesis, Department of Civil and Environmental Engineering, University of Windsor, Windsor, Canada.

Rosset, P. (2005). "Guidelines of Used and Developed Tools for Ambient Noise Analysis." Royal Observatory of Belgium – Koninklijke Sterrenwacht van Belgie, Avenue Circulaire 3 – Ringlaan 3, B-1180 Bruxelles – Brussel.

Rosset, P. (2005). "SPCRATIO", computer program.

Soderstrom, T. (1989). *System Identification*, Prentice Hall, New Jersey.

Trifunac, M. D. (1970). "Ambient Vibration Test of a Thirty-Nine Story Steel Frame Building." California Institute of Technology, Pasadema, California.

Trifunac, M. D. (1972). "Comparisons Between Ambient and Forced Vibration Experiments." *Earthquake Engineering & Structural Dynamics*, 1, p. 133-150.

Udwadia, F. E., and Trifunac, M. D. (1974). "Ambient Vibration tests of Full-Scale

Structures." *Proceedings of the 5th World Conference on Earthquake Engineering*, Rome.

Wenzel, H., and Pichler, D. (2005). *Ambient Vibration Monitoring*, John Wiley & Sons Ltd., Toronto.

Yang, C. Y. (1986). *Random Vibration of Structures*, John Wiley & Sons Inc., Toronto.

Yule, G. U. (1927). "On a Method of Investigating Periodicities in Disturbed Series, with Special Reference to Wolfer's Sunspot Numbers." *Philosophical Transactions of the Royal Society of London*, Series A 266, p. 267-298.

APPENDIX A

MEASUREMENT INVENTORY

Serial No.	Date	Site Name and Address	Floor and Room/Location	Begin Time	Duration (min)	File Name	Wind Speed (km/h)	Wind Direction (0)	Weather Condition	Temp (0C)	Humidity(%)
1	01-Nov-06	MacDonald Building	Floor 04 - Professor's Lounge	15:58	10	061101_1558.txt	20	230	clear	8	51
2	01-Nov-06	MacDonald Building	Floor 03 - Outside Student Affairs Office	16:21	10	061101_1621.txt	20	230	clear	8	51
3	01-Nov-06	MacDonald Building	Floor - 02 - Just outside MD-275	16:49	10	061101_1649.txt	11	220	clear	7	59
4	01-Nov-06	MacDonald Building	Structural Lab - in the Northwest wing\, almost on same axis as SN# 2\, 3 & 4	17:10	10	061101_1710.txt	11	220	clear	7	59
5	03-Nov-06	MacDonald Building - North West Wing	Floor 04 - Professor's Lounge	15:02	10	061103_1502.txt	24	260	clear	5	44
6	03-Nov-06	McDonald Building - North West Wing	Floor 04 - Infront of Elevator	15:43	10	061103_1543.txt	28 - 37	280	clear	4	50
7	03-Nov-06	McDonald Building - North West Wing	Floor 03 - Aligned with SN#7	16:01	10	061103_1601.txt	28 - 37	280	clear	4	50
8	03-Nov-06	McDonald Building - North West Wing	Structure Lab - Aligned with SN#7	16:23	10	061103_1623.txt	28 - 37	280	clear	4	50
9	03-Nov-06	McDonald Building - North East Wing	Floor 04 - Beside SN#6	15:14	10	061103_1514.txt	24	260	clear	5	44
10	03-Nov-06	McDonald Building - North East Wing	Floor 04 - Entrance from stairs near 497	15:55	10	061103_1555.txt	28 - 37	280	clear	4	50
11	03-Nov-06	McDonald Building - North East Wing	Floor 03 - Aligned with SN#11	16:13	10	061103_1613.txt	28 - 37	280	clear	4	50
12	03-Nov-06	McDonald Building - North East Wing	Structure Lab - Aligned with SN#11	16:36	10	061103_1636.txt	28 - 37	280	clear	4	50
13	10-Nov-06	McConnell Building	Basement	15:18	12	061110_1518_McConnel Basement	24-33	270	cloudy	7	67
14	10-Nov-06	McConnell Building	Basement Stationary	15:18	12	061110_1518_McConnel Basement_Stationary	24-33	270	cloudy	7	67
15	10-Nov-06	McConnell Building	Basement Stationary	15:35	12	061110_1535_McConnel Basement_Stationary	20-33	280	cloudy	7	70
16	10-Nov-06	McConnell Building	Floor 01	15:35	12	061110_1535_McConnel Floor1	20-33	280	cloudy	7	70
17	10-Nov-06	McConnell Building	Basement Stationary	15:50	12	061110_1550_McConnel Basement_Stationary	20-33	280	cloudy	7	70
18	10-Nov-06	McConnell Building	Floor 03	15:50	12	061110_1550_McConnel Floor3	20-33	280	cloudy	7	70
19	10-Nov-06	McConnell Building	Floor 05	16:06	12	061110_1606_McConnel Floor5	20-33	280	cloudy	7	70
20	10-Nov-06	McConnell Building	Basement Stationary	16:07	12	061110_1607_McConnel Basement_Stationary	20-33	280	cloudy	7	70
21	10-Nov-06	McConnell Building	Basement Stationary	16:22	12	061110_1622_McConnel Basement_Stationary	20-33	280	cloudy	7	70

22	10-Nov-06	McConnell Building	Floor 07	16:22	12	061110_1622_McConnel Floor7	20-33	280	cloudy	7	70
23	17-Nov-06	Burnside Building	Floor 2, Location 2	16:17	10	Burnside Basement Moving Floor 2 061117_1617	30	240	cloudy	8.5	68
24	17-Nov-06	Burnside Building	Floor 6, Location 2	16:58	10	Burnside Basement Moving Floor 6 061117_1658	35	230	cloudy	7	78
25	17-Nov-06	Burnside Building	Floor 9, Location 2	16:45	10	Burnside Basement Moving Floor 9 061117_1645	35	230	cloudy	7	78
26	17-Nov-06	Burnside Building	Floor 12, Location 2	16:31	10	Burnside Basement Moving Floor 12 061117_1631	35	230	cloudy	7	78
27	17-Nov-06	Burnside Building	Basement, Location 2	15:26	10	Burnside Basement Moving Basement 10 min 061117_1526	41	230	cloudy	9	68
28	17-Nov-06	Burnside Building	Basement Stationary, Location 2	15:26	10	Burnside Basement Stationary 061117_1526	41	230	cloudy	9	68
29	17-Nov-06	Burnside Building	Basement Stationary, Location 2	16:16	10	Burnside Basement Stationary 061117_1616	30	240	cloudy	8.5	68
30	17-Nov-06	Burnside Building	Basement Stationary, Location 2	16:31	10	Burnside Basement Stationary 061117_1631	35	230	cloudy	7	78
31	17-Nov-06	Burnside Building	Basement Stationary, Location 2	16:44	10	Burnside Basement Stationary 061117_1644	35	230	cloudy	7	78
32	17-Nov-06	Burnside Building	Basement Stationary, Location 2	16:58	10	Burnside Basement Stationary 061117_1658	35	230	cloudy	7	78
33	24-Nov-06	Burnside Building	Floor 3, Location 1	13:32	10	Burnside Center Floor 3_061124_1332	9	ENE	sunny	5	50
34	24-Nov-06	Burnside Building	Floor 3, Location 3	13:32	10	Burnside Center West Floor 3_061124_1332	9	ENE	sunny	5	50
35	24-Nov-06	Burnside Building	Floor 6, Location 1	13:49	10	Burnside Center Floor 6_061124_1349	9	ENE	sunny	5	50
36	24-Nov-06	Burnside Building	Floor 6, Location 3	13:49	10	Burnside Center West Floor 6_061124_1349	9	ENE	sunny	5	50
37	24-Nov-06	Burnside Building	Floor 9 , Location 1	14:04	10	Burnside Center Floor 9_061124_1404	9	ENE	sunny	5	50
38	24-Nov-06	Burnside Building	Floor 9 , Location 3	14:03	10	Burnside Center West Floor 9_061124_1403	9	ENE	sunny	5	50
39	24-Nov-06	Burnside Building	Floor 12, Location 1	14:18	10	Burnside Center Floor 12_061124_1418	9	ENE	sunny	5	50
40	24-Nov-06	Burnside Building	Floor 12, Location 3	14:18	10	Burnside Center West Floor 12_061124_1418	9	ENE	sunny	5	50
41	24-Nov-06	Burnside Building	Floor 9, Location 4	14:35	10	Burnside Corner Floor 9_061124_1435	9	ENE	sunny	5	50
42	24-Nov-06	Burnside Building	Floor 12, Location 4	14:35	10	Burnside Corner Floor 12_061124_1434	9	ENE	sunny	5	50
43	25-Nov-06	Burnside Building	Floor 3, Location 1	9:08	10	Burnside Center Floor 03_061125_0908.txt	5	SSE	sunny	0	84
44	25-Nov-06	Burnside Building	Floor 6, Location 1	9:29	10	Burnside Center Floor 06_061125_0929.txt	5	SSE	sunny	0	84

45	25-Nov-06	Burnside Building	Floor 9, Location 1	9:44	10	Burnside Center Floor 09_01_061125_0944.txt	0	0	sunny	2	78
46	25-Nov-06	Burnside Building	Floor 9, Location 1	9:55	10	Burnside Center Floor 09_02_061125_0955.txt	0	0	sunny	2	78
47	25-Nov-06	Burnside Building	Floor 12, Location 1	10:39	10	Burnside Center Floor 12_01_061125_1039.txt	4	N	sunny	3	70
48	25-Nov-06	Burnside Building	Floor 12, Location 1	10:50	10	Burnside Center Floor 12_02_061125_1050.txt	4	N	sunny	3	70
49	25-Nov-06	Burnside Building	Floor 9, Location 5	10:08	10	Burnside East Corner Floor 09_01_061125_1008.txt	0	0	sunny	2	78
50	25-Nov-06	Burnside Building	Floor 9, Location 5	10:20	10	Burnside East Corner Floor 09_01_061125_1020.txt	0	0	sunny	2	78
51	25-Nov-06	Burnside Building	Floor 12, Location 5	11:02	10	Burnside East Corner Floor 12_01_061125_1102.txt	4	N	sunny	3	70
52	25-Nov-06	Burnside Building	Floor 12, Location 5	11:13	10	Burnside East Corner Floor 12_02_061125_1113.txt	4	N	sunny	3	70
53	25-Nov-06	Burnside Building	Floor 3, Location 3	9:08	10	Burnside East Floor 03_061125_0908.txt	5	SSE	sunny	0	84
54	25-Nov-06	Burnside Building	Floor 6, Location 3	9:29	10	Burnside East Floor 06_061125_0929.txt	5	SSE	sunny	0	84
55	25-Nov-06	Burnside Building	Floor 9, Location 3	9:44	10	Burnside East Floor 09_01_061125_0944.txt	0	0	sunny	2	78
56	25-Nov-06	Burnside Building	Floor 9, Location 3	9:55	10	Burnside East Floor 09_02_061125_0955.txt	0	0	sunny	2	78
57	25-Nov-06	Burnside Building	Floor 9, Location 4	10:09	10	Burnside West Corner Floor 09_01_061125_1009.txt	4	N	sunny	3	70
58	25-Nov-06	Burnside Building	Floor 9, Location 4	10:20	10	Burnside West Corner Floor 09_02_061125_1020.txt	4	N	sunny	3	70
59	25-Nov-06	Burnside Building	Floor 12, Location 4	11:02	10	Burnside West Corner Floor 12_01_061125_1102.txt	4	N	sunny	3	70
60	25-Nov-06	Burnside Building	Floor 12, Location 4	11:13	10	Burnside West Corner Floor 12_02_061125_1113.txt	4	N	sunny	3	70
61	25-Nov-06	Burnside Building	Floor 12, Location 3	10:39	10	Burnside West Floor 12_01_061125_1039.txt	4	N	sunny	3	70

APPENDIX B

FREQUENCY SPECTRA

Date of Measurement: November 17, 2006
Building: Burnside Hall Building

Location: Basement, Location 2

Direct Fourier Transformation Spectrum

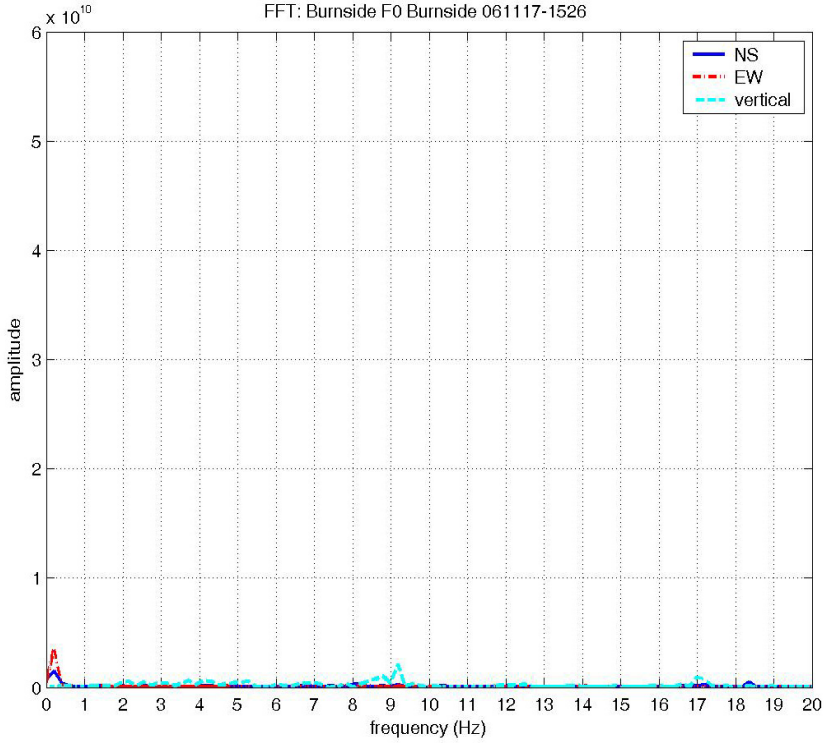

Power Spectral Density Spectrum

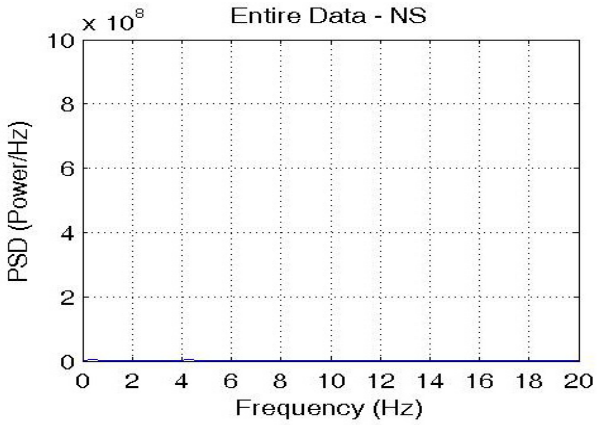

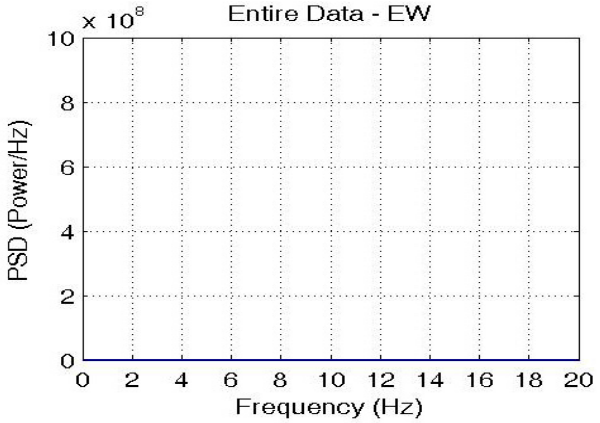

Auto-Regressive-Moving-Average Spectrum

NS component

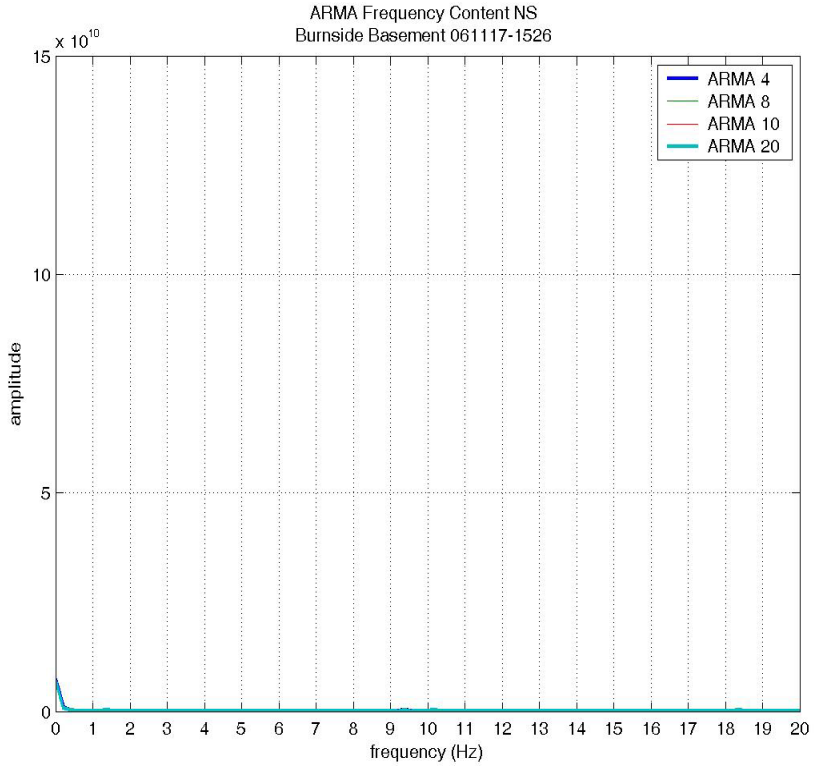

EW component

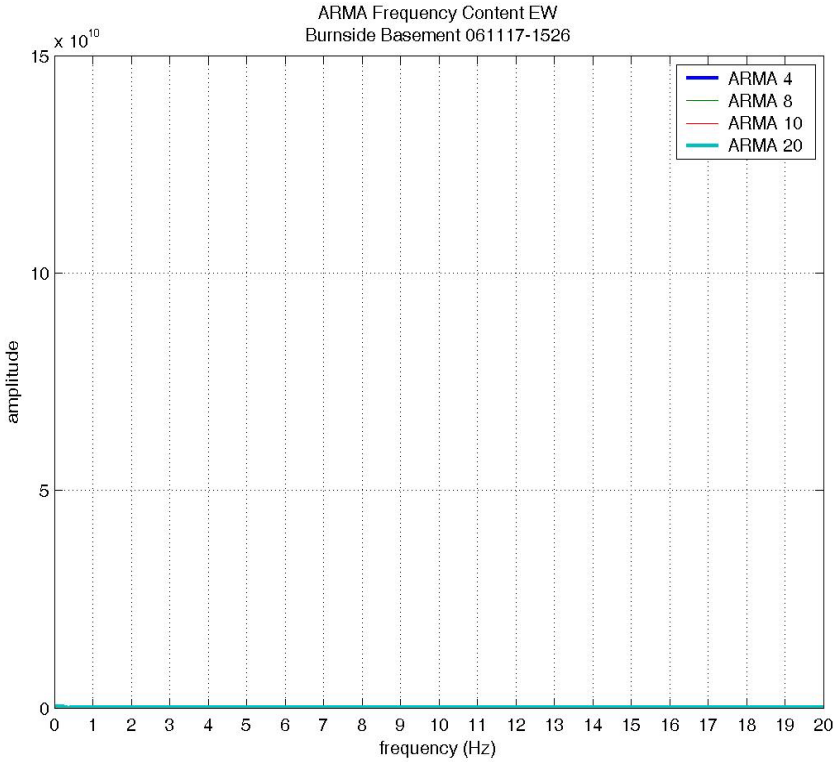

Location: Floor 2, Location 2

Direct Fourier Transformation Spectrum

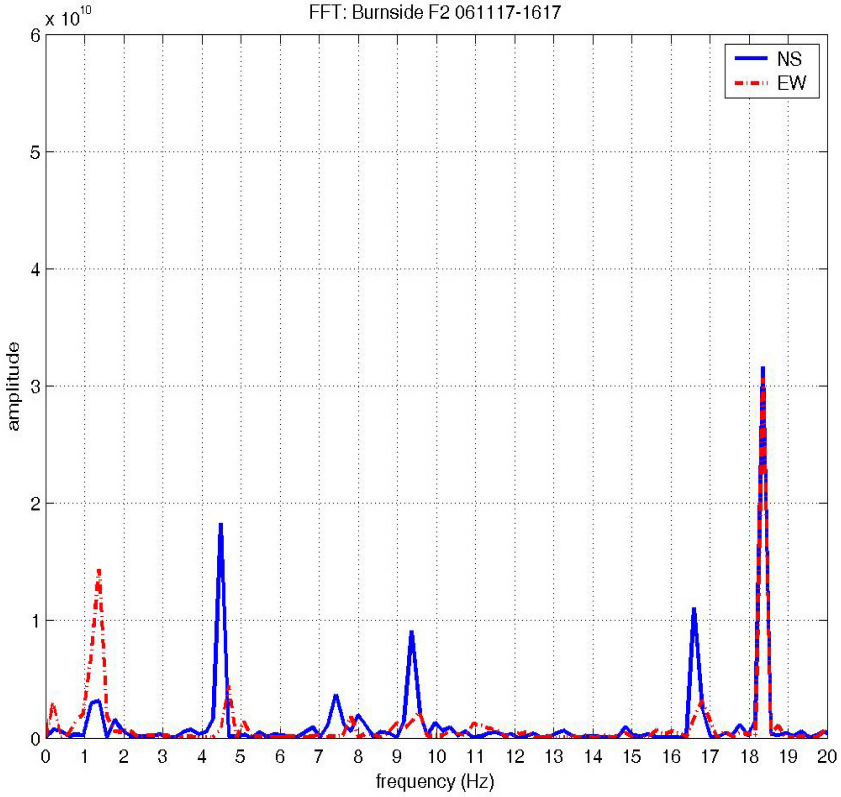

Power Spectral Density Spectrum

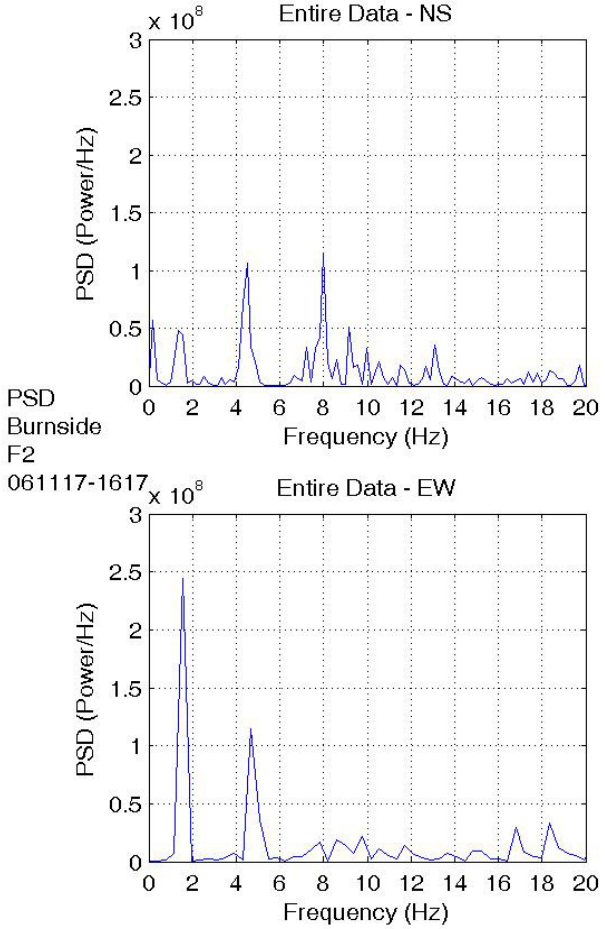

Auto-Regressive-Moving-Average Spectrum

NS component

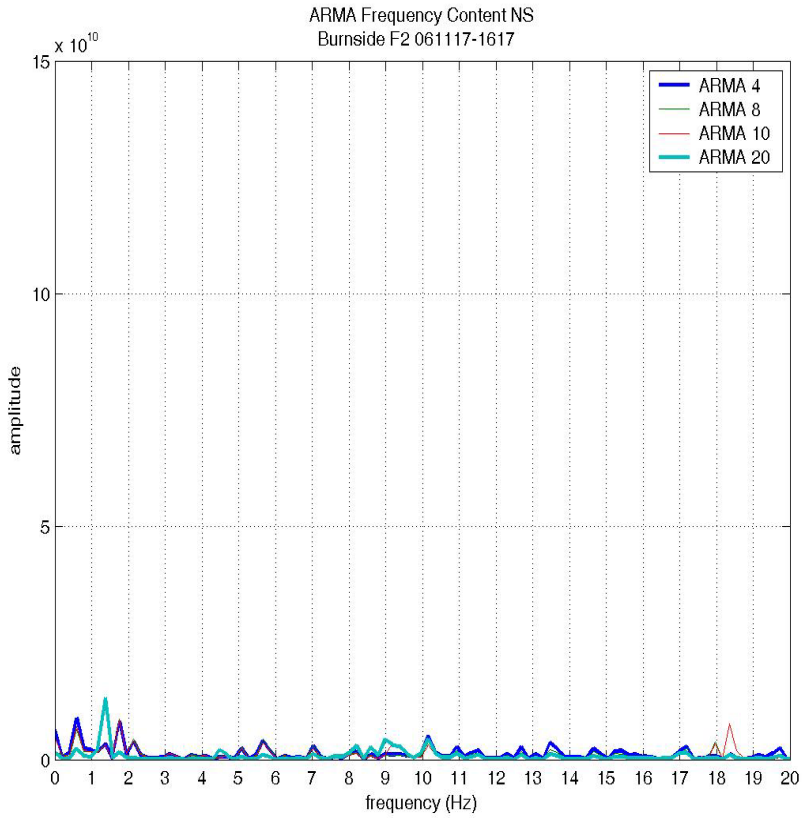

EW component

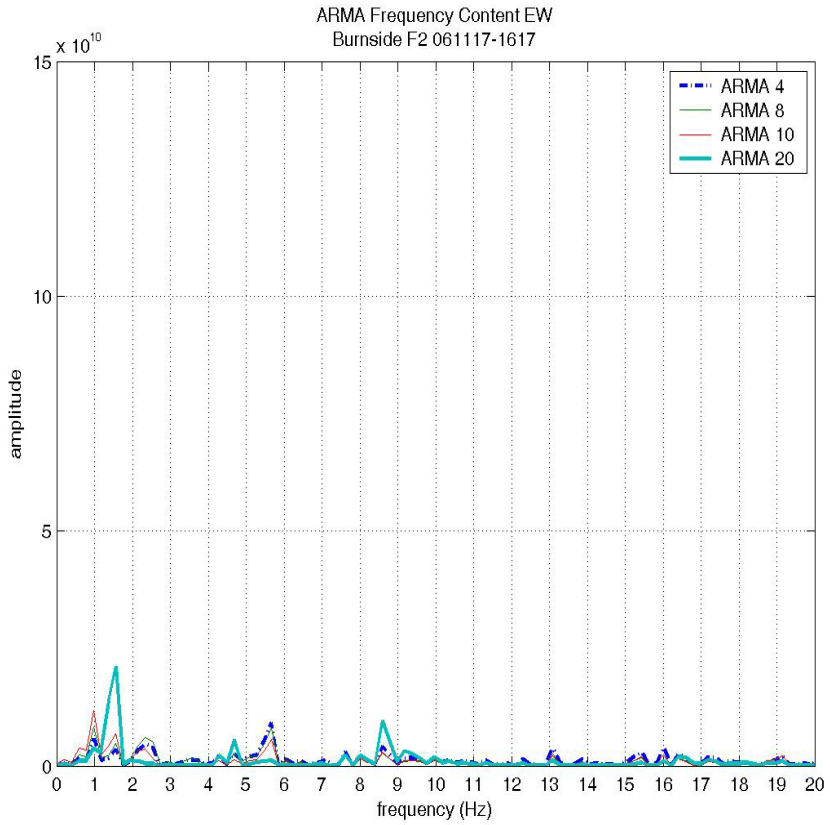

Location: Floor 6, Location 2

Direct Fourier Transformation Spectrum

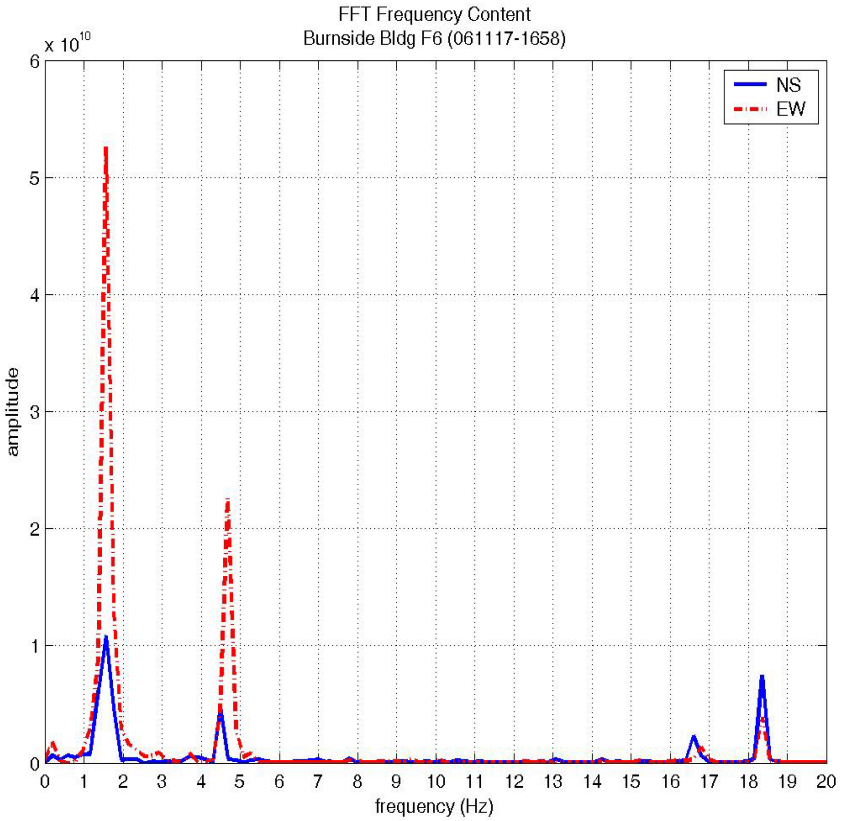

Power Spectrum Density Spectrum

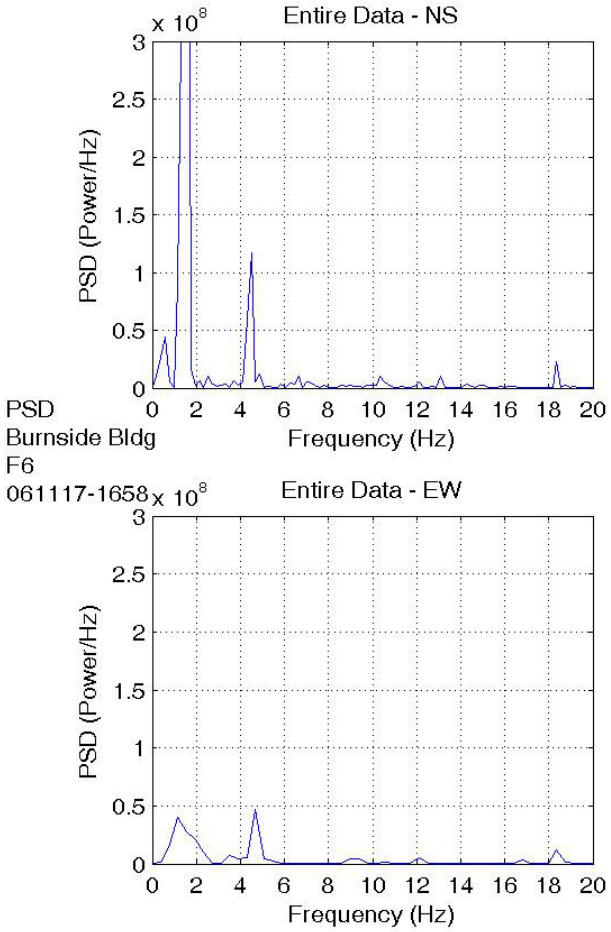

Auto-Regressive-Moving-Average Spectrum

NS component

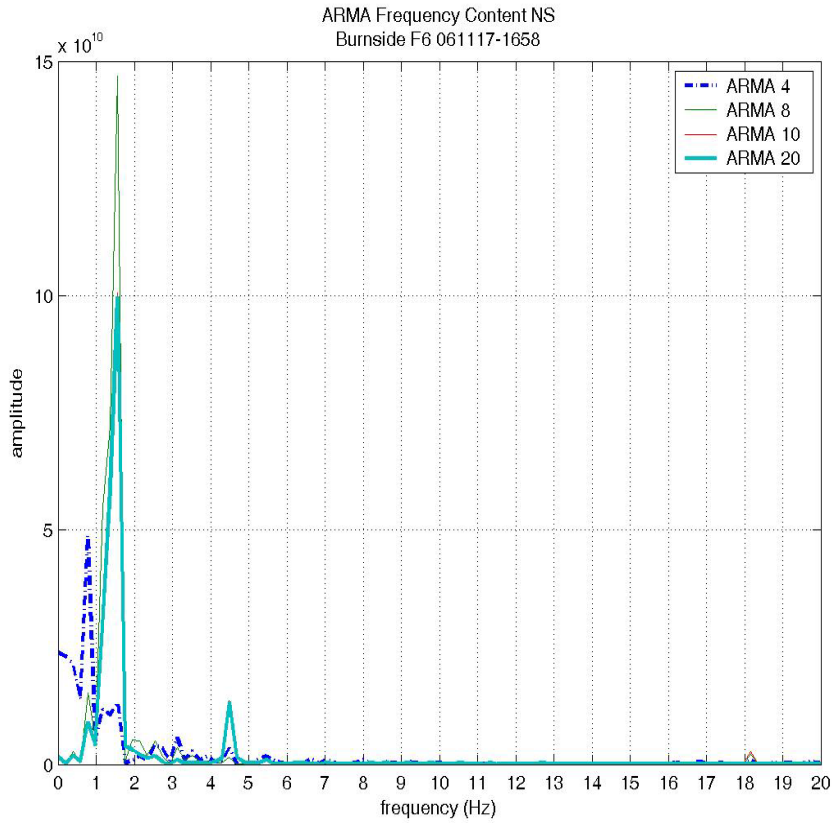

EW component

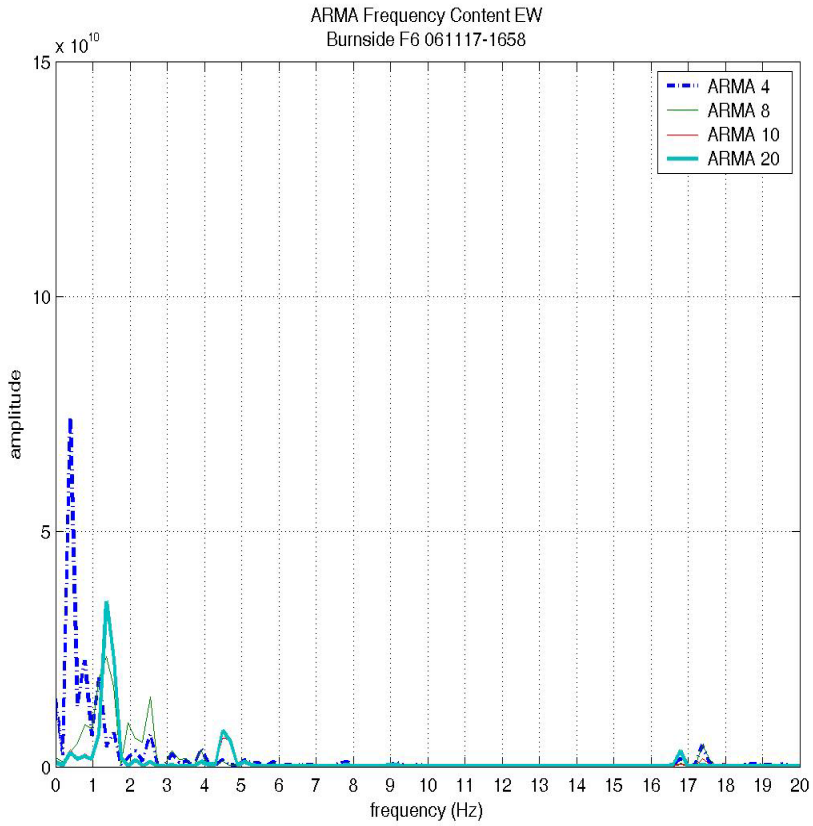

Location: Floor 9, Location 2

Direct Fourier Transformation Spectrum

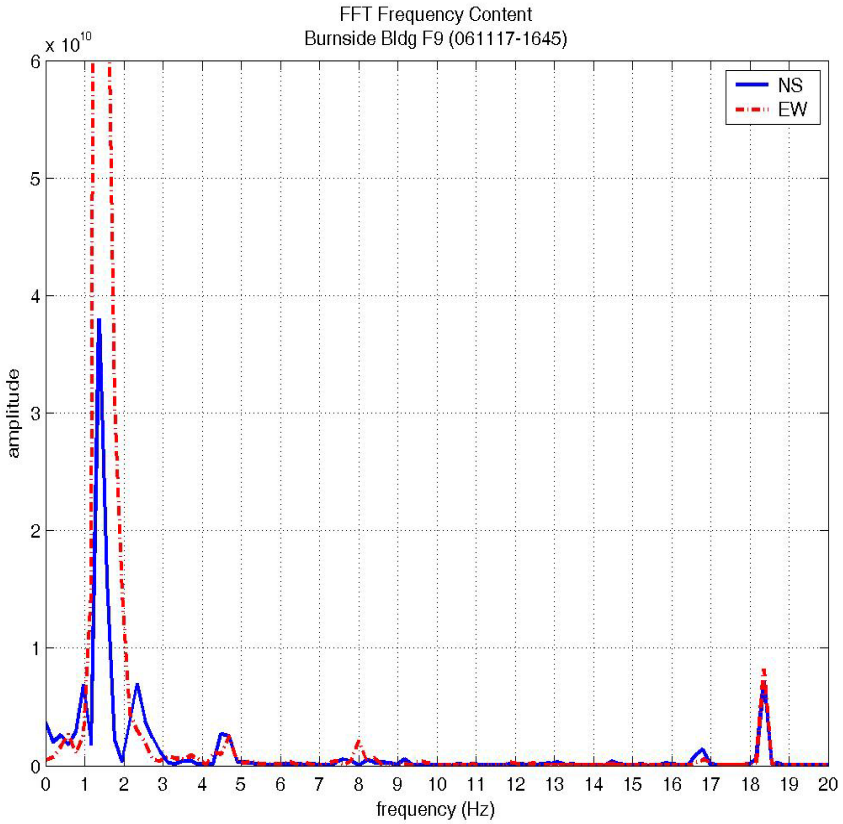

Power Spectrum Density Spectrum

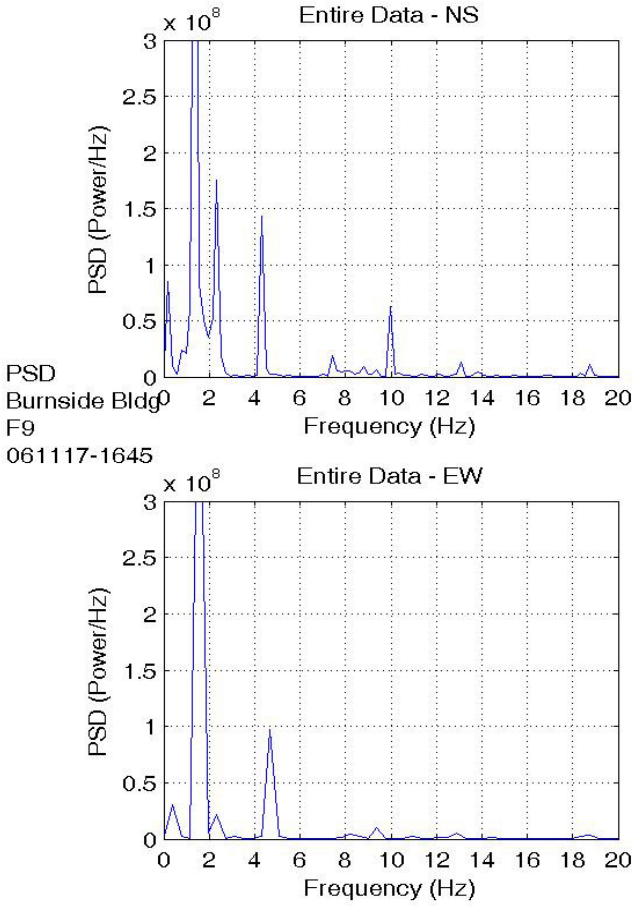

Auto-Regressive-Moving-Average Spectrum

NS component

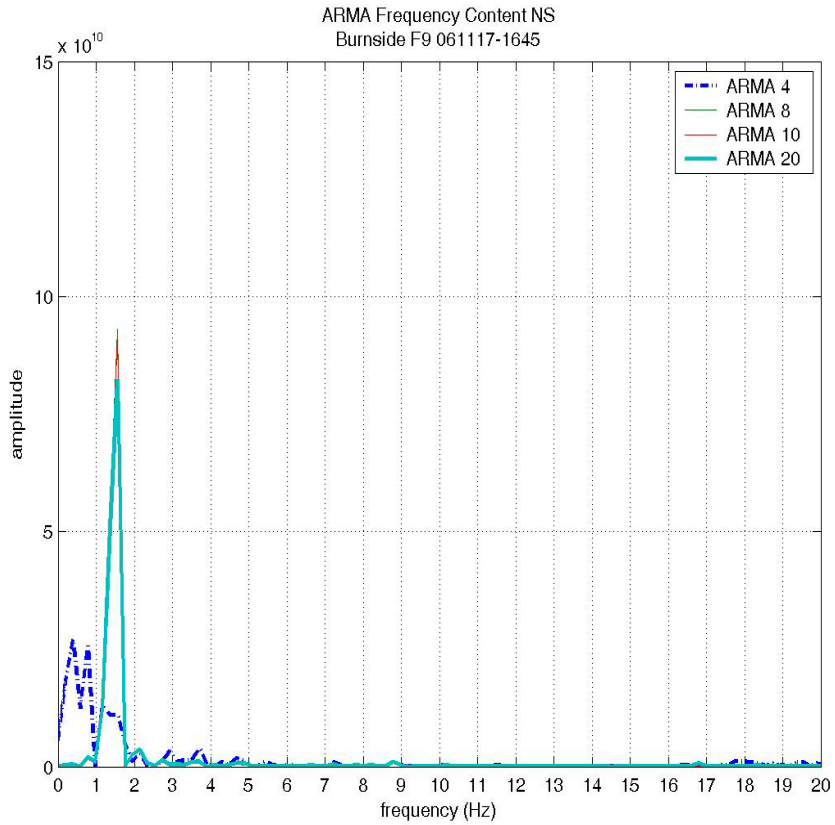

EW component

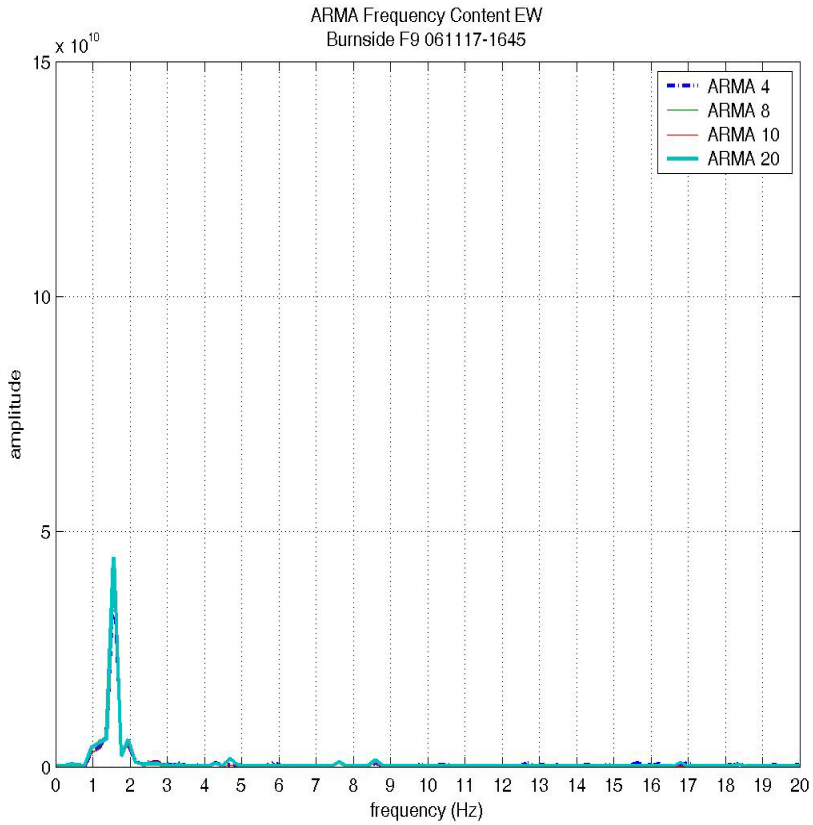

Location: Floor 12, Location 2

Direct Fourier Transformation Spectrum

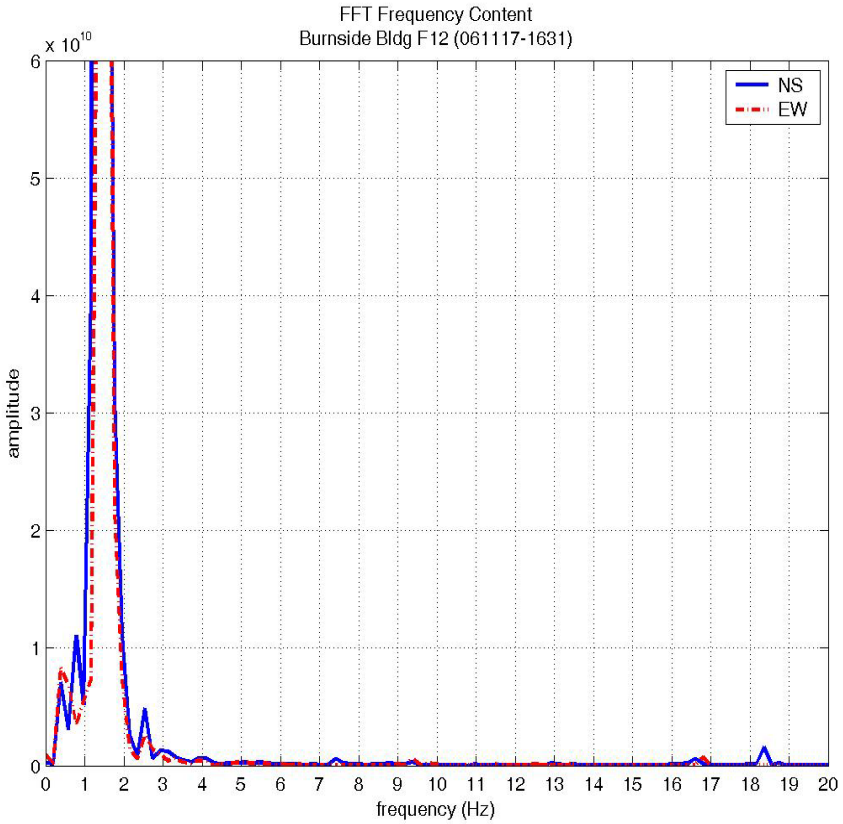

Power Spectrum Density Spectrum

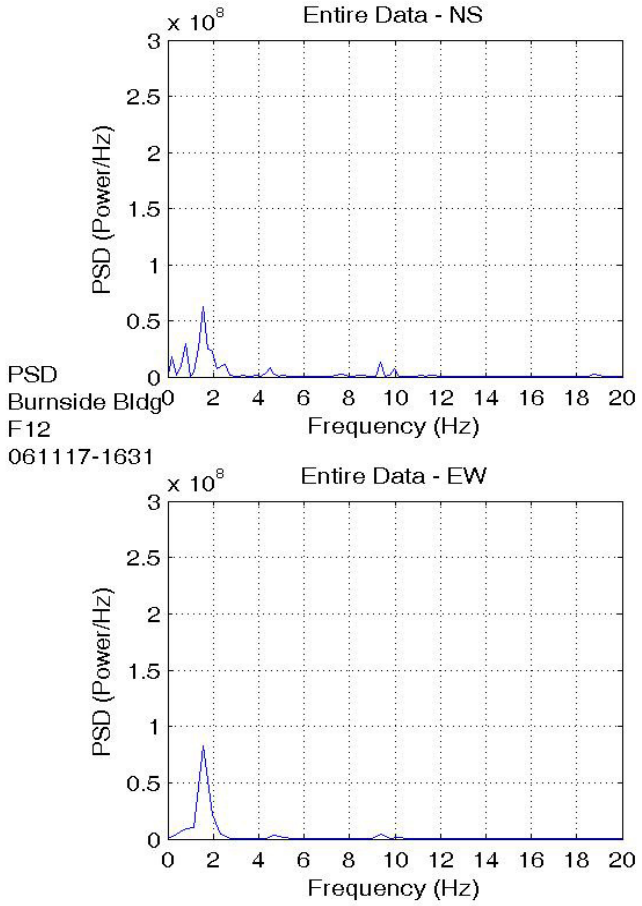

Auto-Regressive-Moving-Average Spectrum

NS component

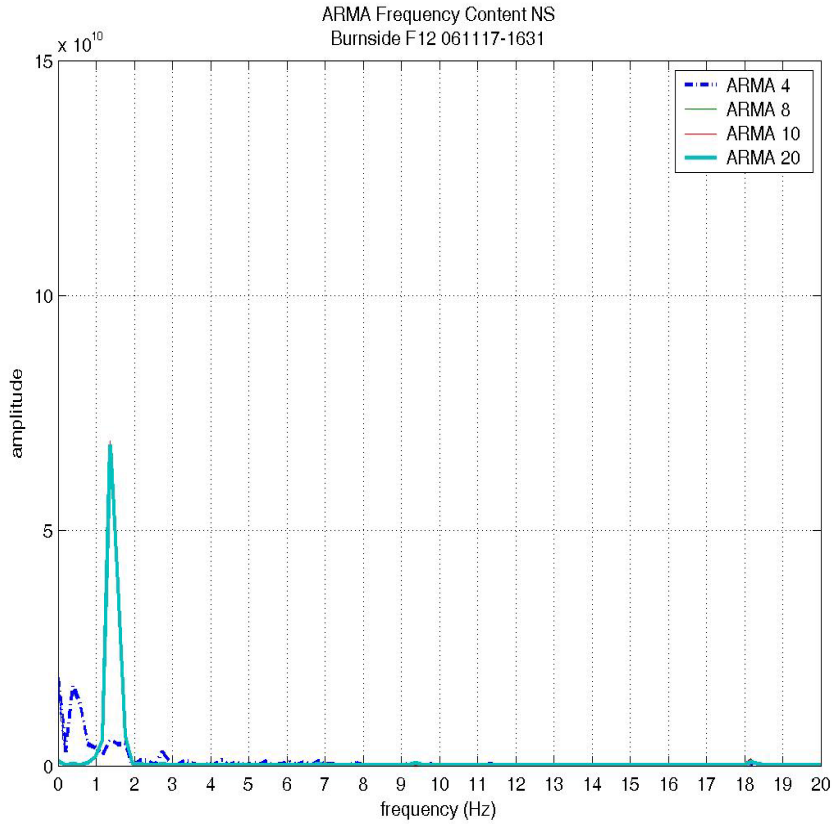

EW component

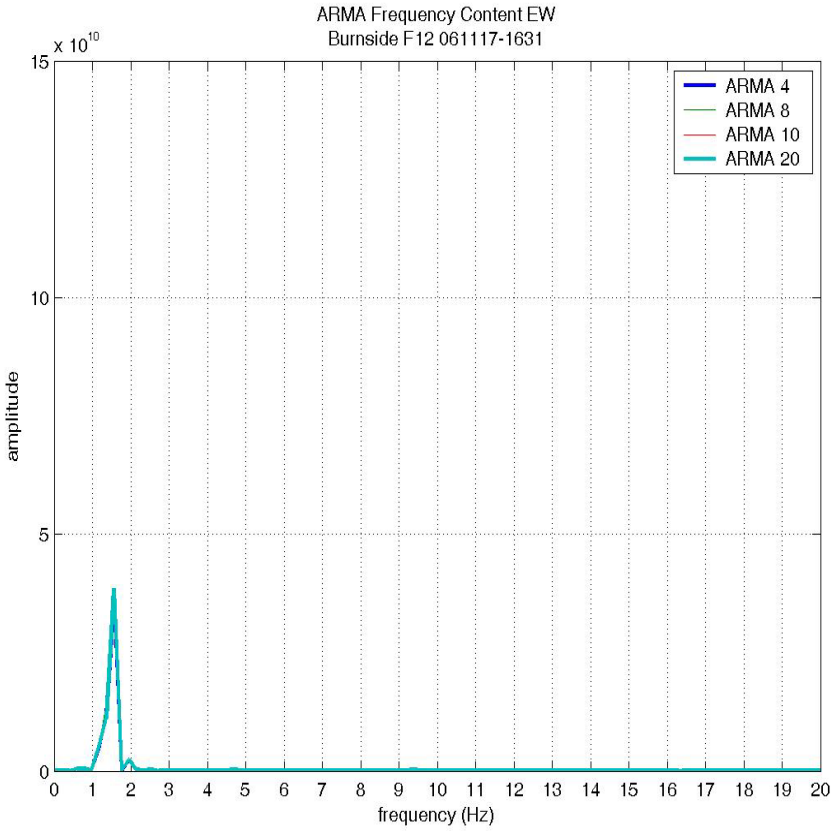

Date of Measurement: November 24, 2006
Building: Burnside Hall Building

Location: Floor 3, Location 1

Direct Fourier Transformation Spectrum

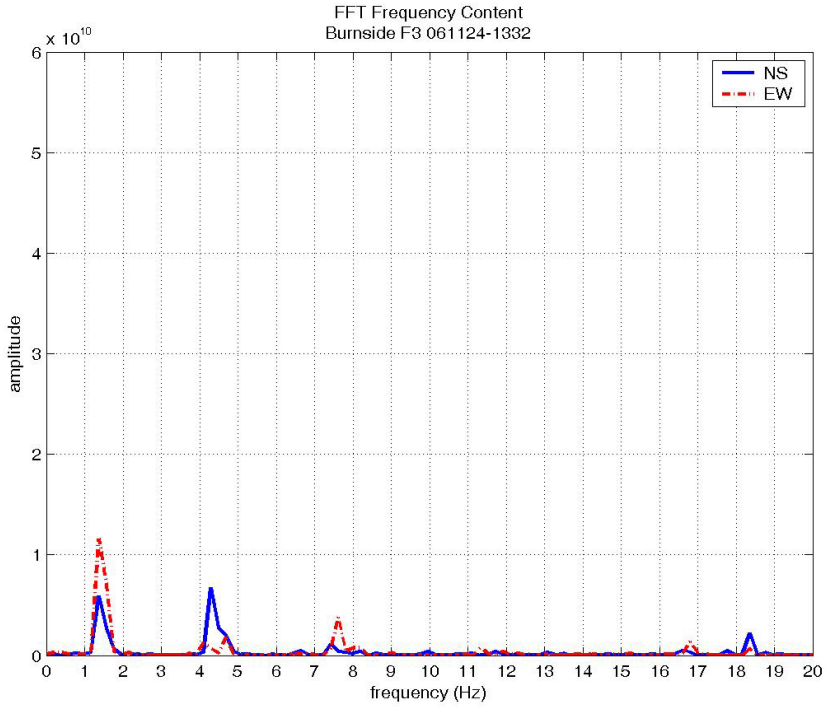

Power Spectrum Density Spectrum

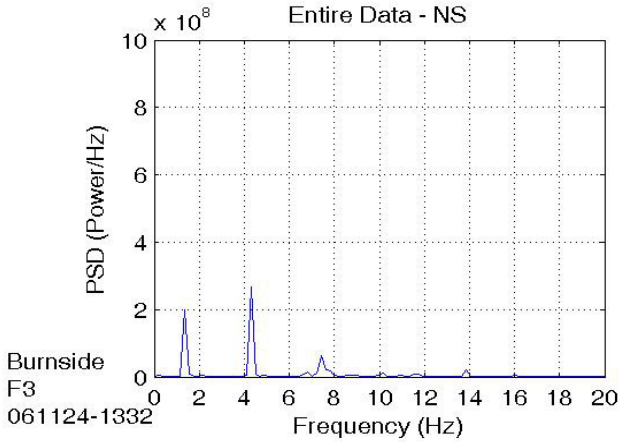

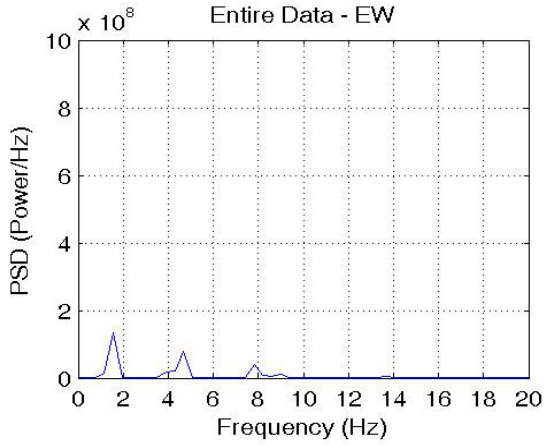

Auto-Regressive-Moving-Average Spectrum

NS component

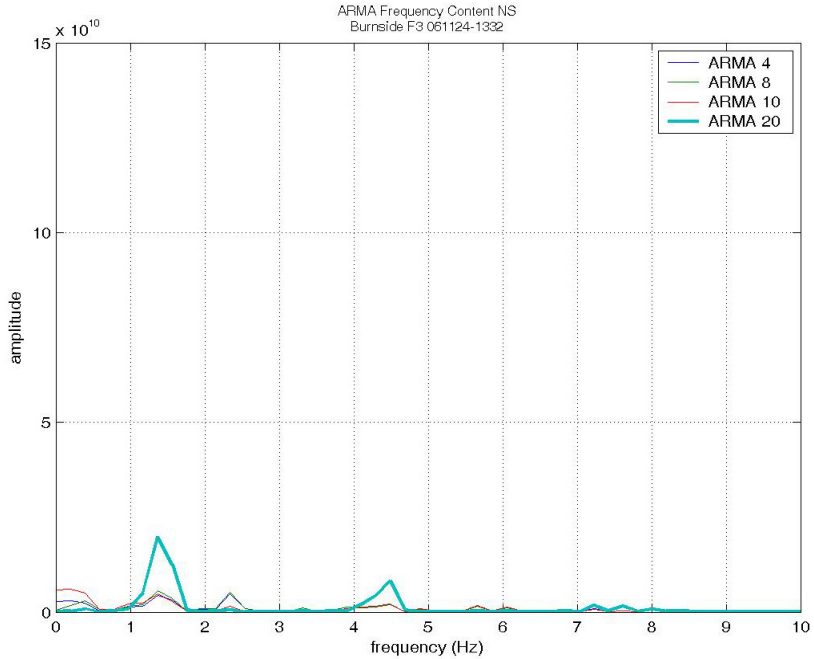

EW component

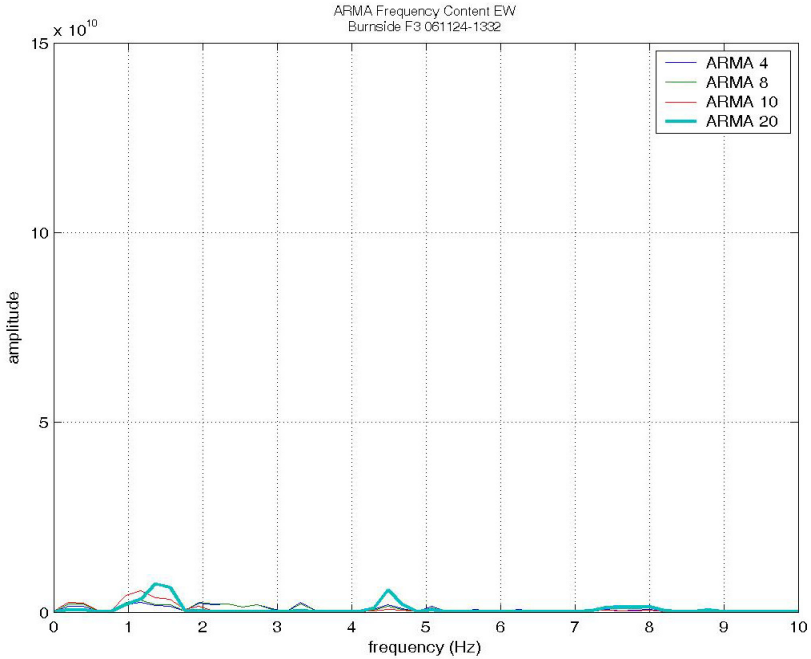

Location: Floor 6, Location 1

Direct Fourier Transformation Spectrum

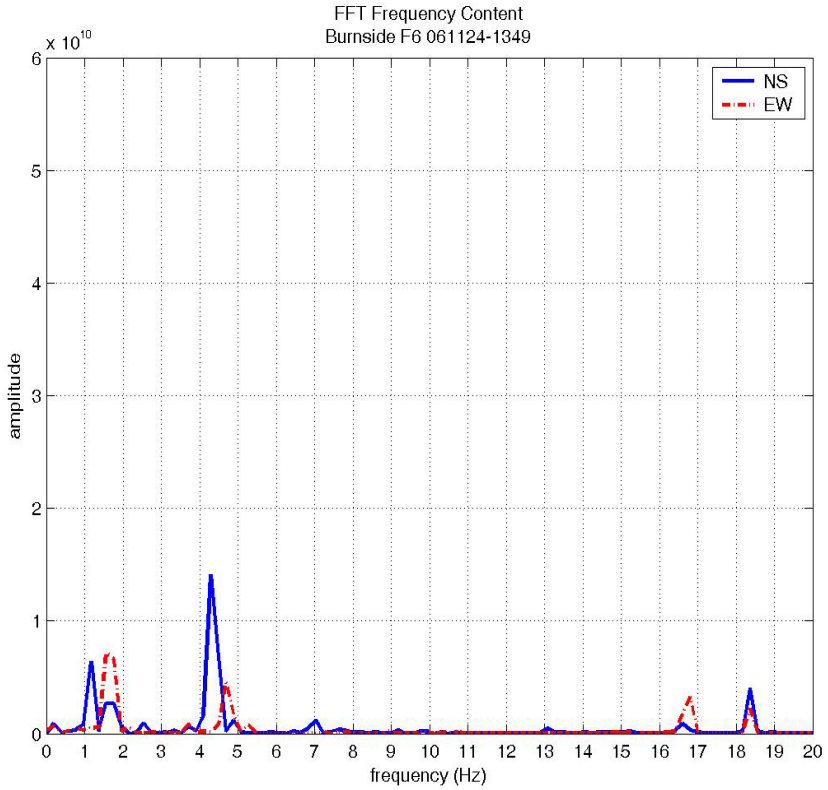

Power Spectrum Density Spectrum

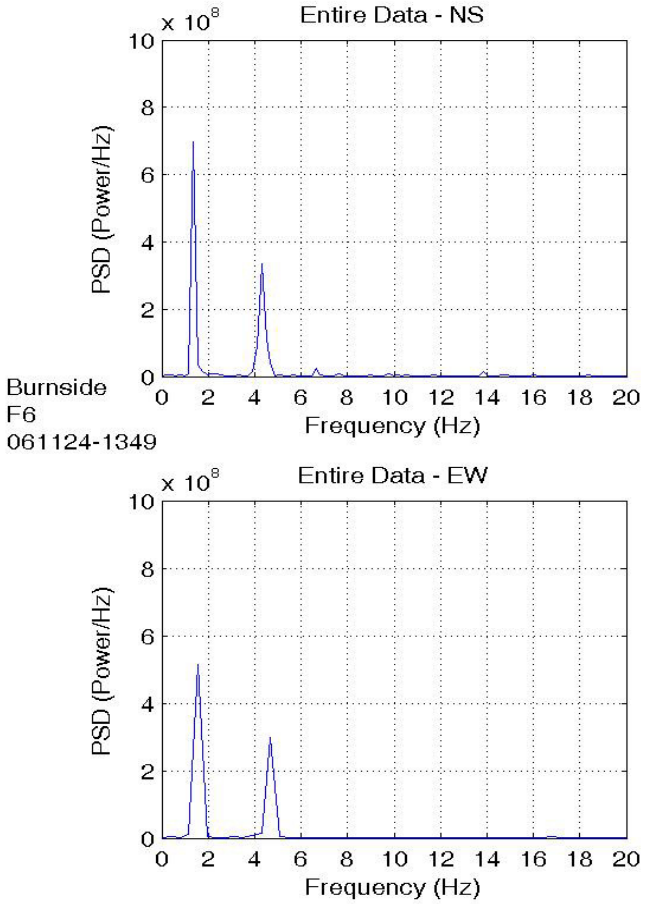

Auto-Regressive-Moving-Average Spectrum

NS component

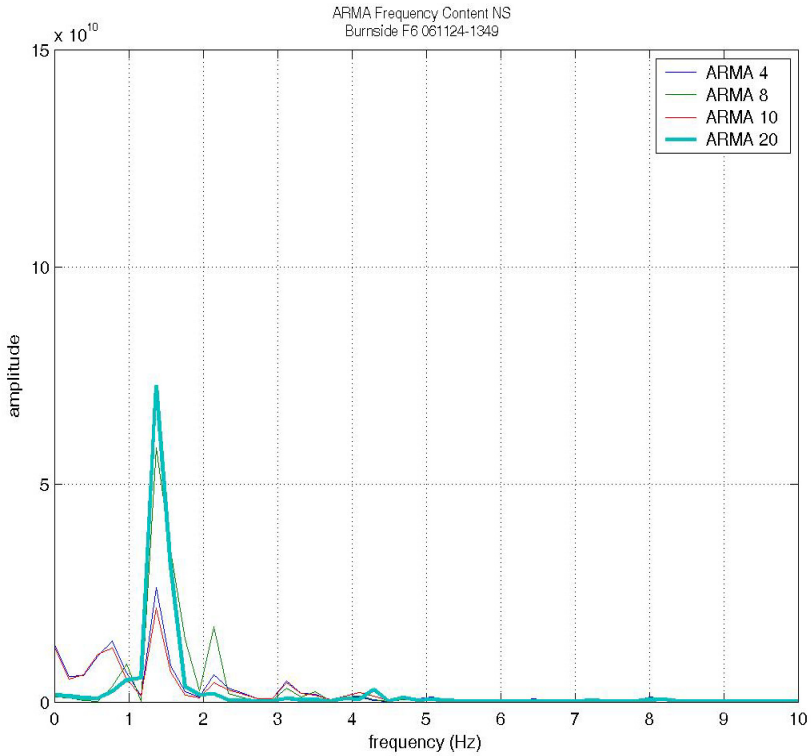

EW component

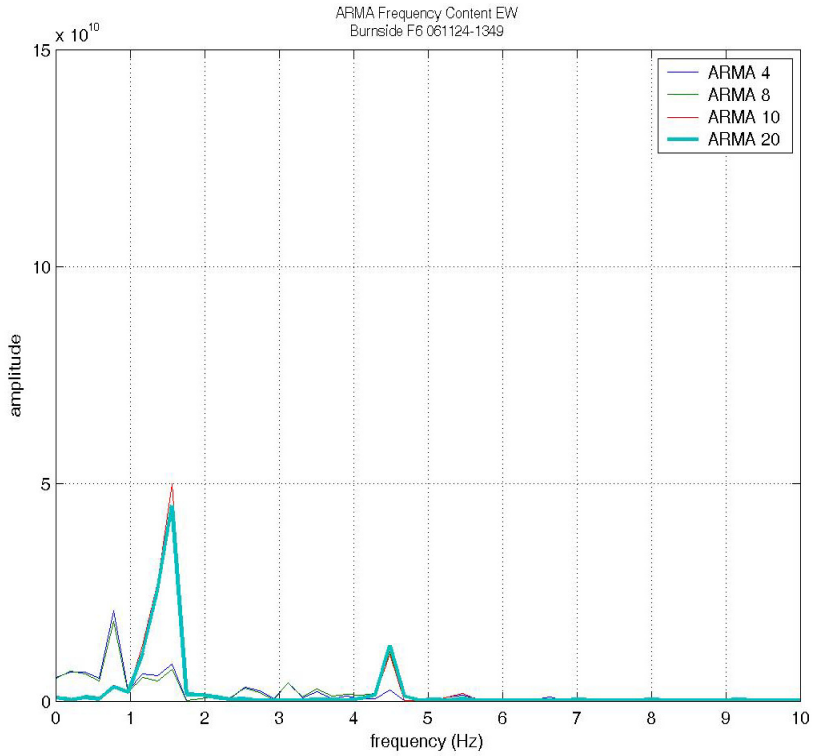

Location: Floor 9, Location 1

Direct Fourier Transformation Spectrum

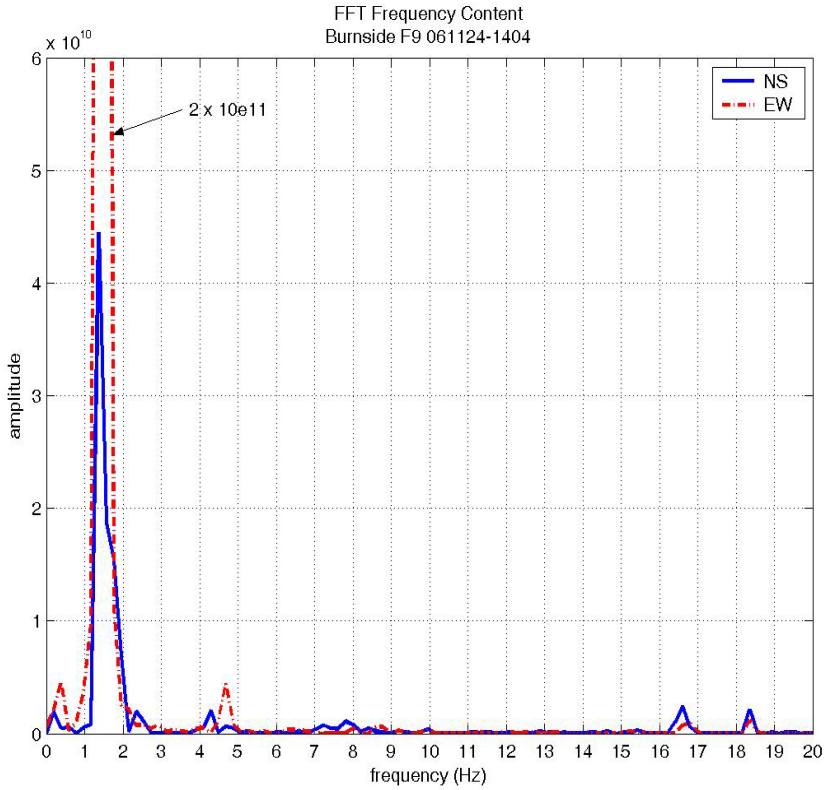

Power Spectrum Density Spectrum

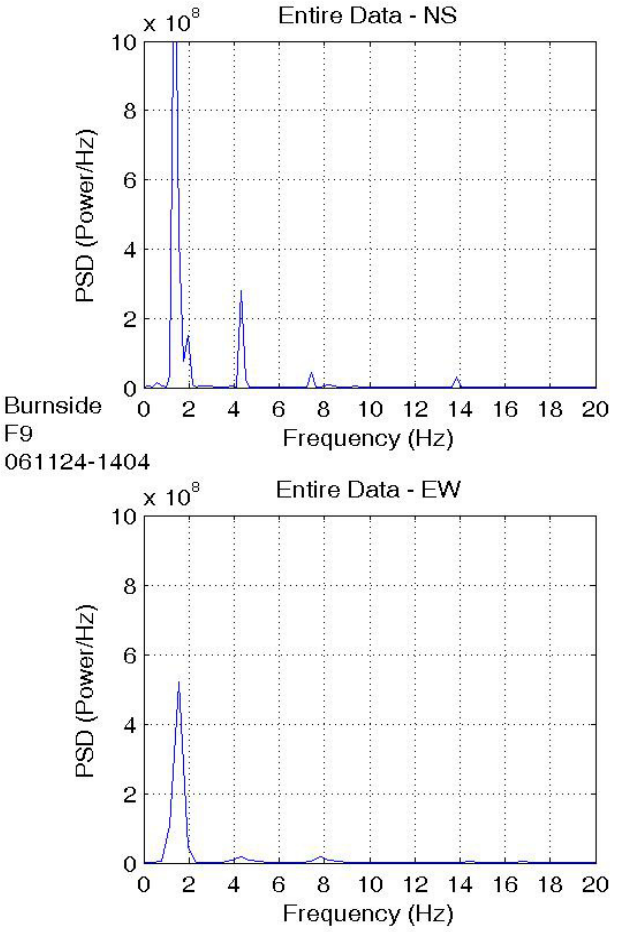

Auto-Regressive-Moving-Average Spectrum

NS component

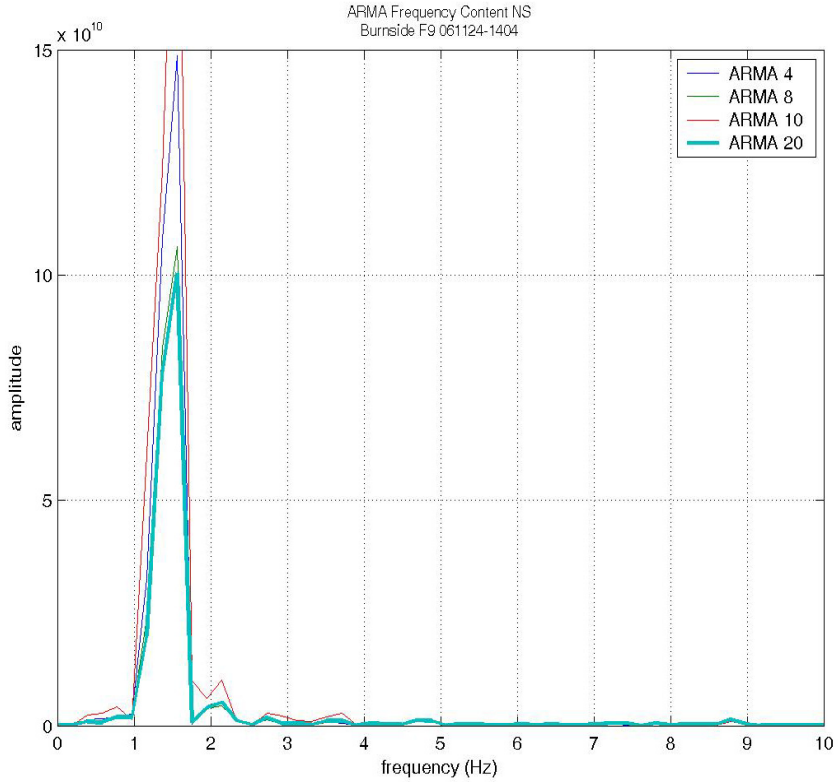

EW component

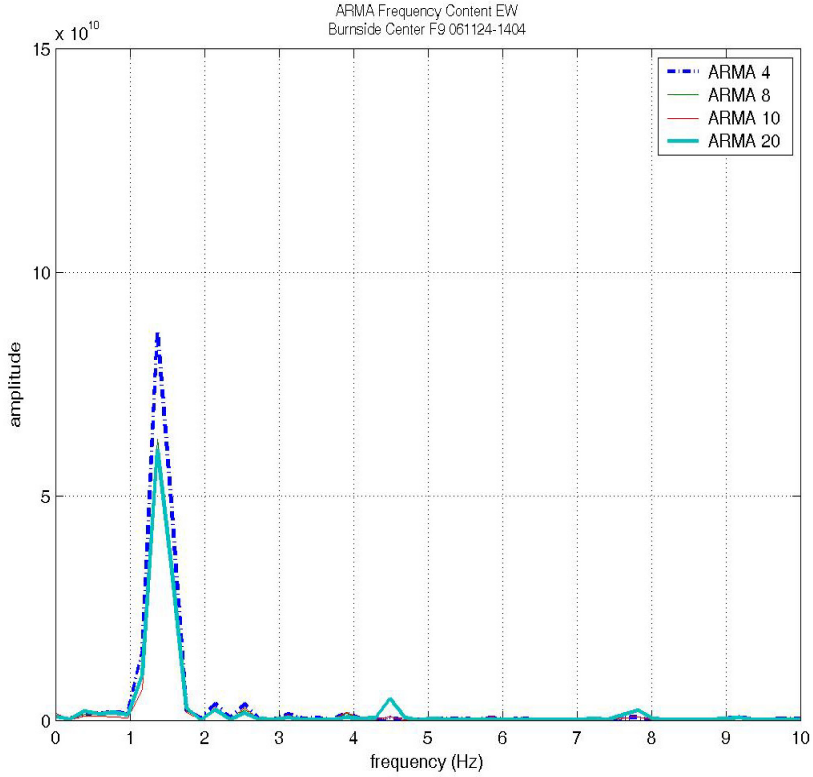

Location: Floor 12, Location 1

Direct Fourier Transformation Spectrum

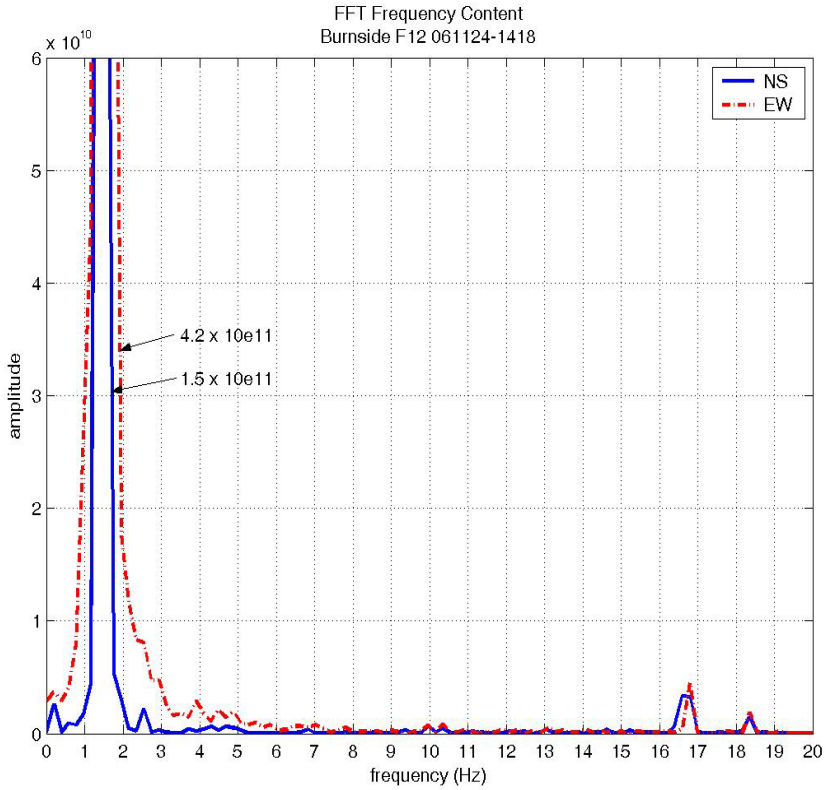

Power Spectrum Density Spectrum

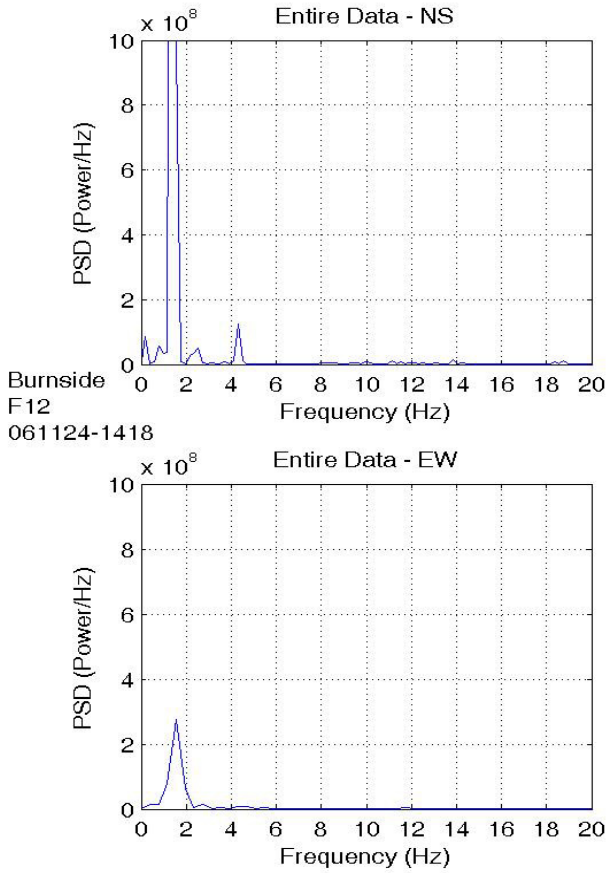

Auto-Regressive-Moving-Average Spectrum

NS component

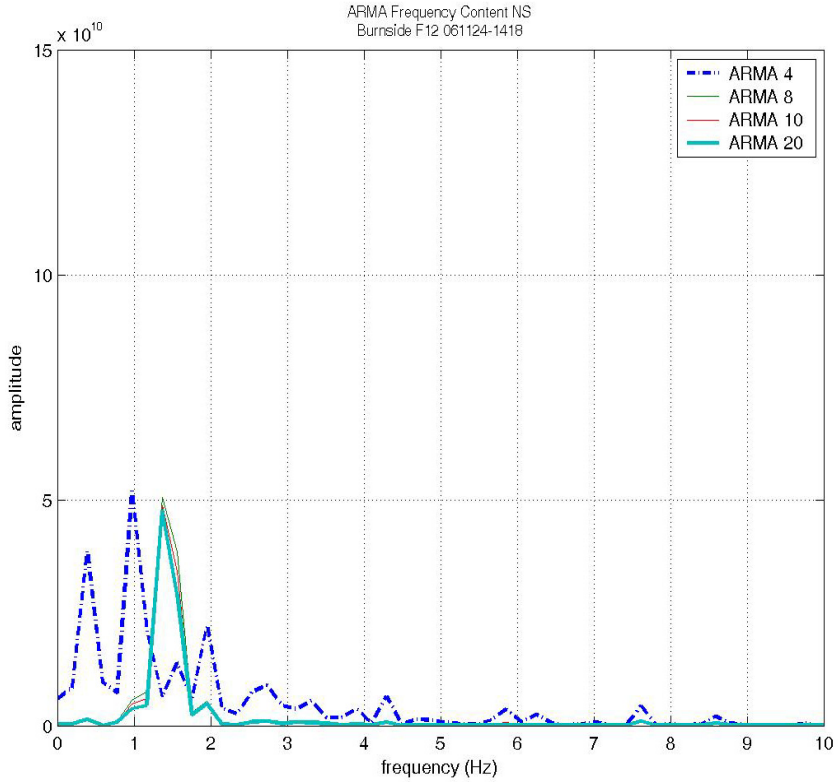

EW component

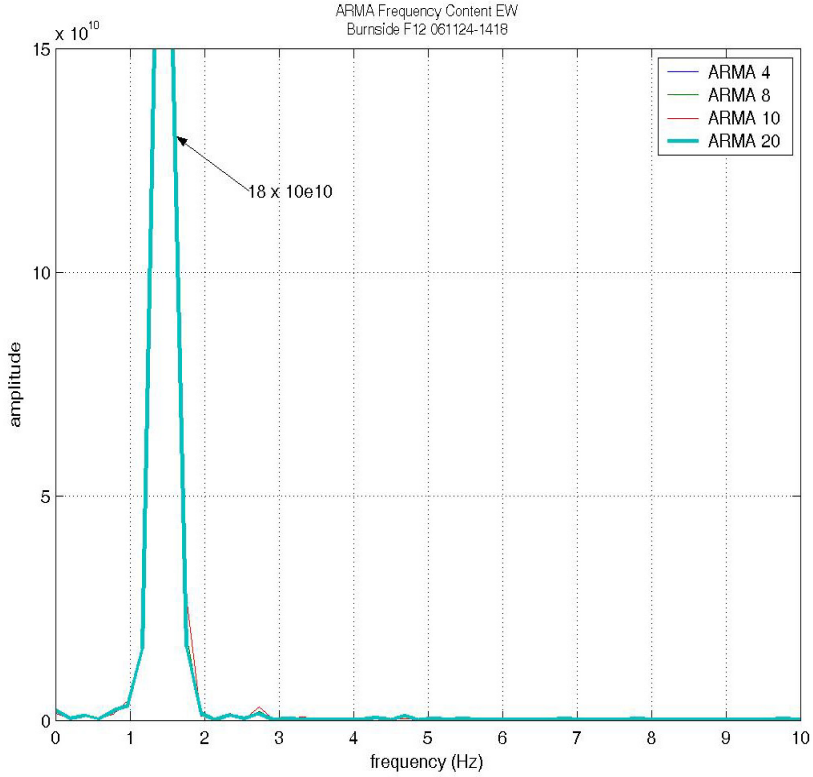

Location: Floor 3, Location 3

Direct Fourier Transformation Spectrum

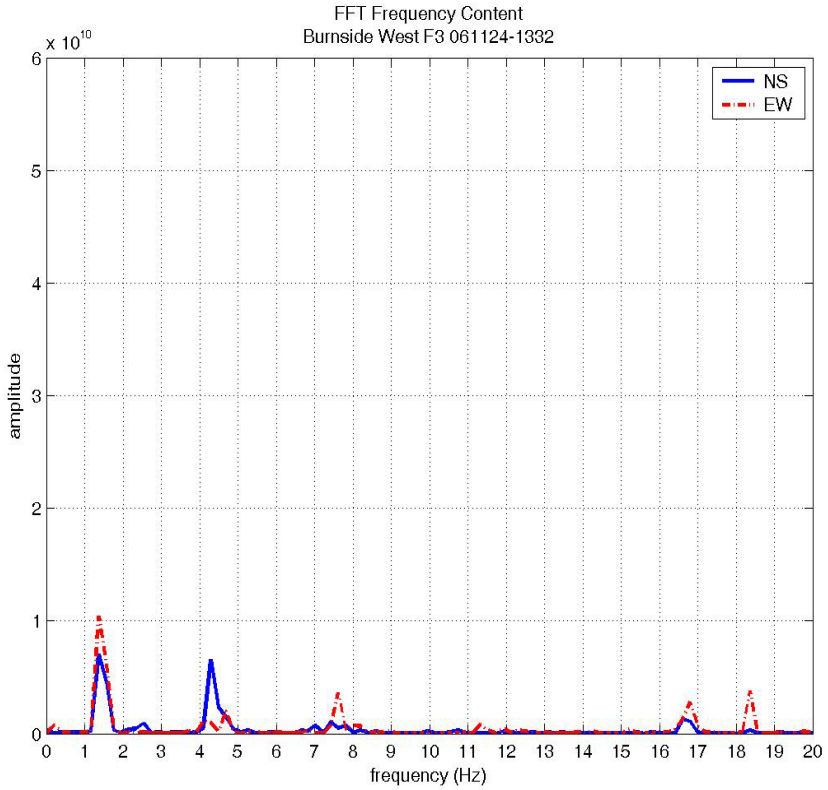

Power Spectrum Density Spectrum

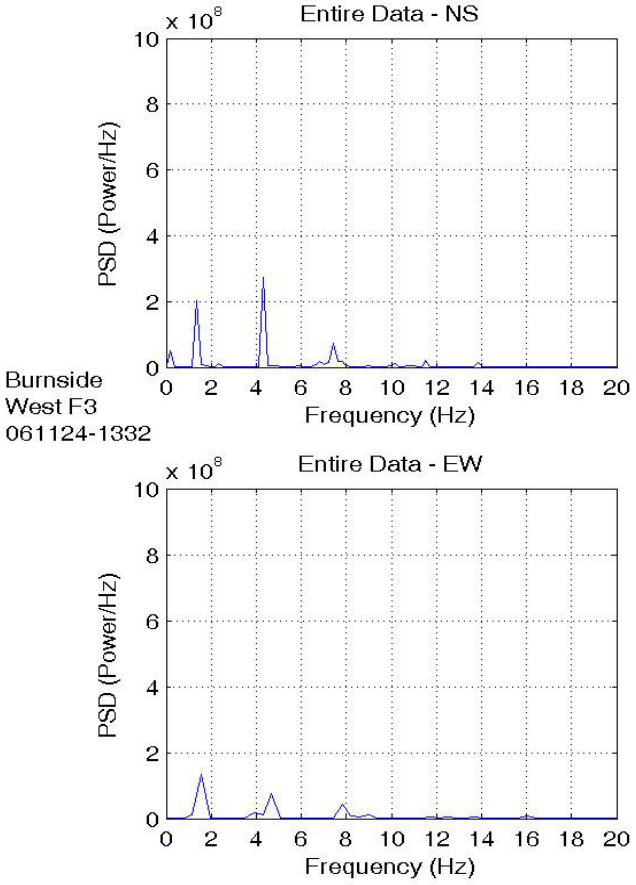

Auto-Regressive-Moving-Average Spectrum

NS component

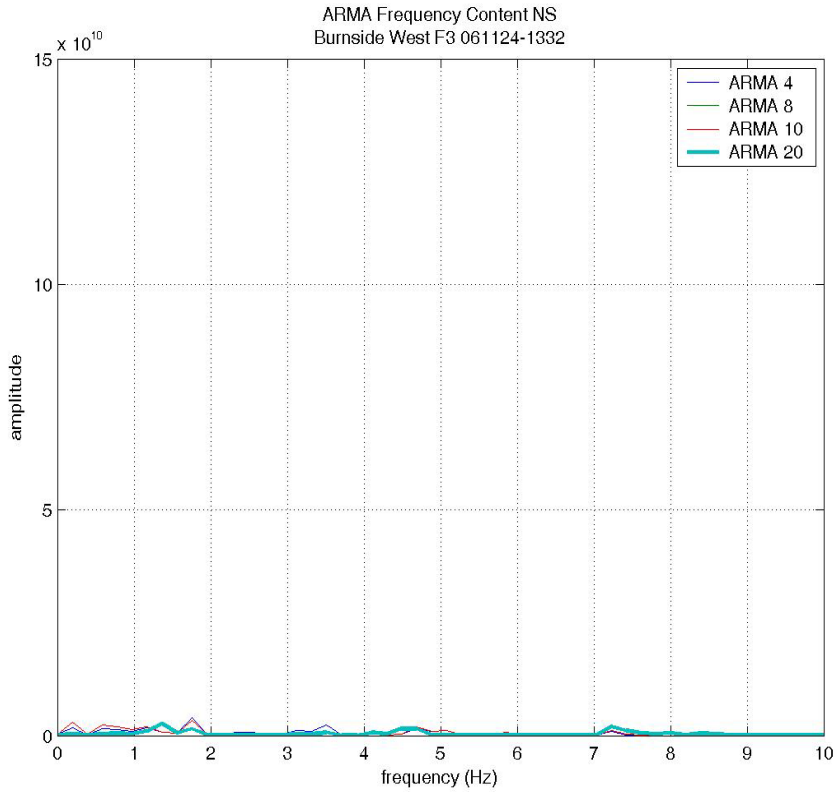

EW component

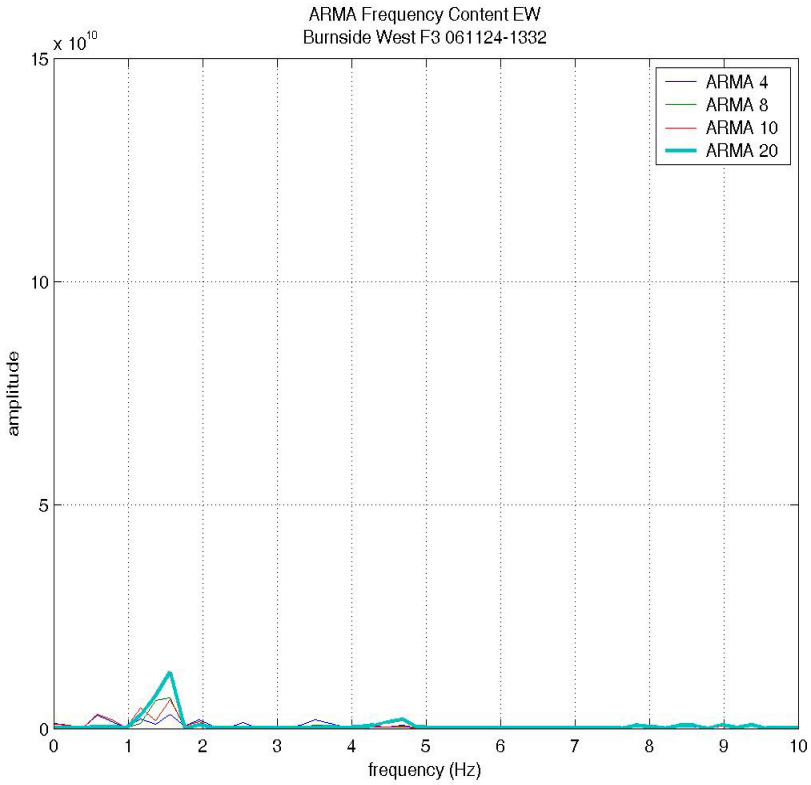

Location: Floor 6, Location 3

Direct Fourier Transformation Spectrum

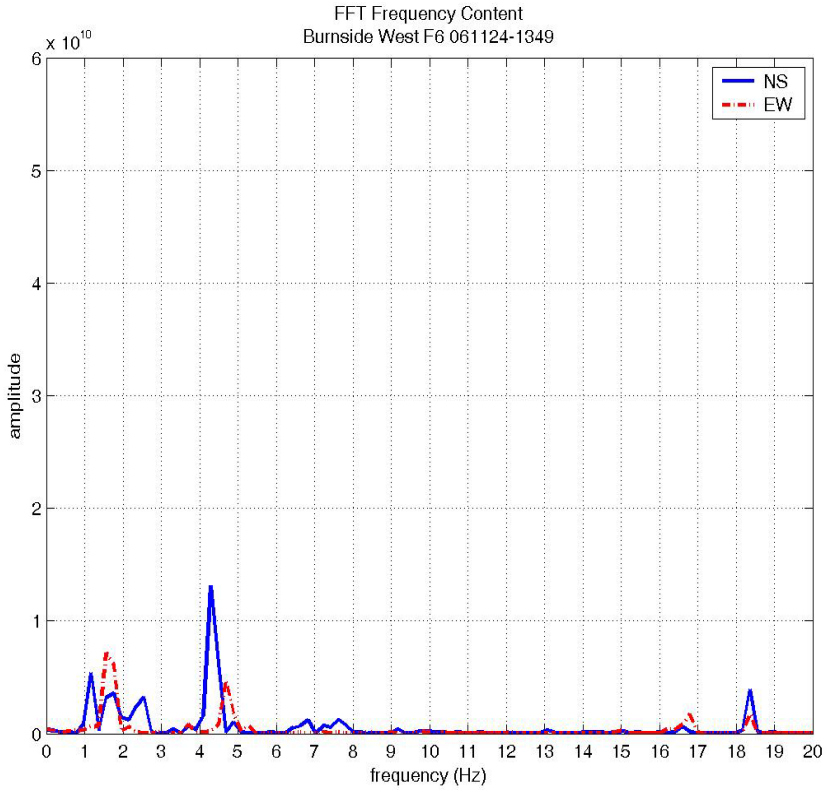

Power Spectrum Density Spectrum

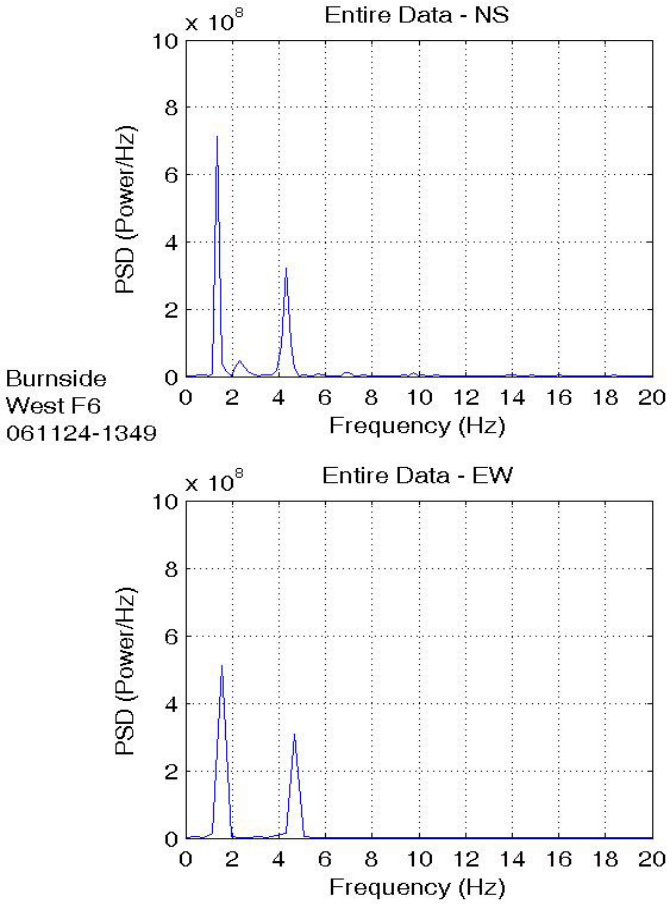

Auto-Regressive-Moving-Average Spectrum

NS component

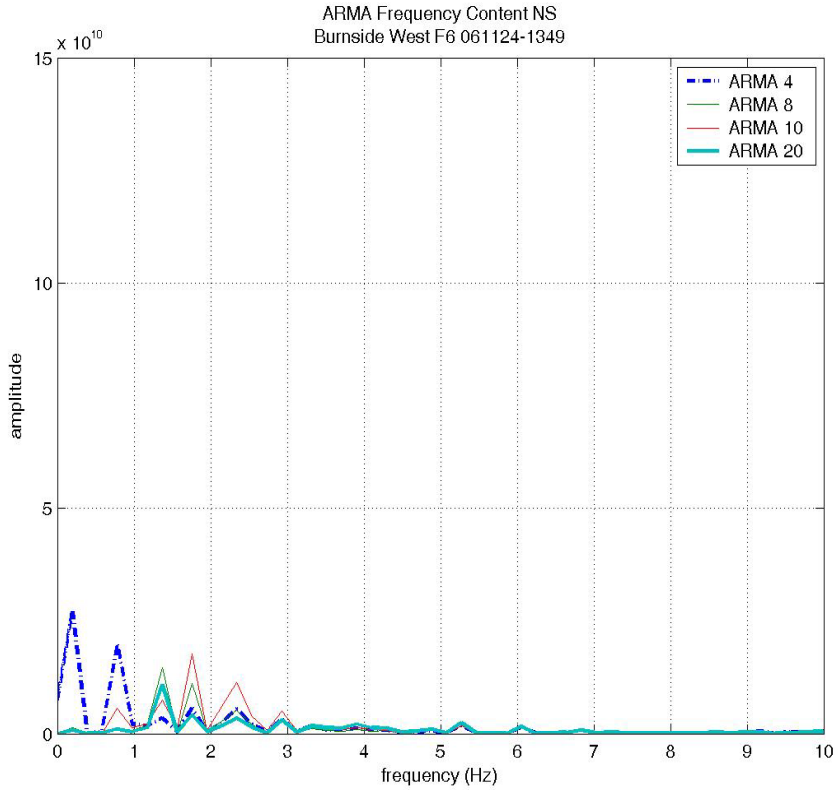

EW component

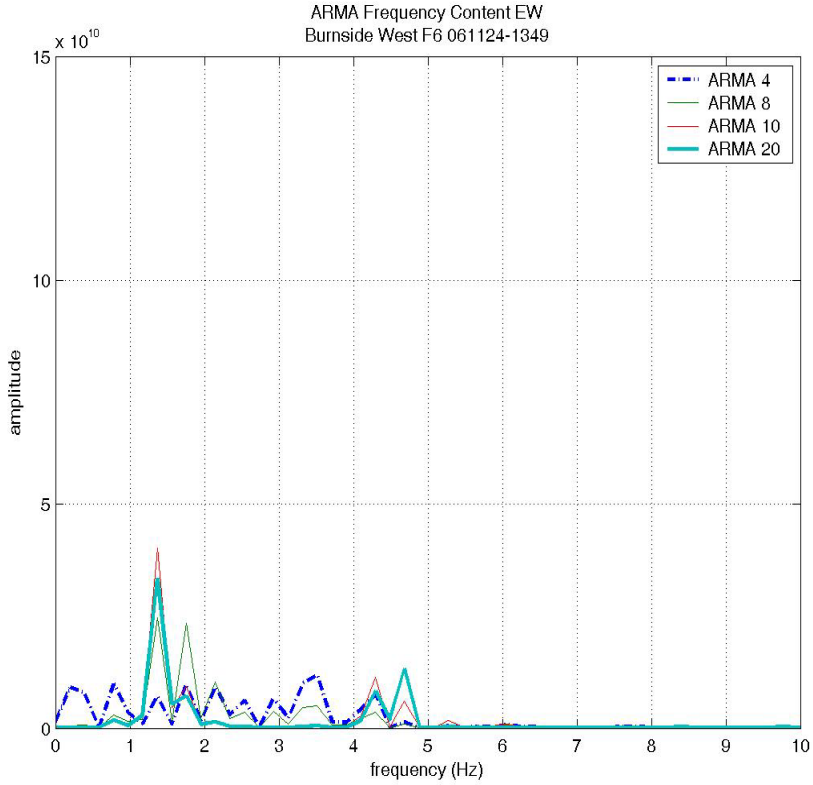

Location: Floor 9, Location 3

Direct Fourier Transformation Spectrum

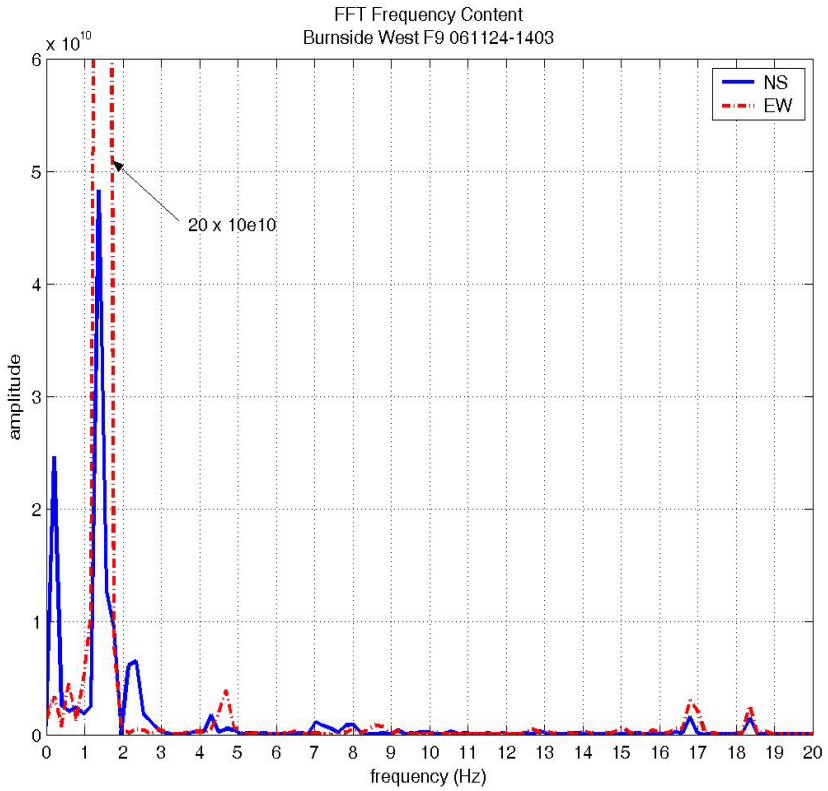

Power Spectrum Density Spectrum

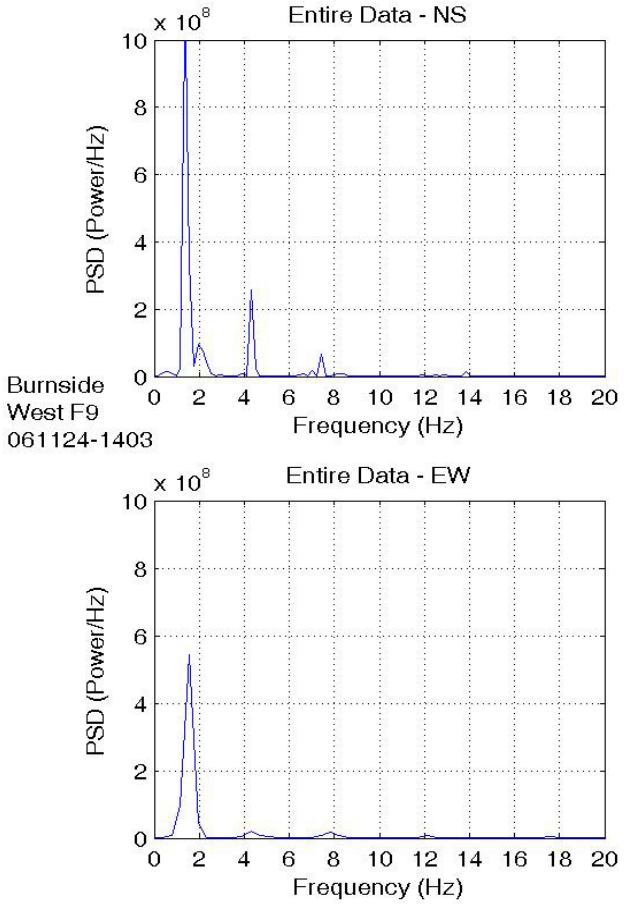

Auto-Regressive-Moving-Average Spectrum

NS component

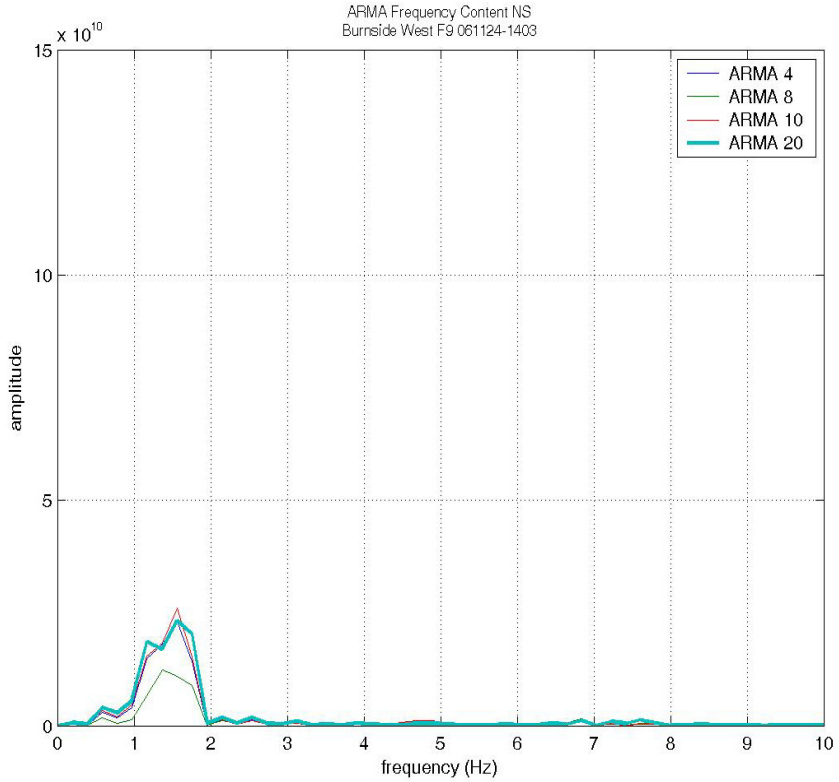

EW component

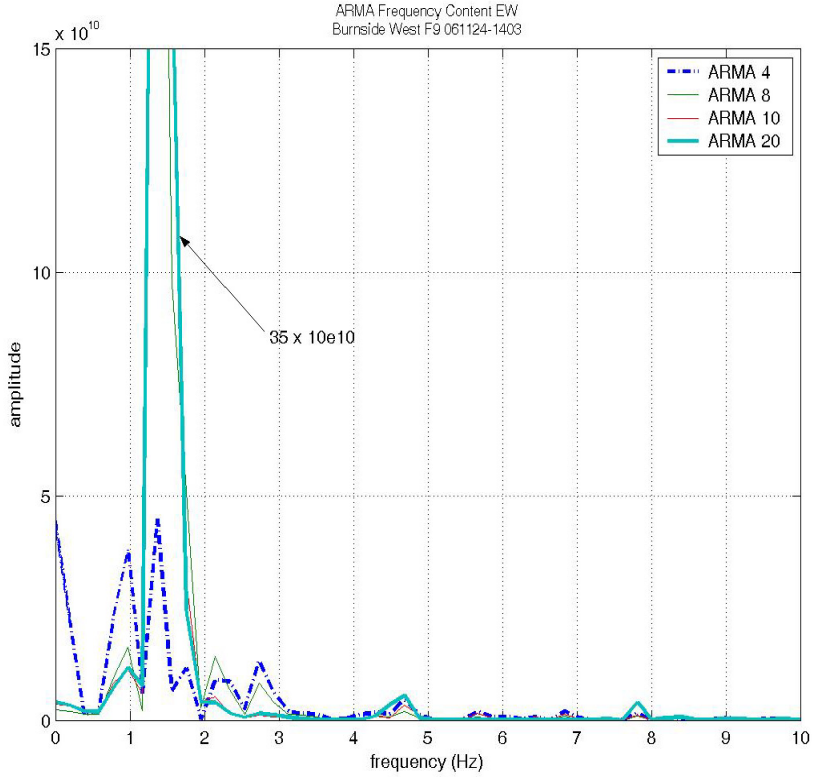

Location: Floor 12, Location 3

Direct Fourier Transformation Spectrum

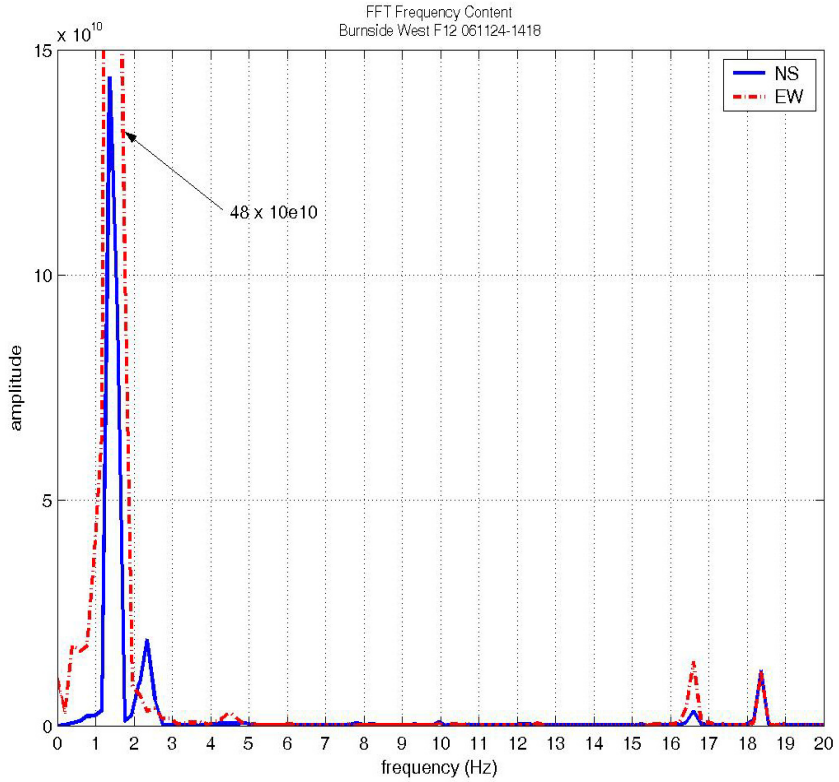

Power Spectrum Density Spectrum

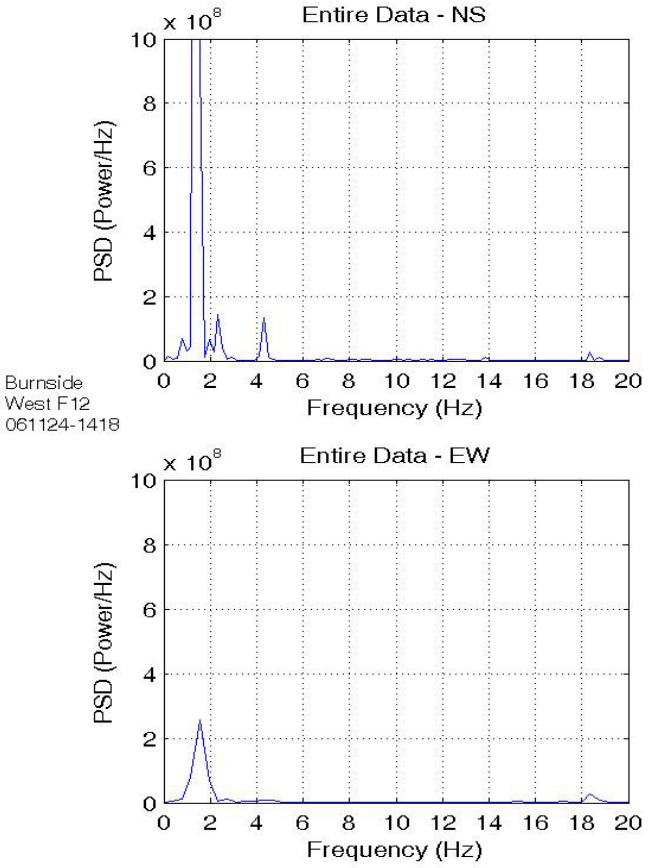

Auto-Regressive-Moving-Average Spectrum

NS component

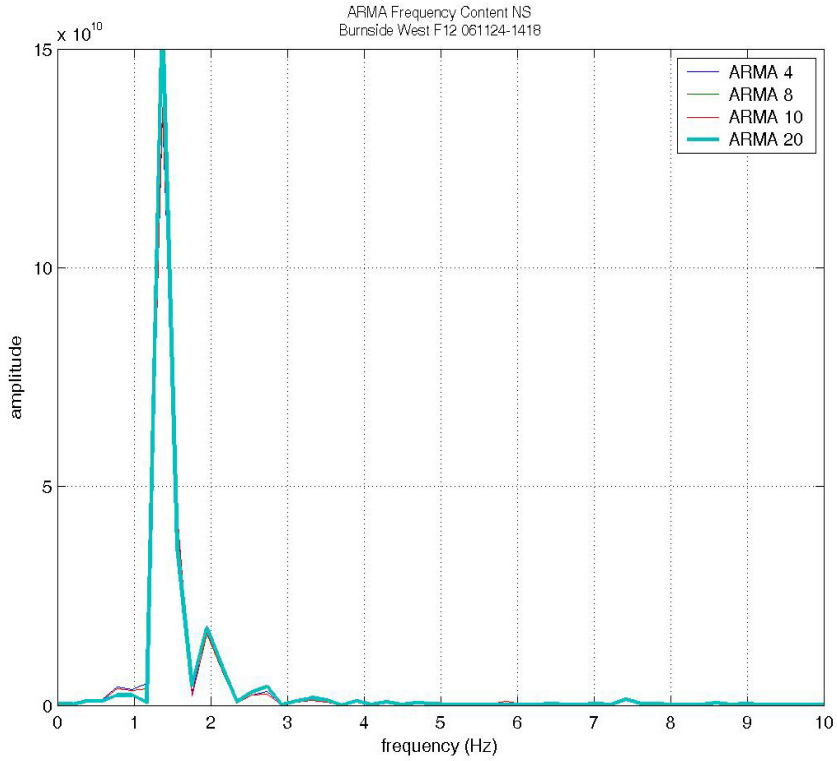

EW component

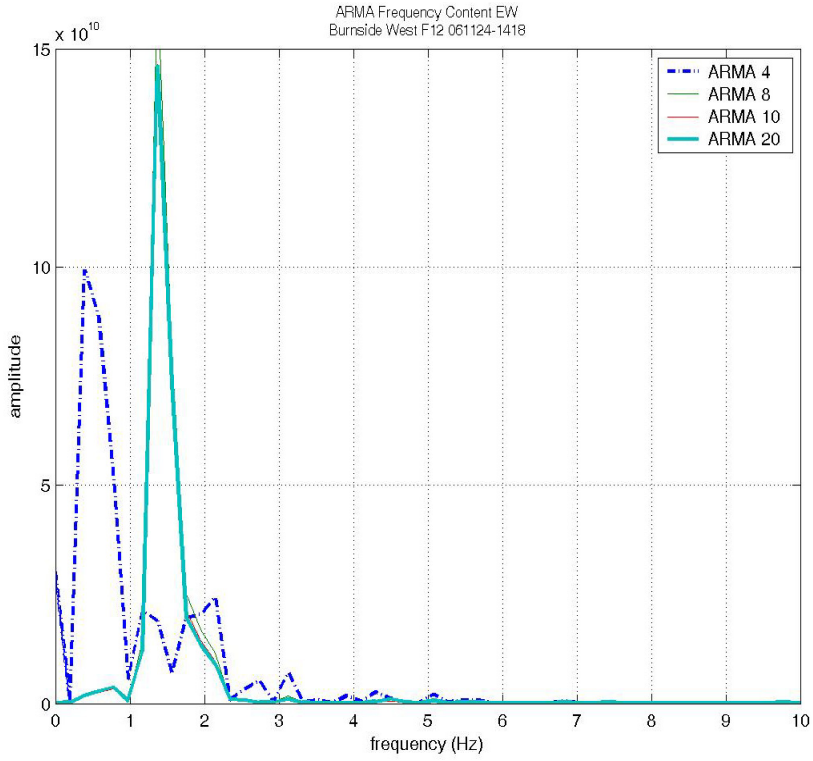

Location: Floor 9, Location 4

Direct Fourier Transformation Spectrum

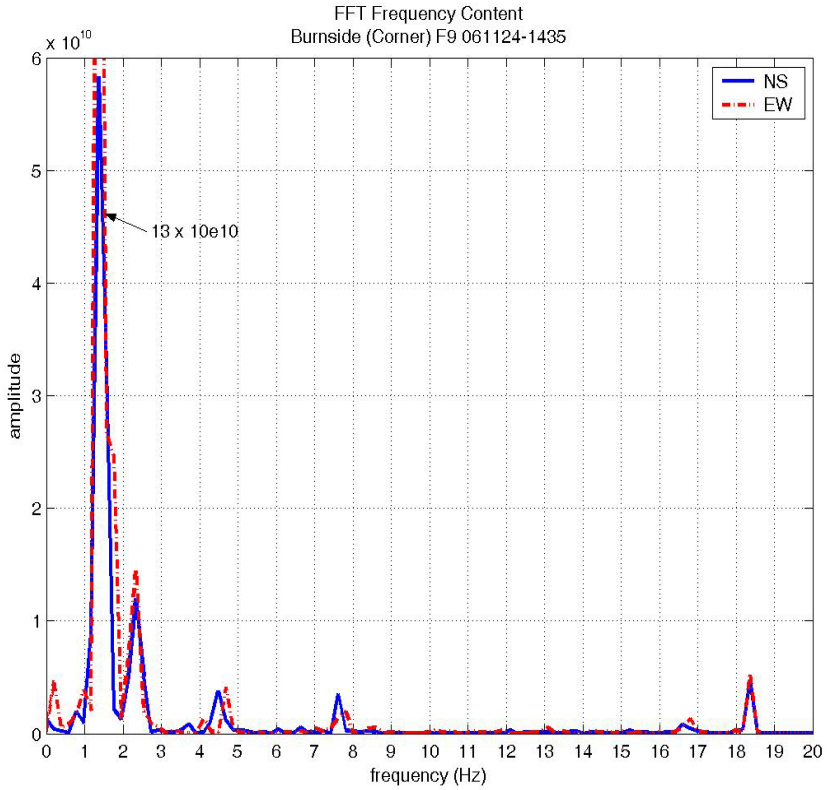

Power Spectrum Density Spectrum

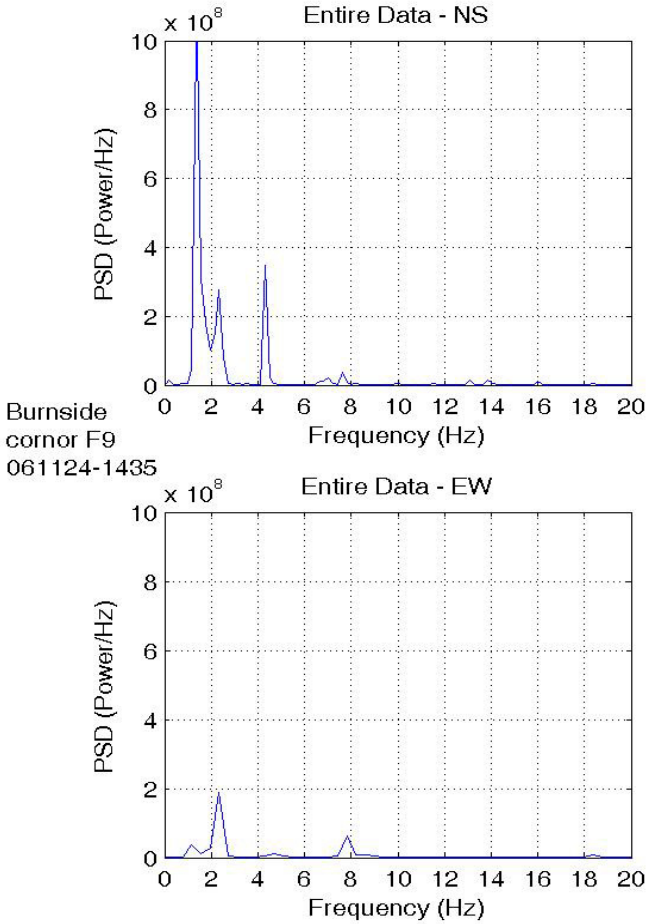

Auto-Regressive-Moving-Average Spectrum

NS component

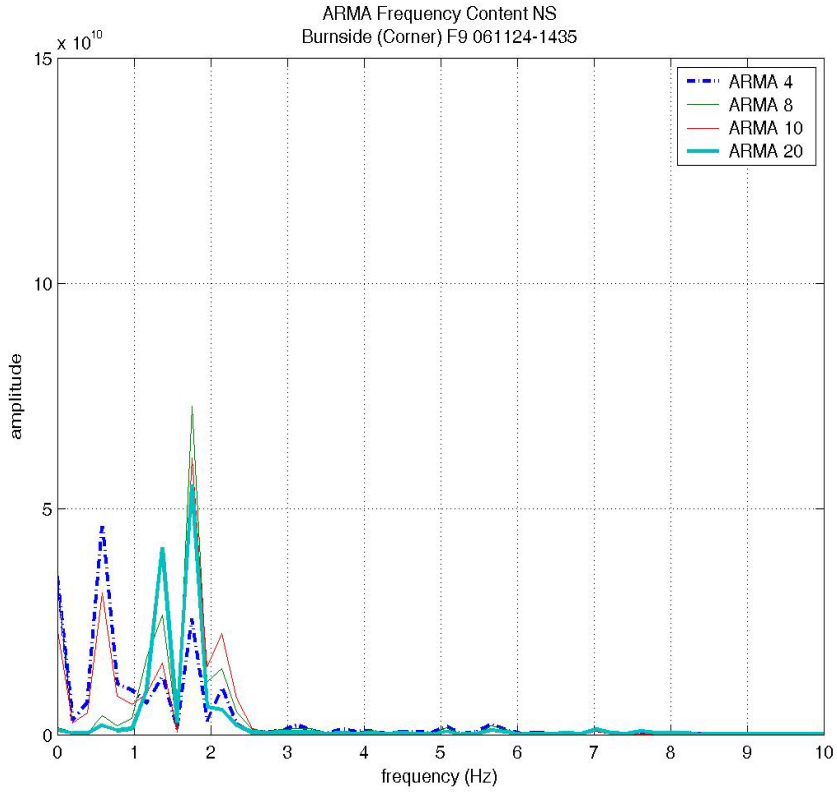

EW component

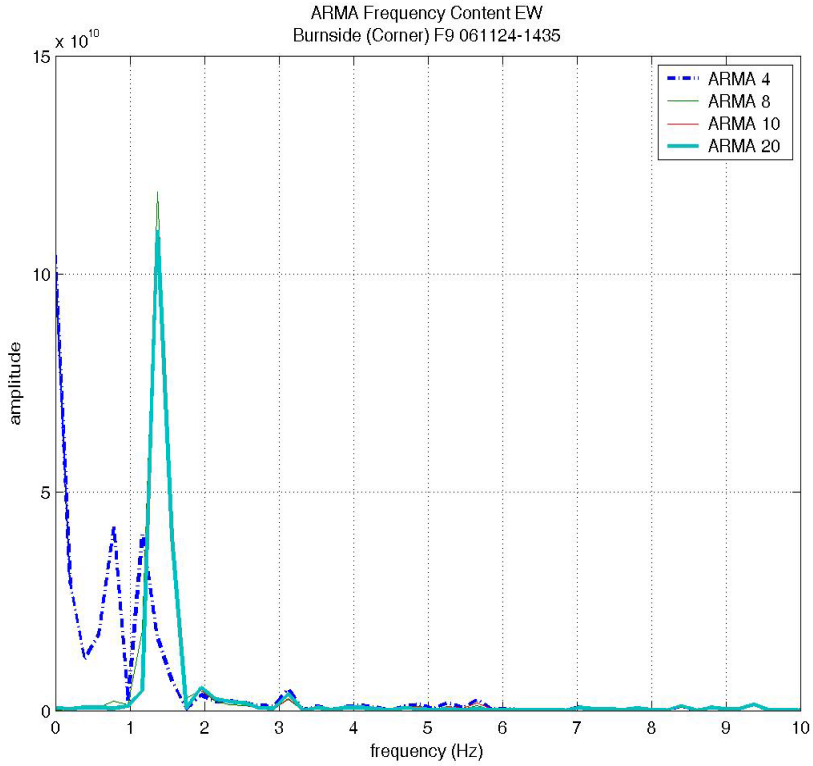

Location: Floor 12, Location 4

Direct Fourier Transformation Spectrum

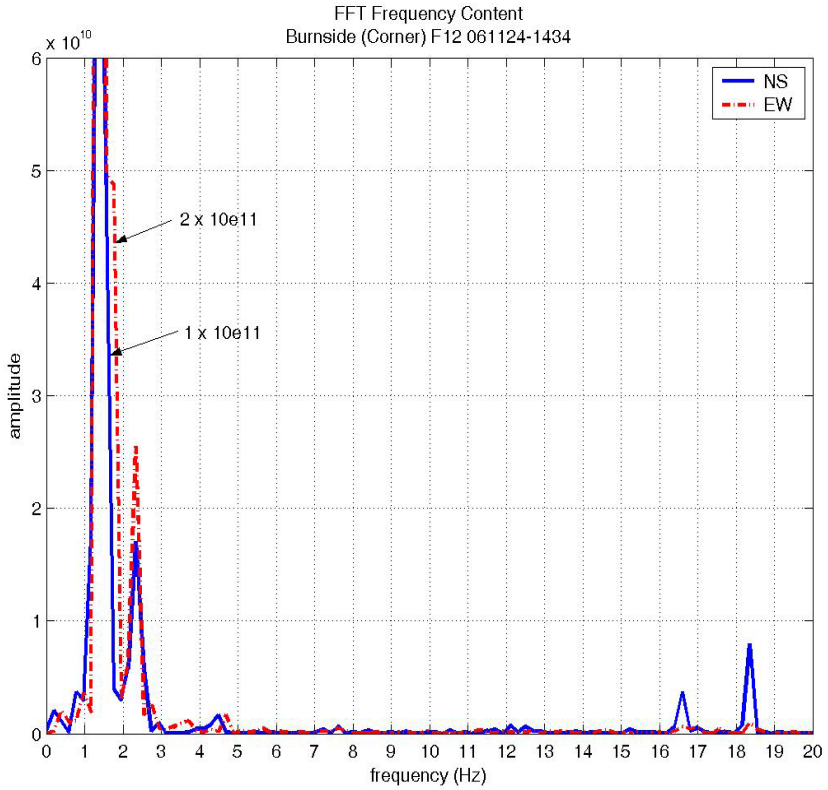

Power Spectrum Density Spectrum

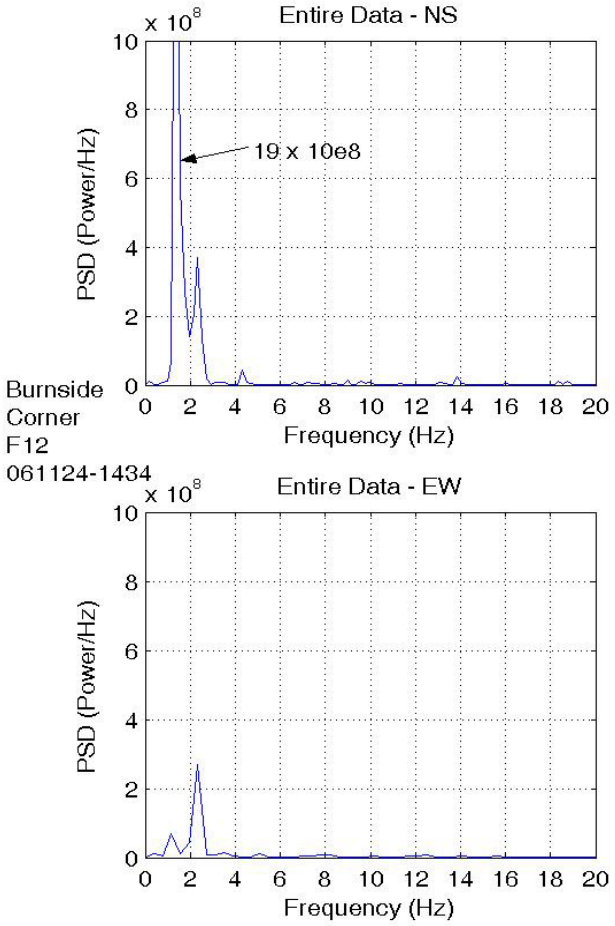

Auto-Regressive-Moving-Average Spectrum

NS component

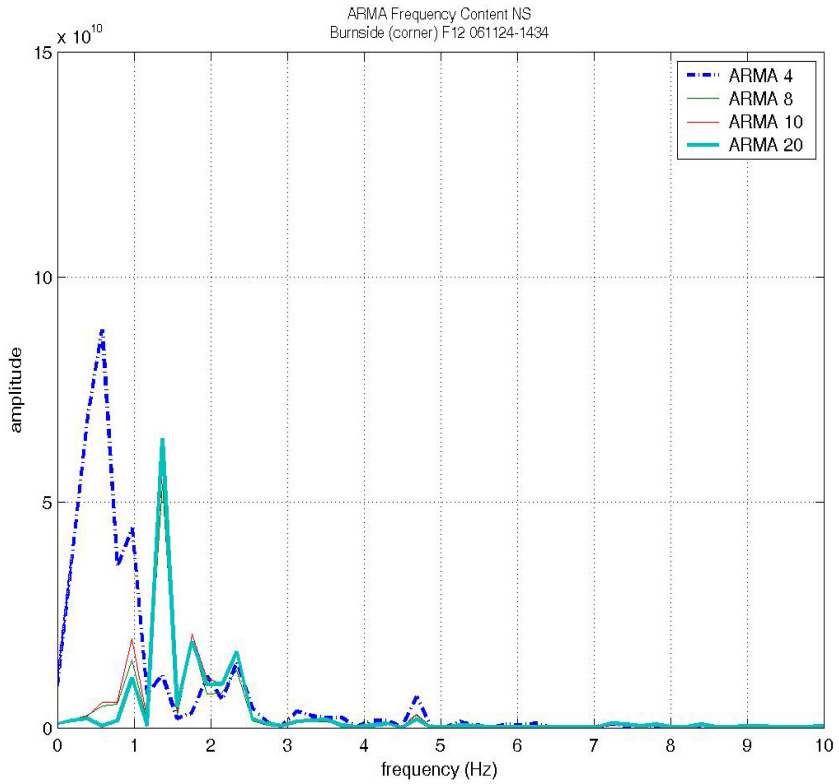

EW component

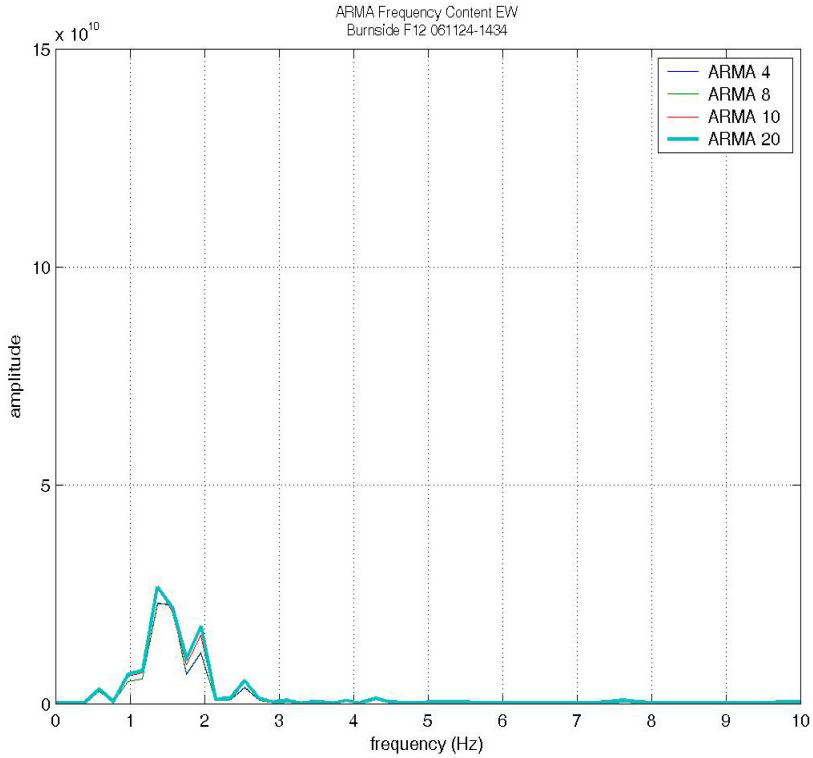

Date of Measurement: November 25, 2006
Building: Burnside Hall Building

Location: Floor 3, Location 1

Direct Fourier Transformation Spectrum

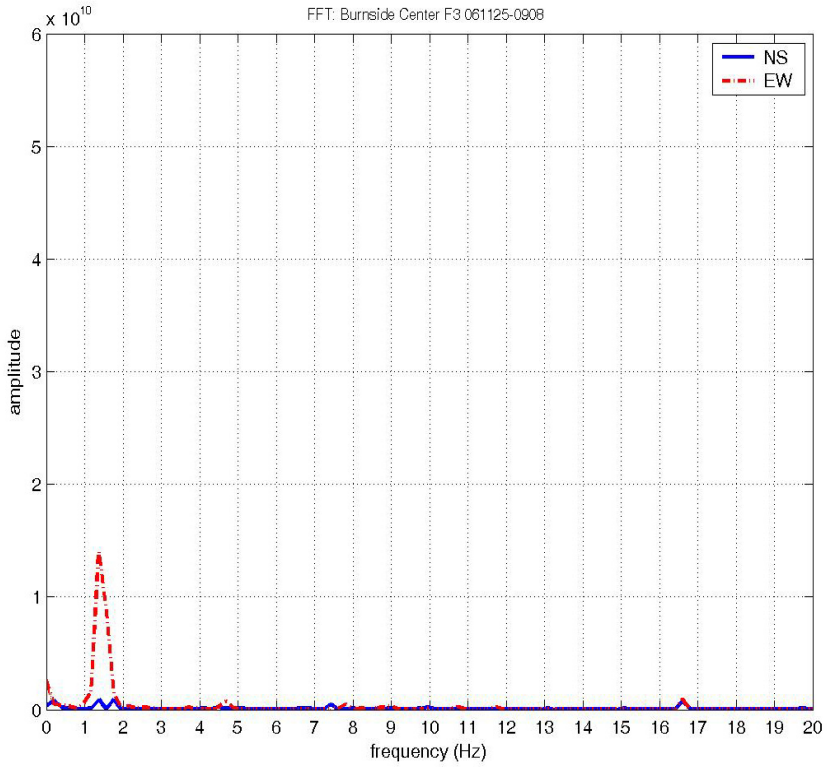

Power Spectrum Density Spectrum

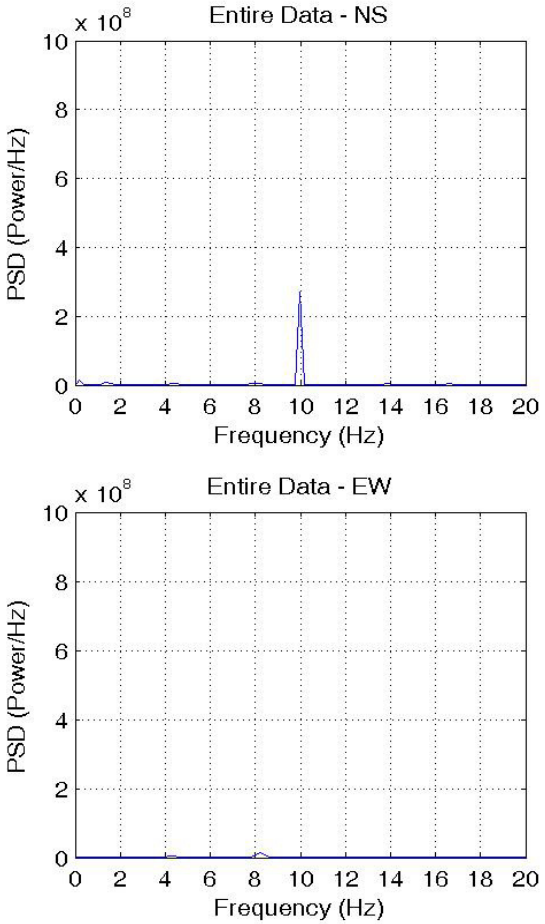

Auto-Regressive-Moving-Average Spectrum

NS component

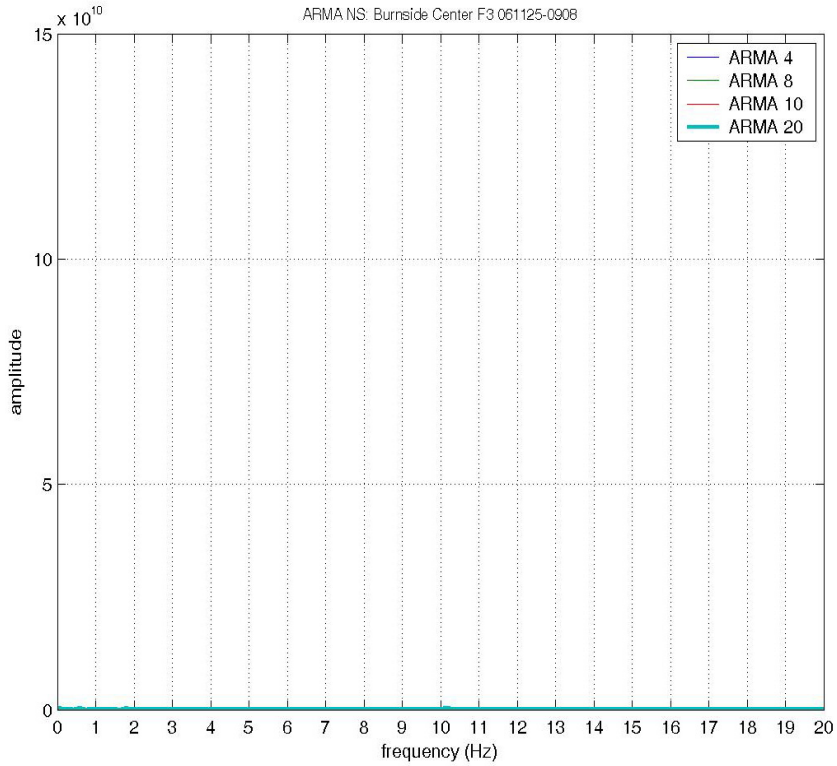

EW component

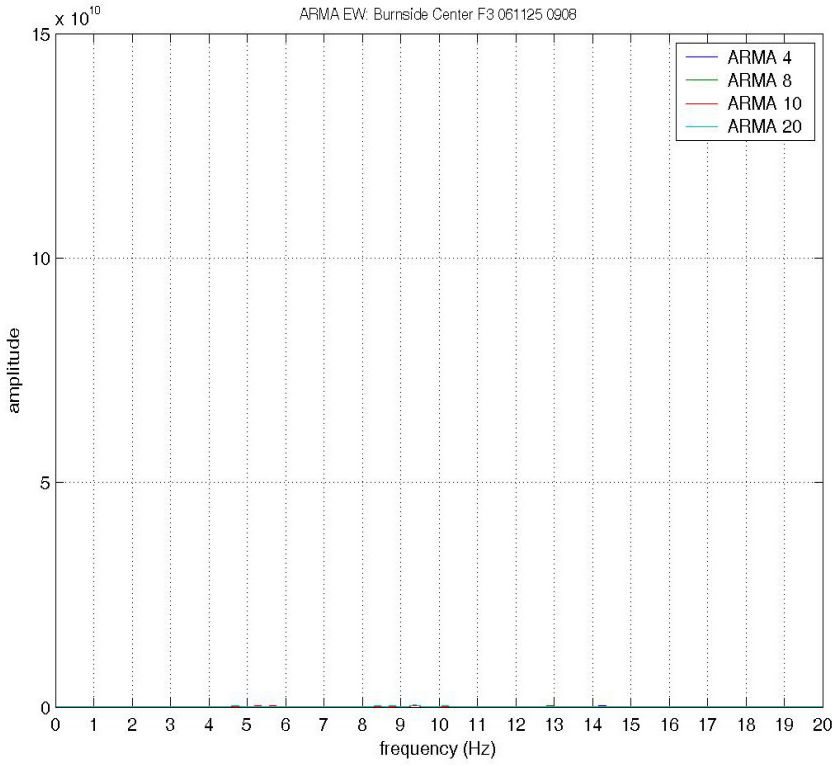

Location: Floor 6, Location 1

Direct Fourier Transformation Spectrum

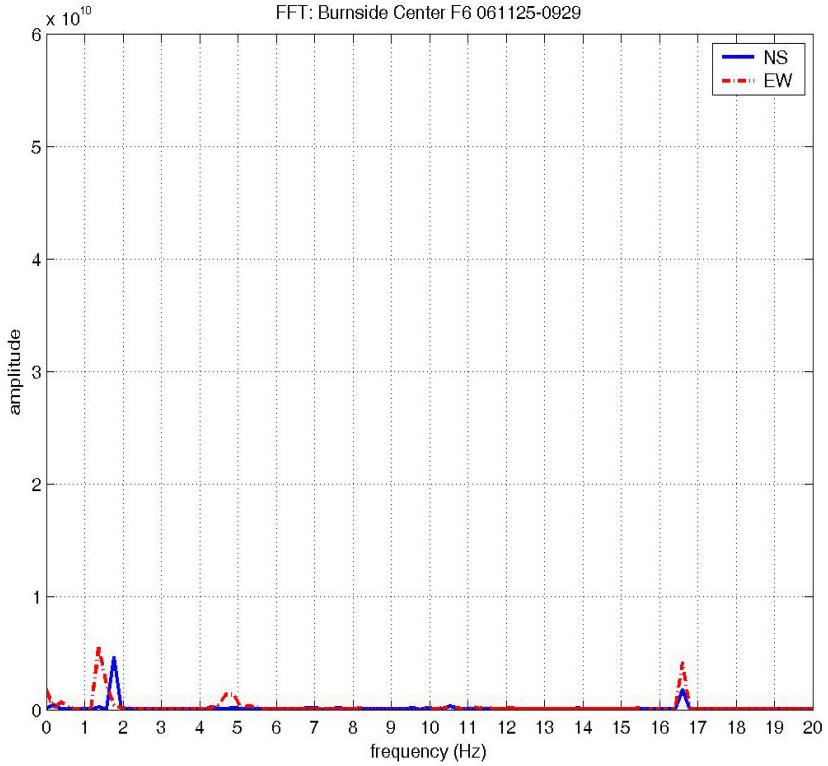

Power Spectrum Density Spectrum

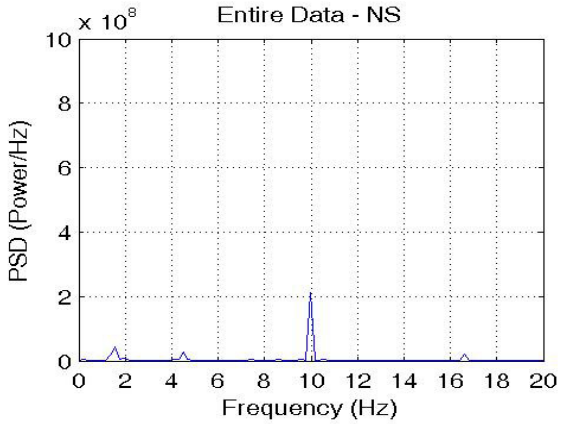

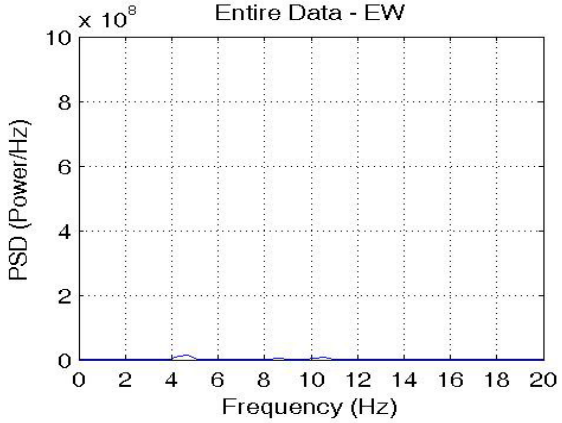

Auto-Regressive-Moving-Average Spectrum

NS component

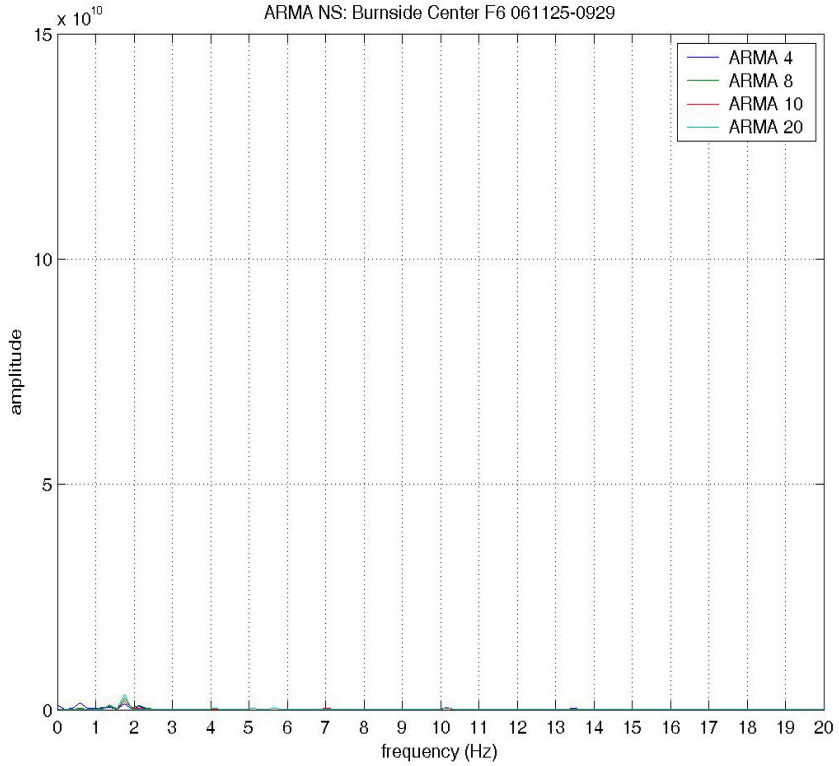

EW component

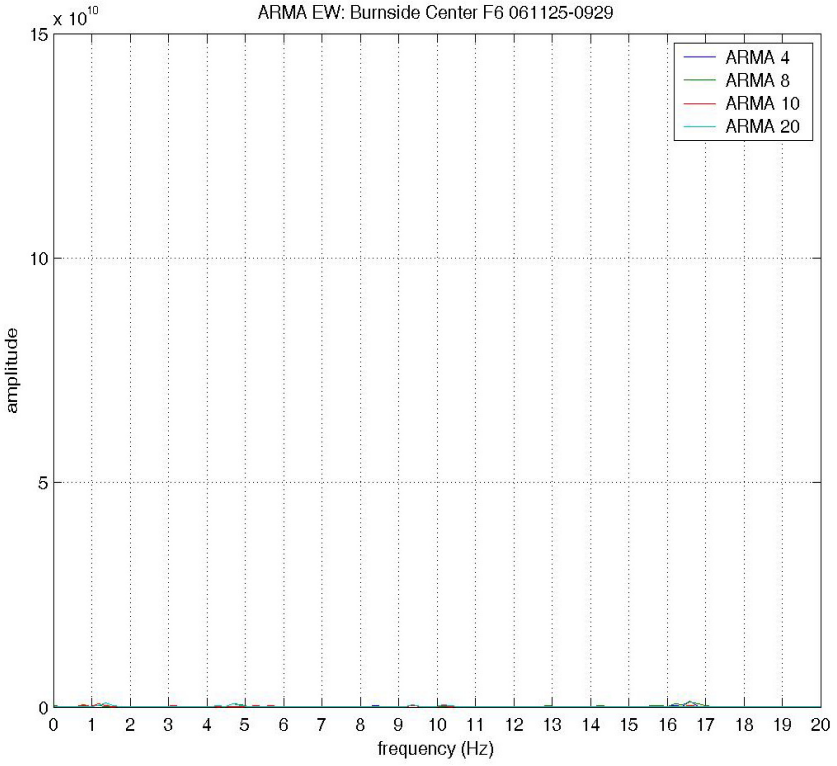

Location: Floor 9, Location 1

Direct Fourier Transformation Spectrum

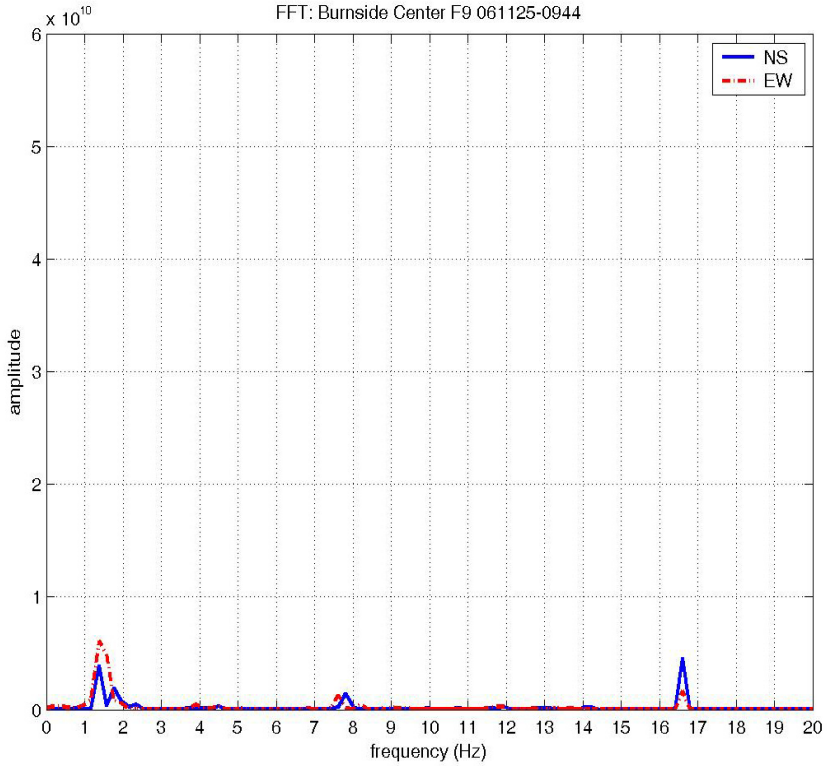

Power Spectrum Density Spectrum

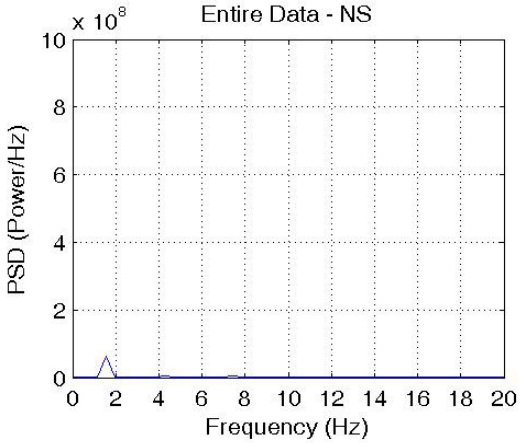

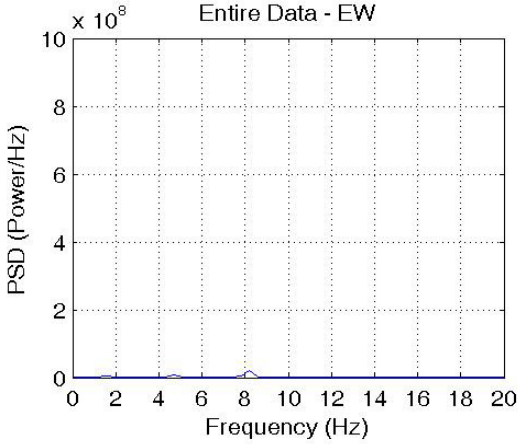

Auto-Regressive-Moving-Average Spectrum

NS component

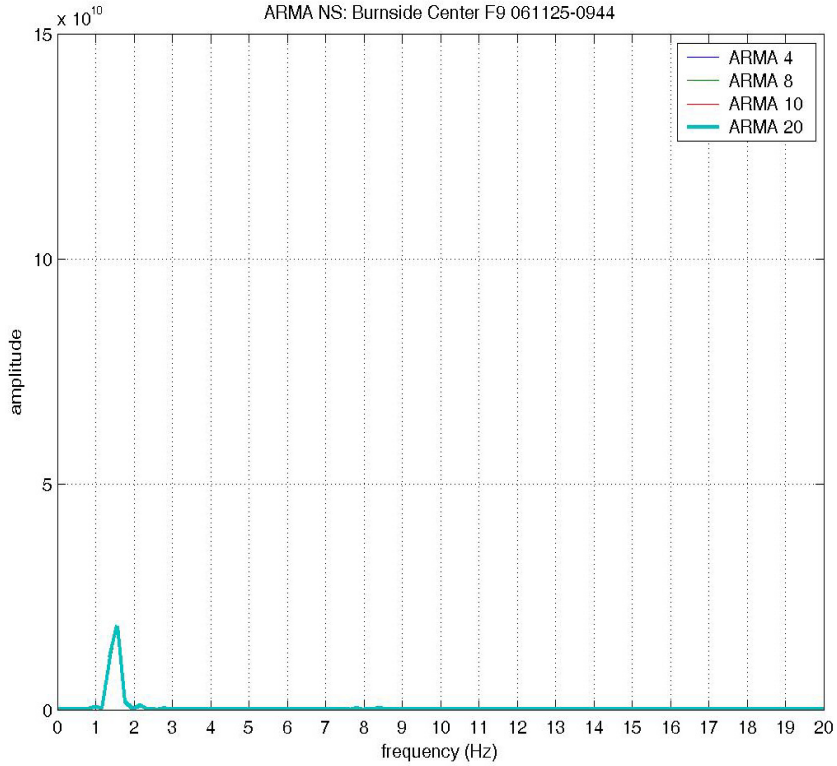

EW component

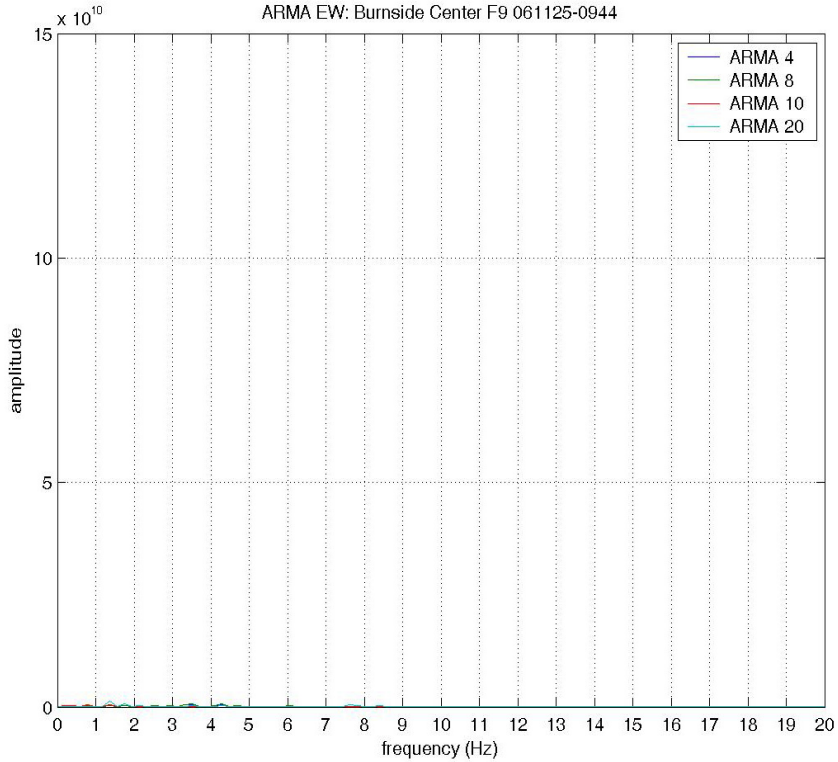

Location: Floor 12, Location 1

Direct Fourier Transformation Spectrum

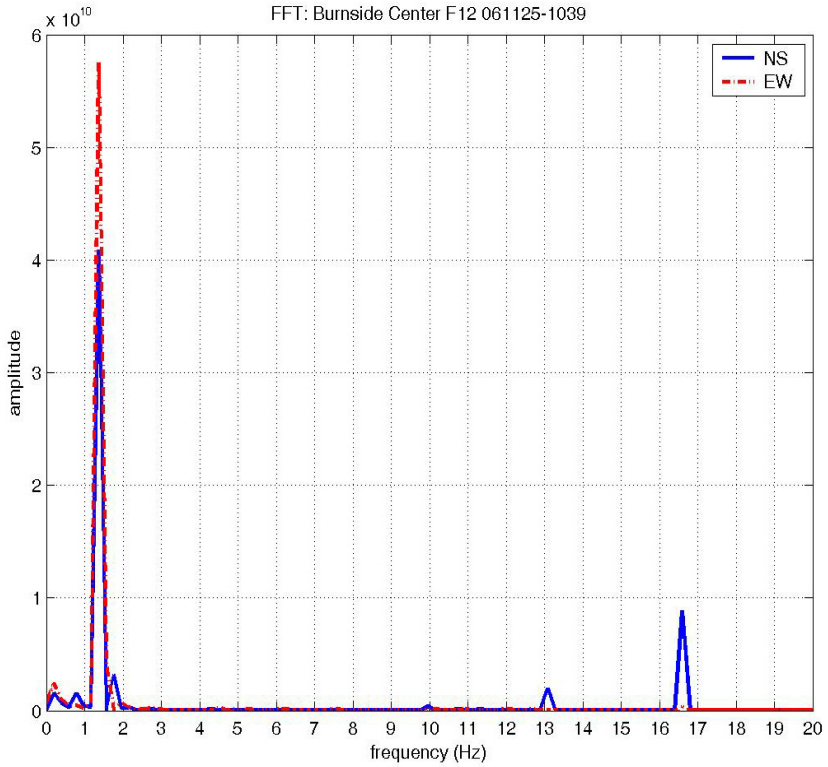

Power Spectrum Density Spectrum

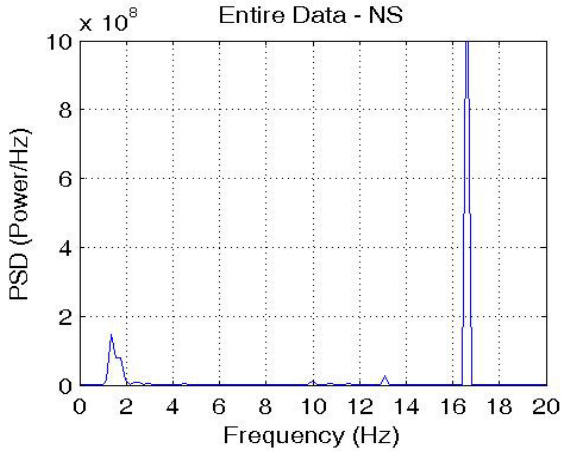

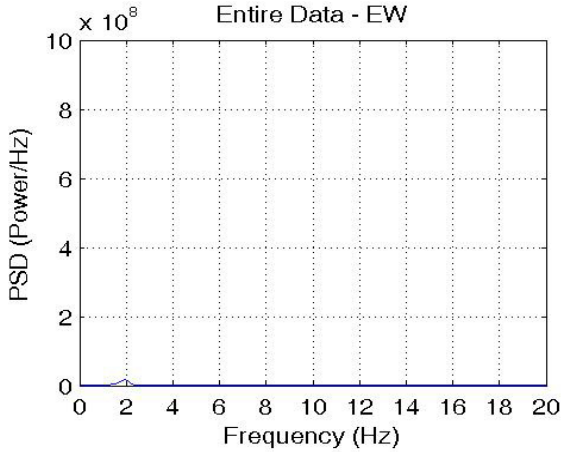

Auto-Regressive-Moving-Average Spectrum

NS component

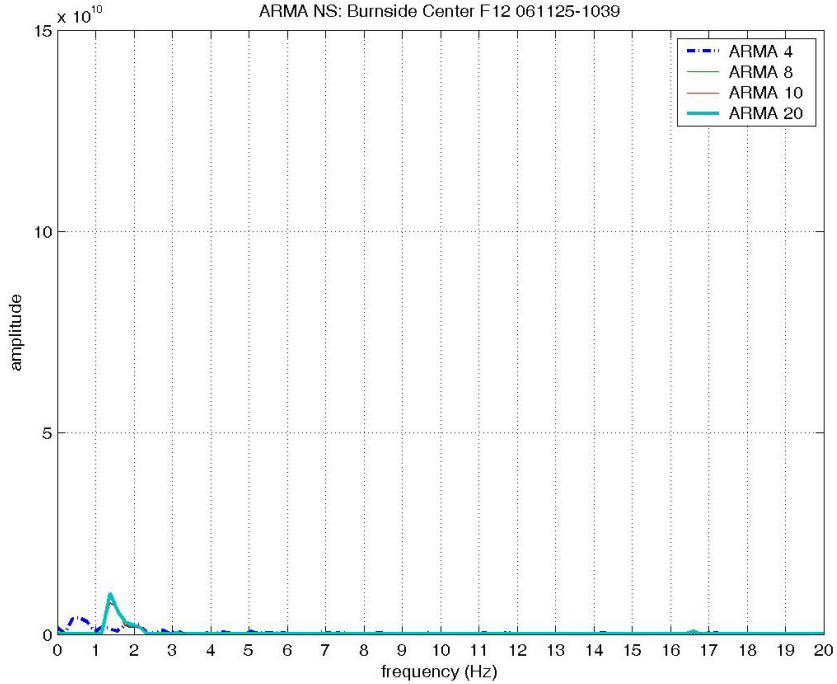

EW component

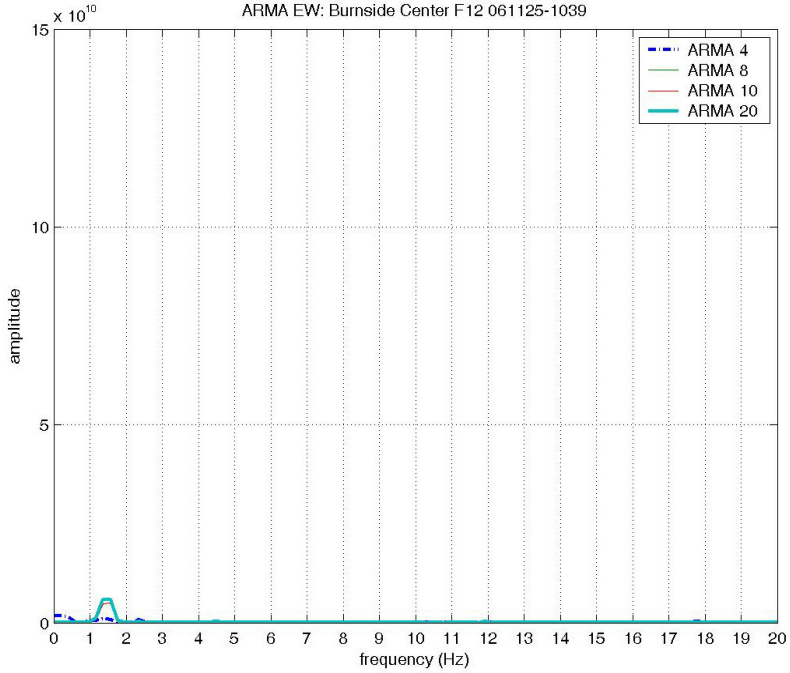

Location: Floor 3, Location 3

Direct Fourier Transformation Spectrum

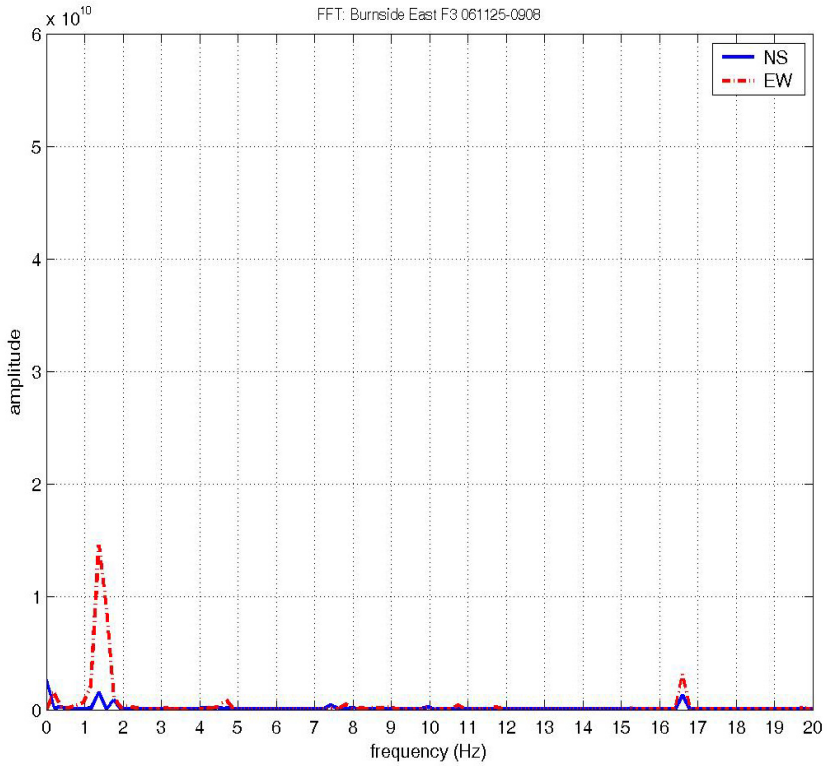

Power Spectrum Density Spectrum

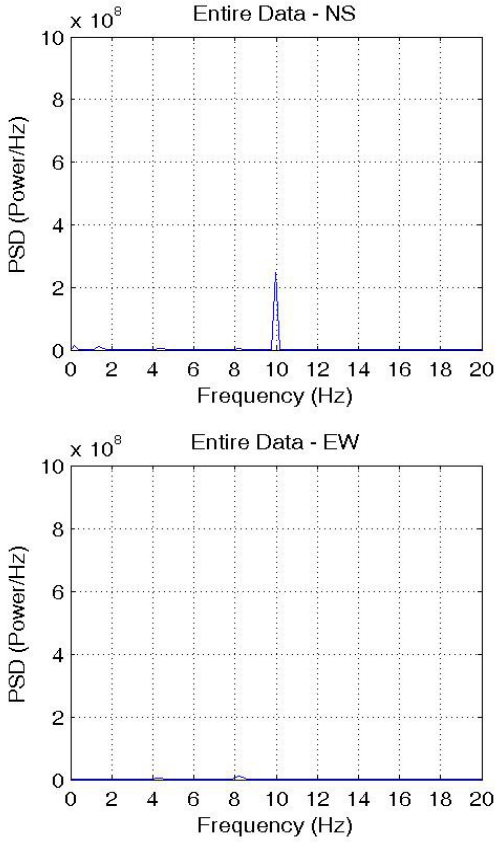

Auto-Regressive-Moving-Average Spectrum

NS component

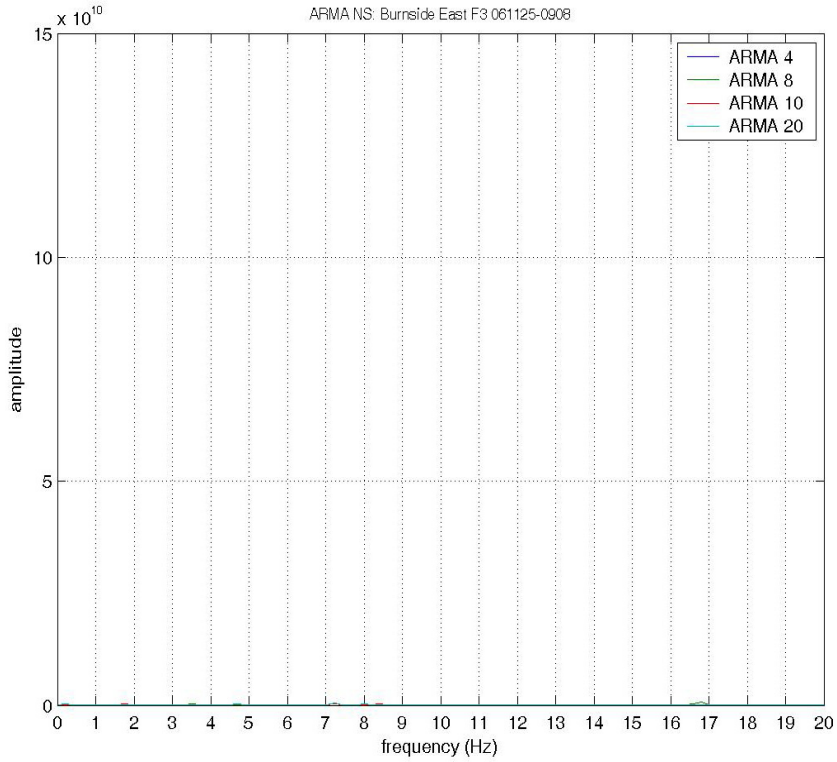

EW component

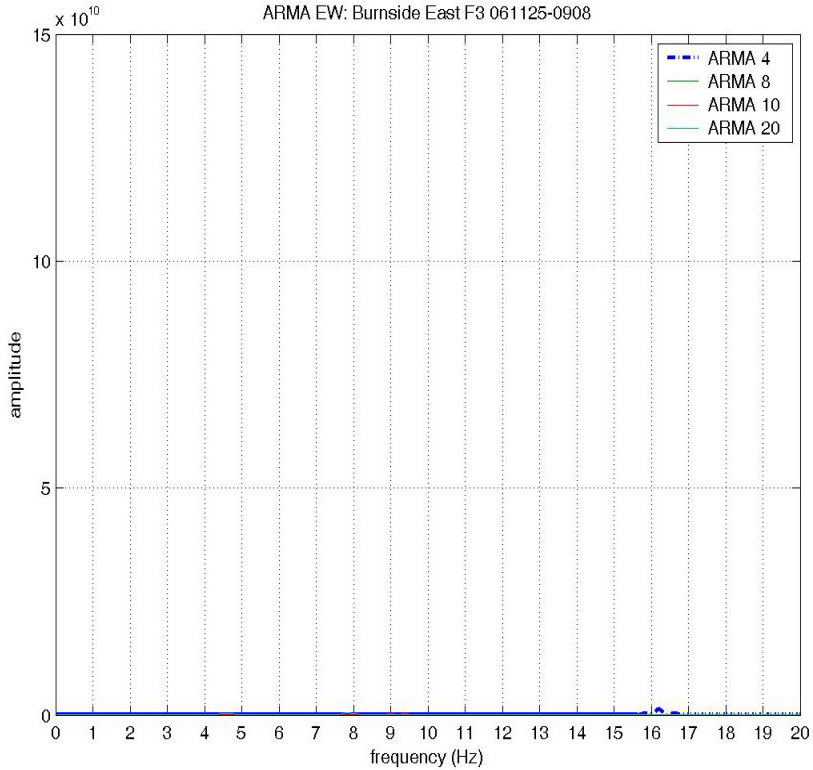

Location: Floor 6, Location 3

Direct Fourier Transformation Spectrum

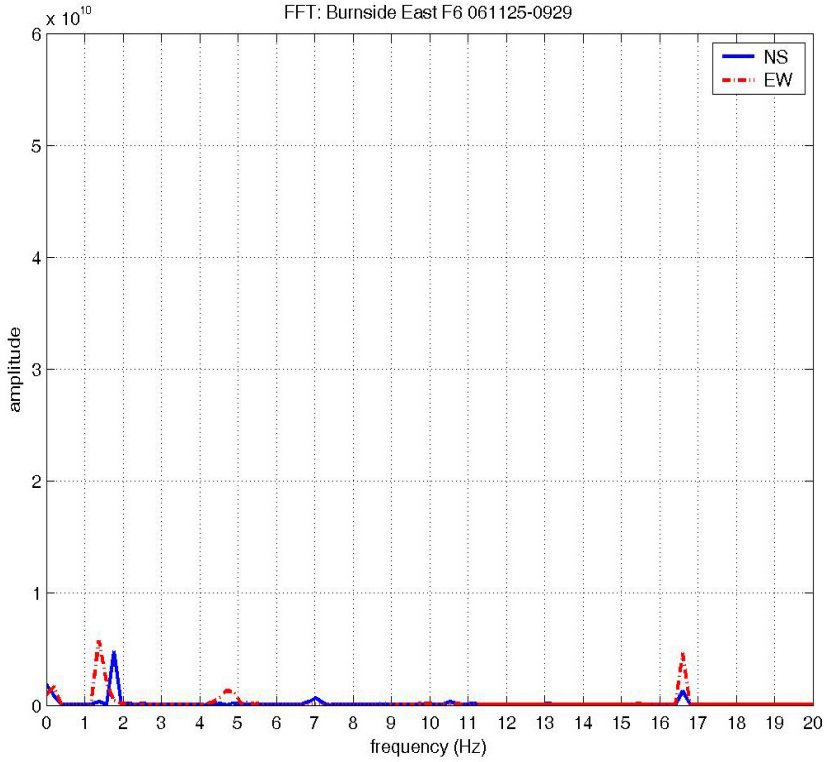

Power Spectrum Density Spectrum

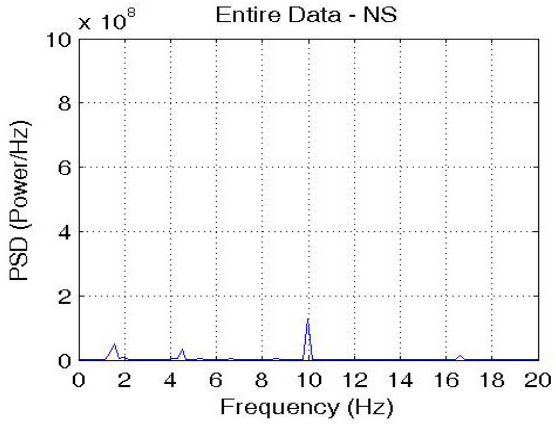

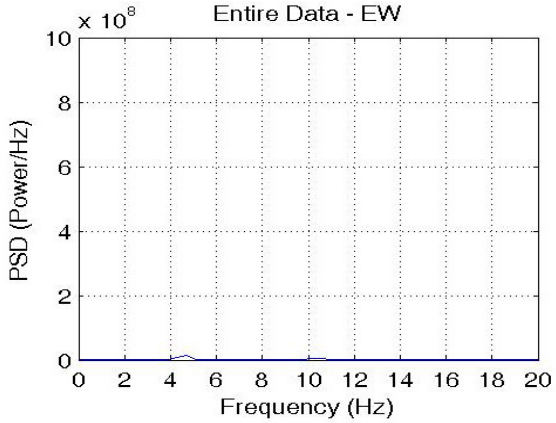

Auto-Regressive-Moving-Average Spectrum

NS component

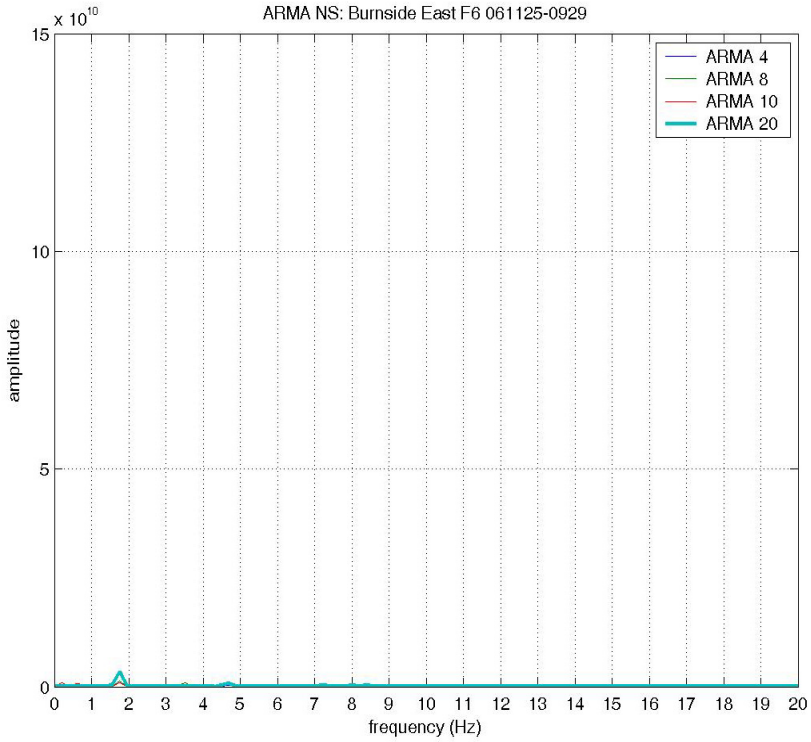

EW component

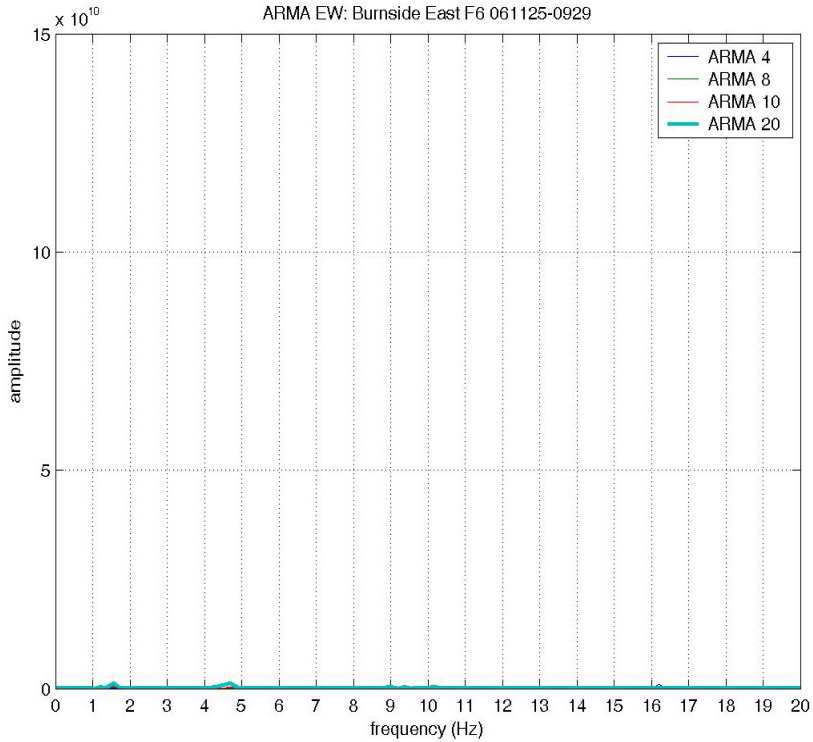

Location: Floor 9, Location 3

Direct Fourier Transformation Spectrum

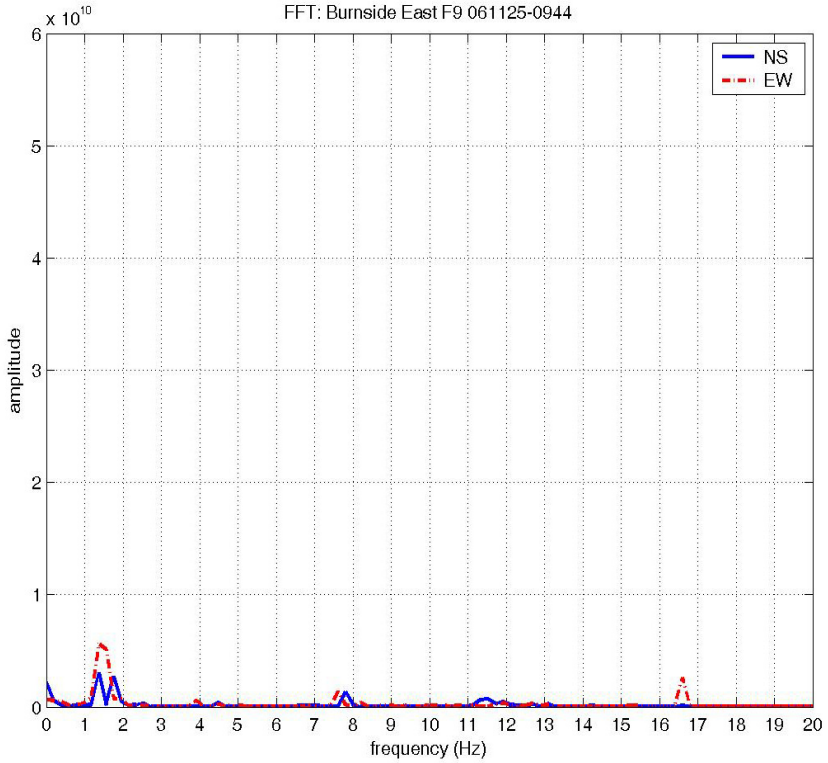

Power Spectrum Density Spectrum

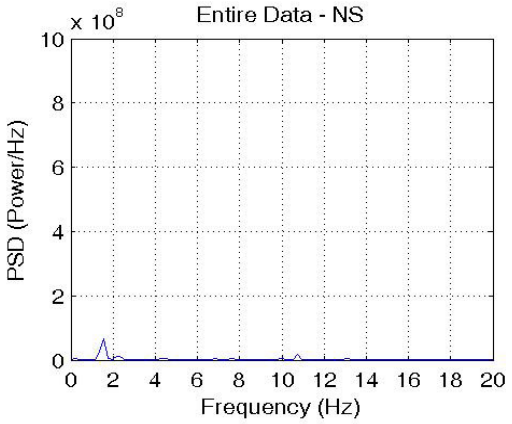

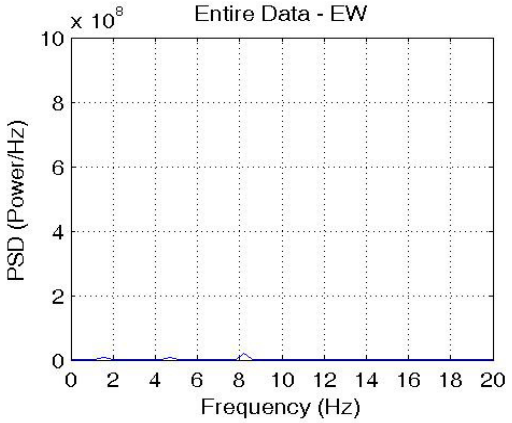

Auto-Regressive-Moving-Average Spectrum

NS component

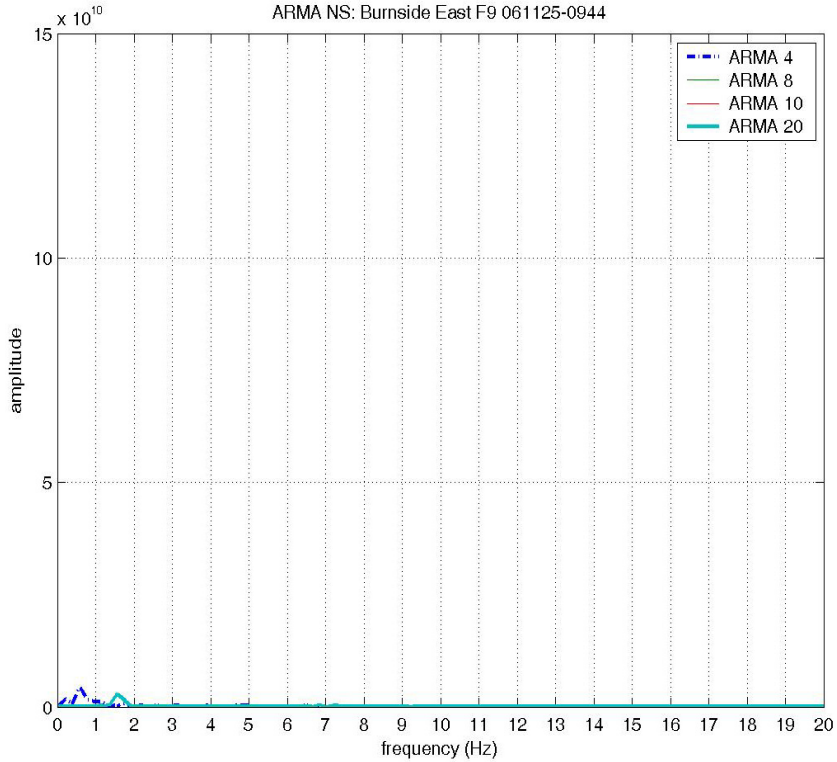

EW component

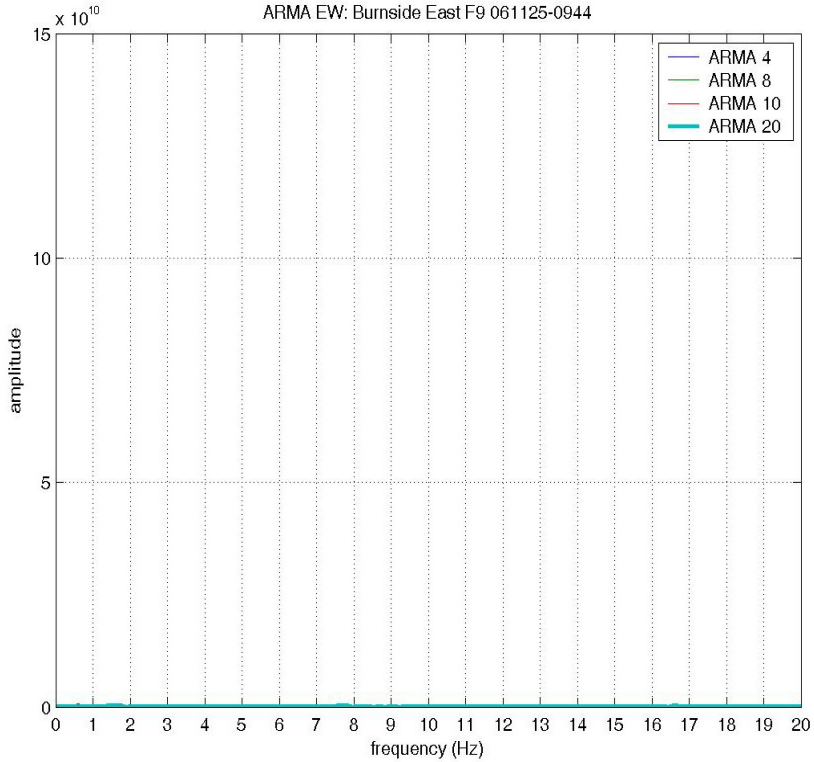

Location: Floor 12, Location 3

Direct Fourier Transformation Spectrum

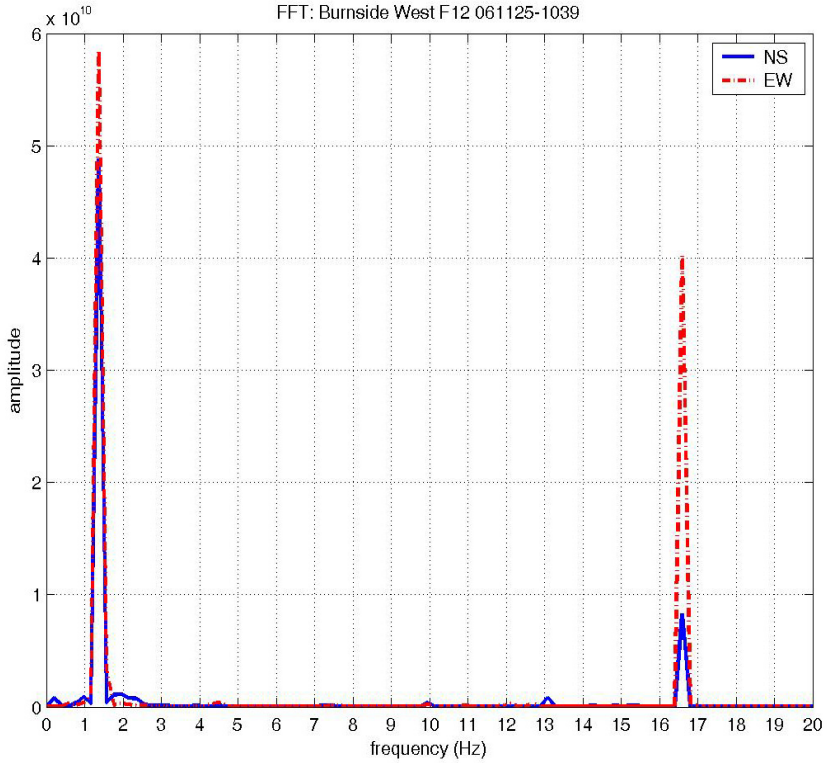

Power Spectrum Density Spectrum

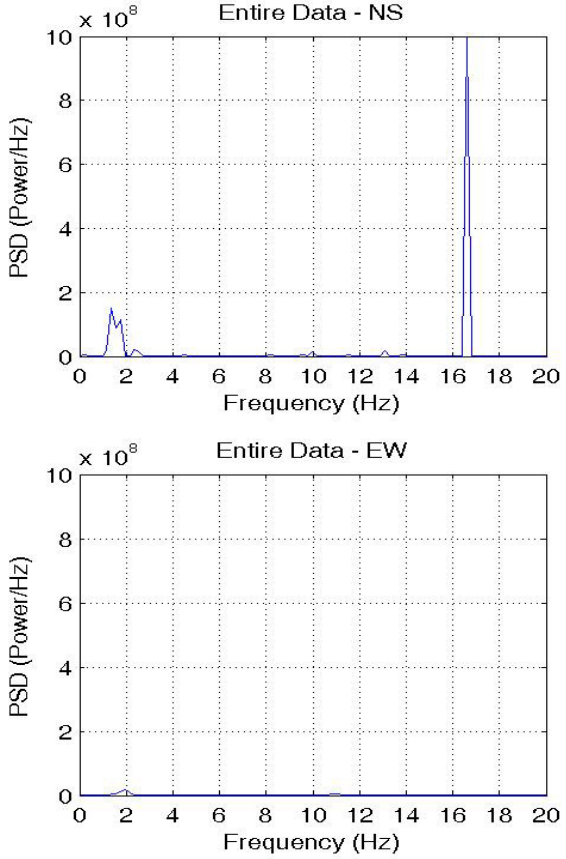

Auto-Regressive-Moving-Average Spectrum

NS component

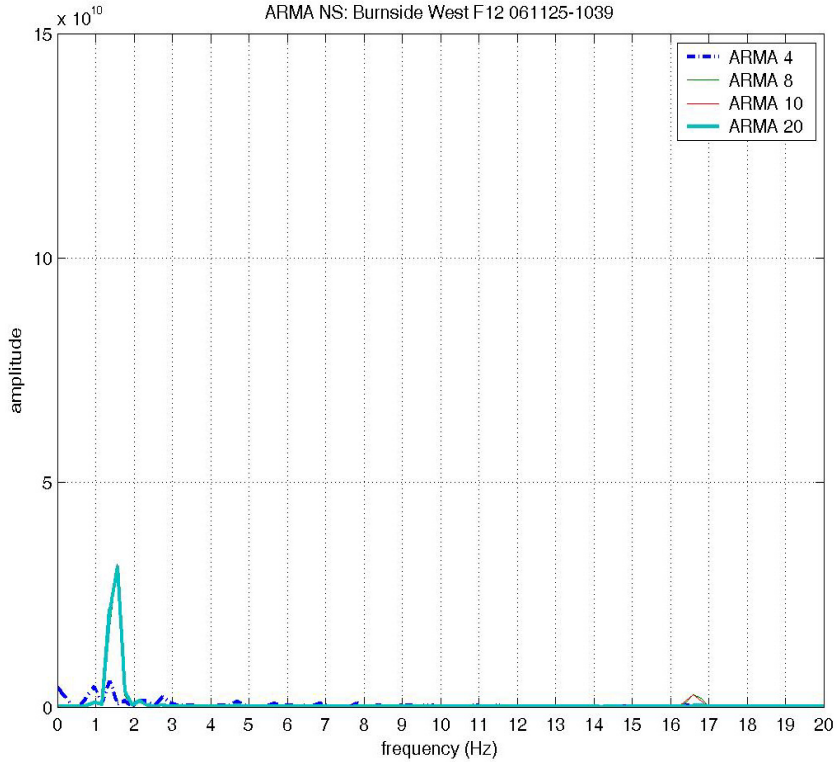

EW component

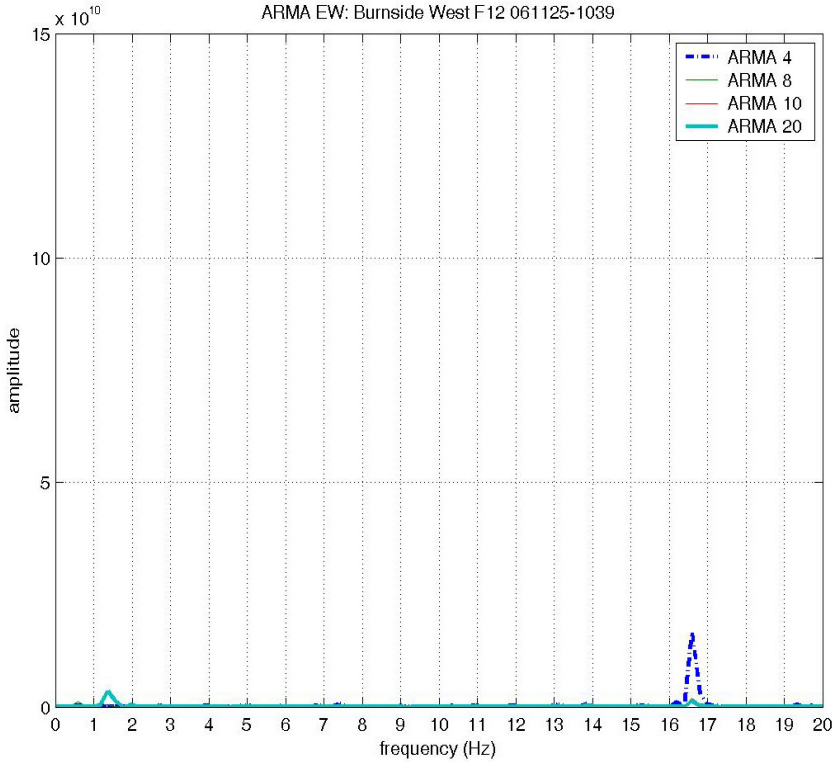

Location: Floor 9, Location 4

Direct Fourier Transformation Spectrum

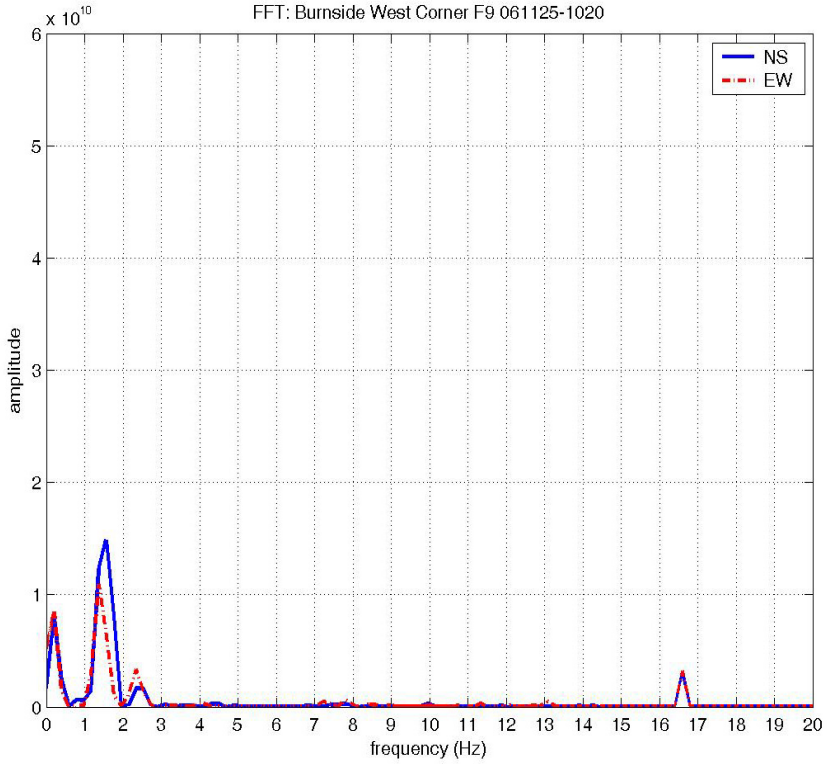

Power Spectrum Density Spectrum

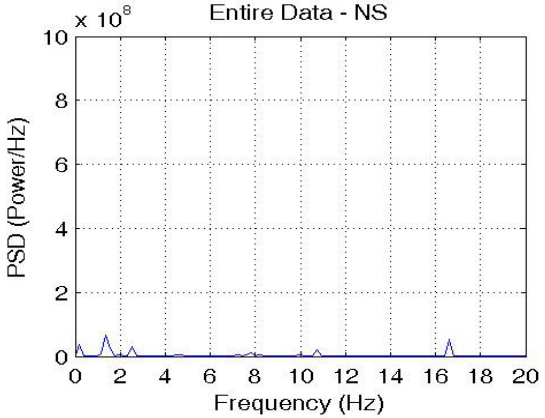

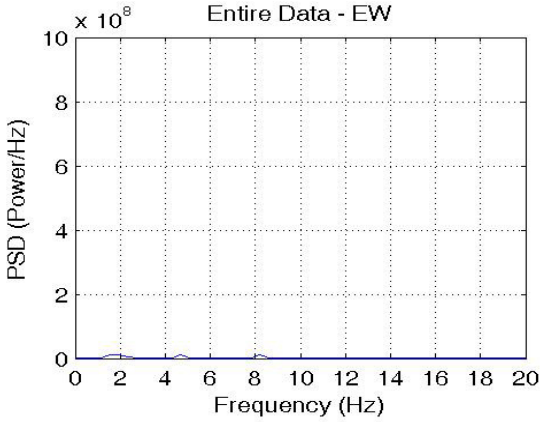

Auto-Regressive-Moving-Average Spectrum

NS component

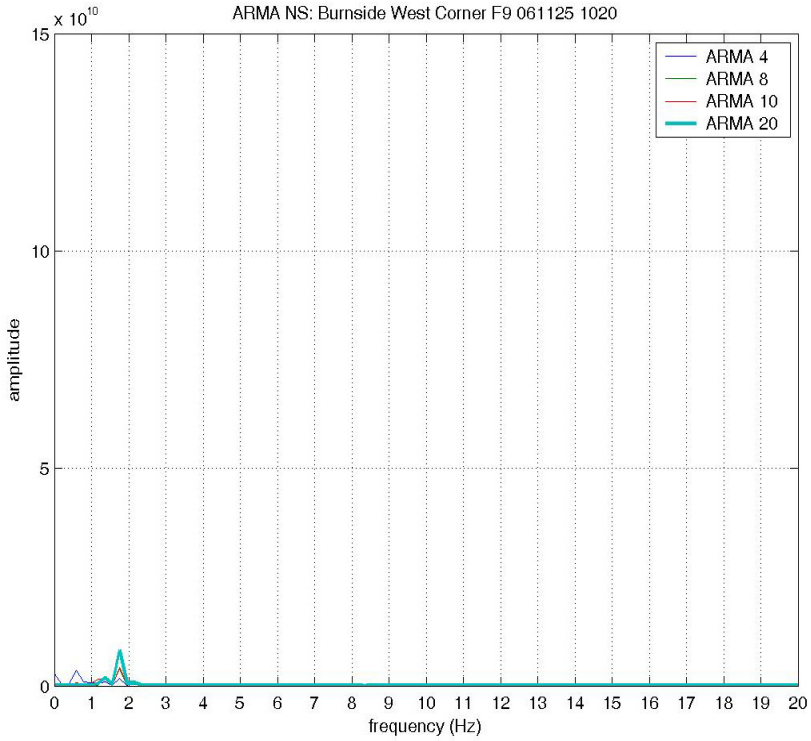

EW component

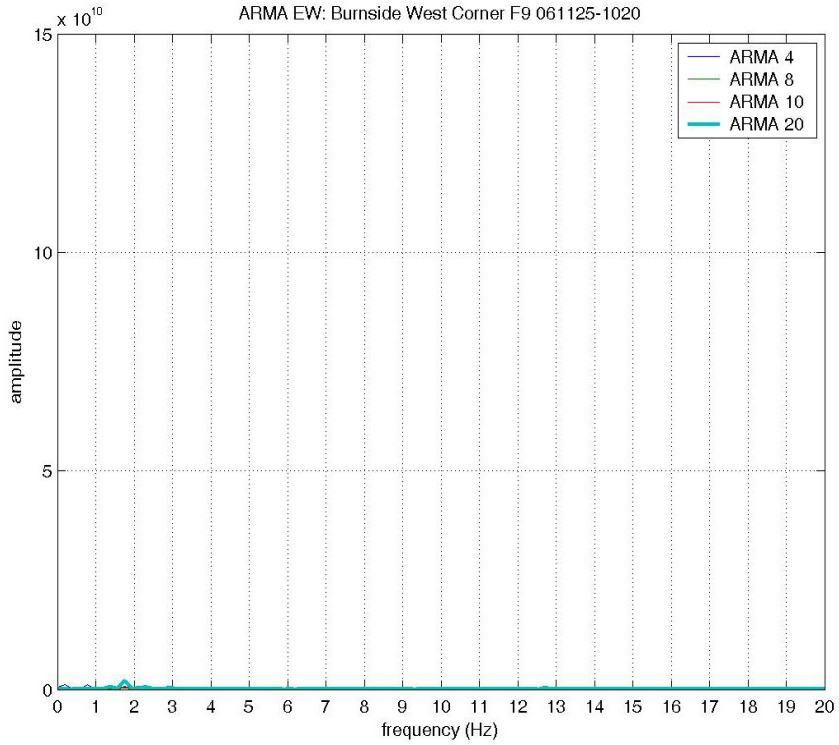

Location: Floor 12, Location 4

Direct Fourier Transformation Spectrum

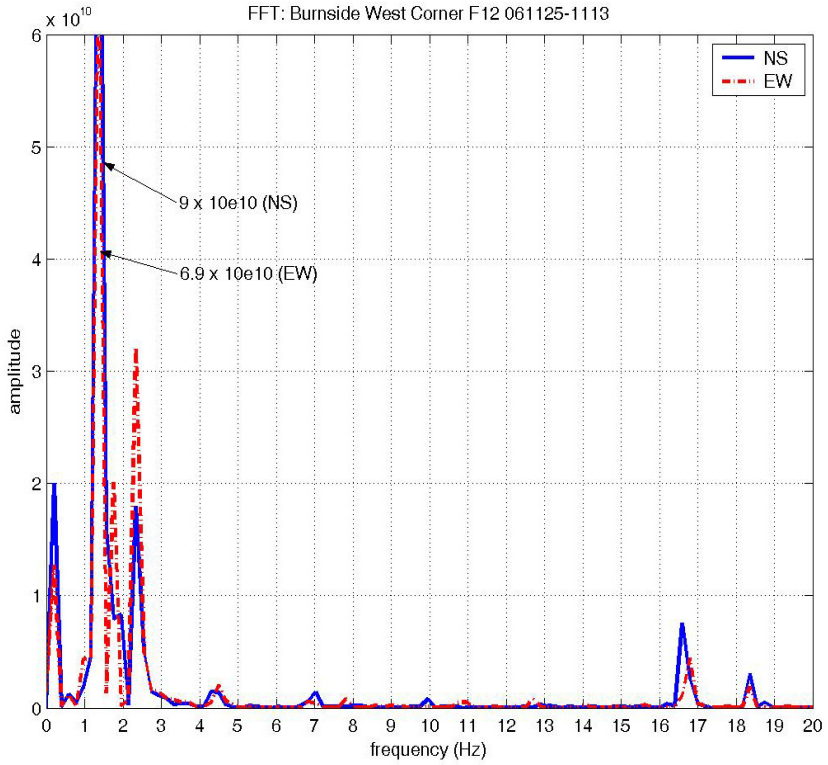

Power Spectrum Density Spectrum

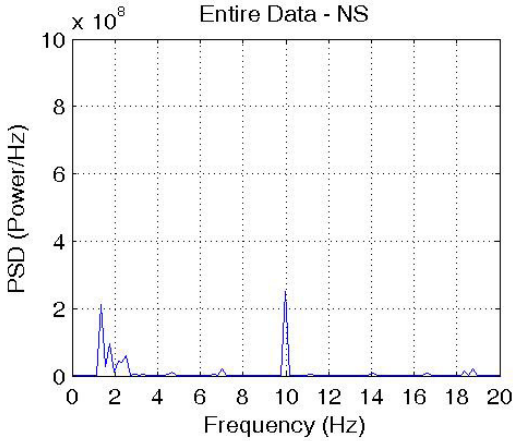

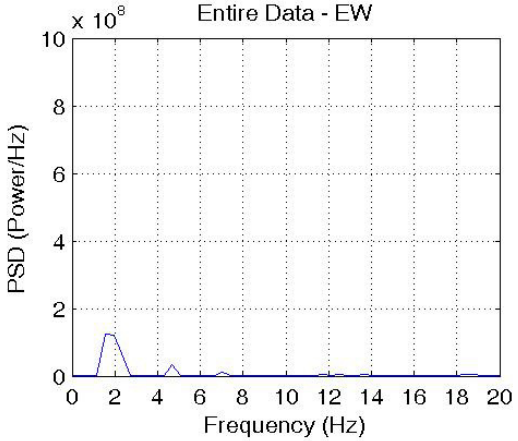

Auto-Regressive-Moving-Average Spectrum

NS component

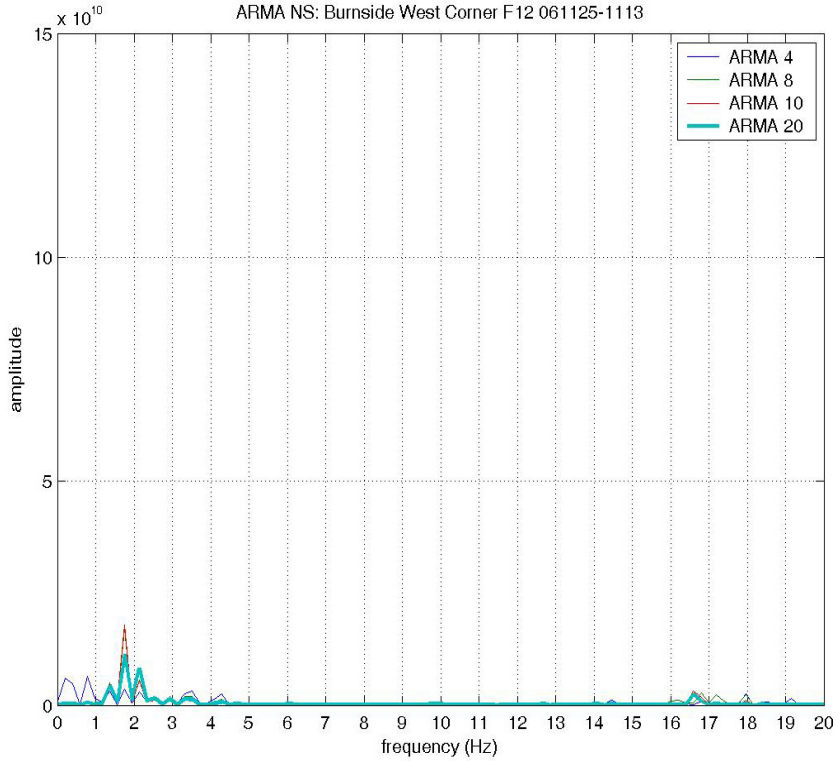

EW component

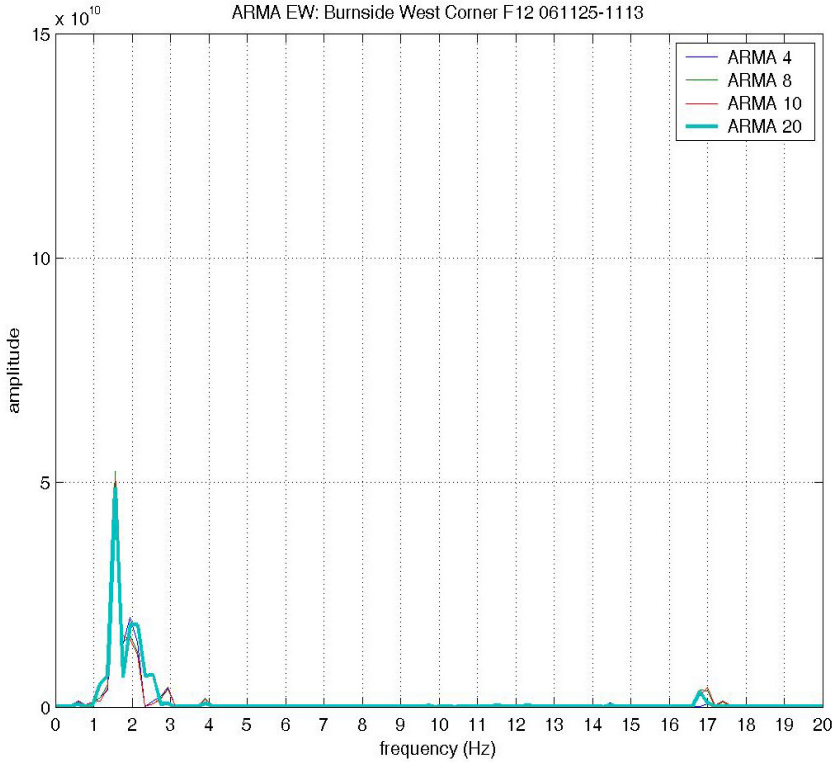

Location: Floor 9, Location 5

Direct Fourier Transformation Spectrum

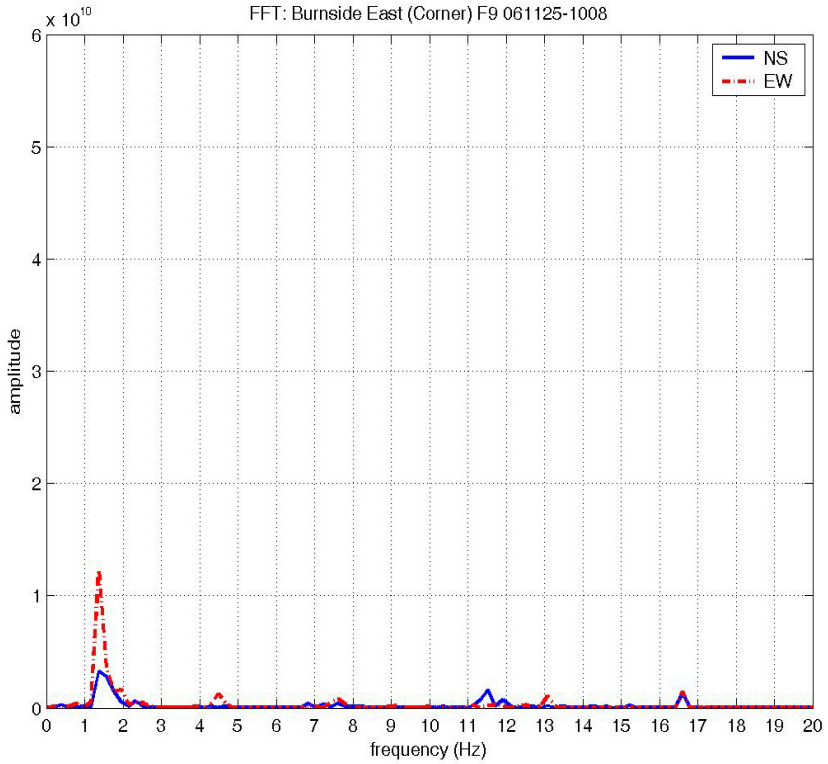

Power Spectrum Density Spectrum

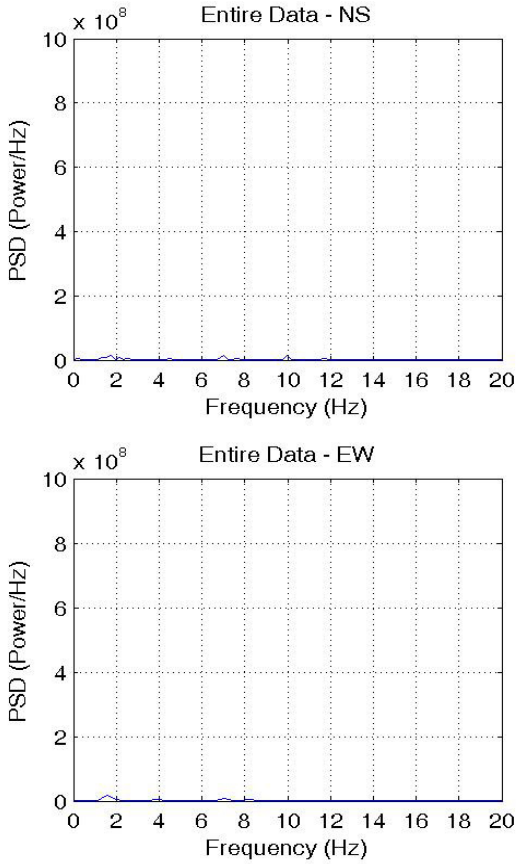

Auto-Regressive-Moving-Average Spectrum

NS component

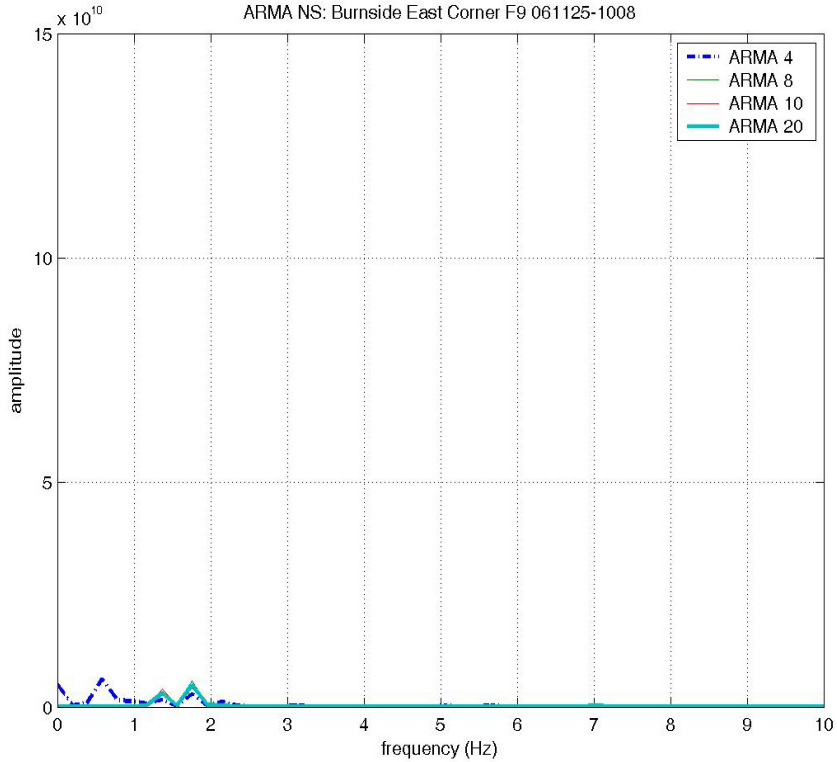

EW component

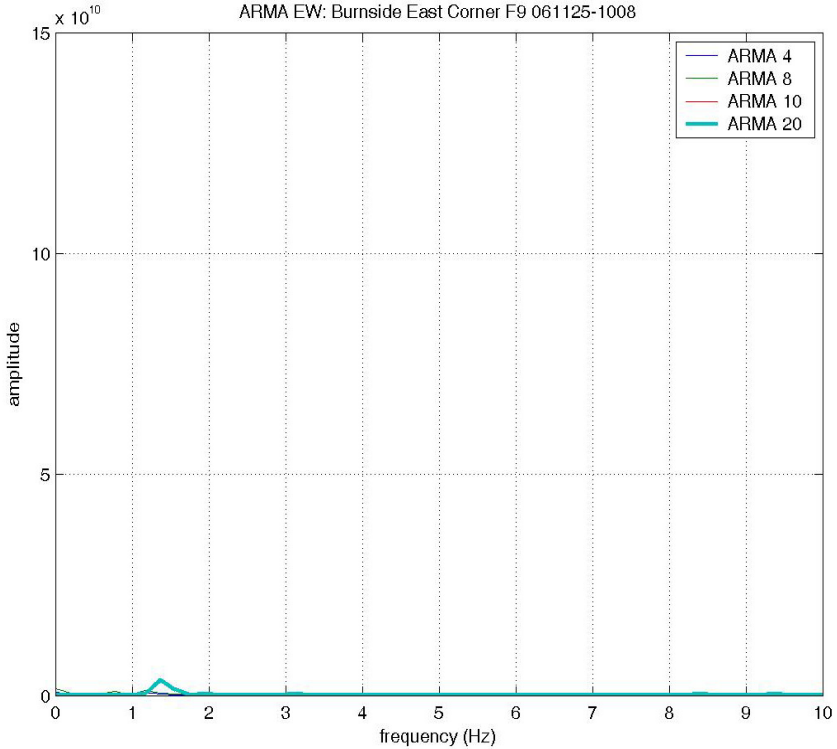

Location: Floor 12, Location 5

Direct Fourier Transformation Spectrum

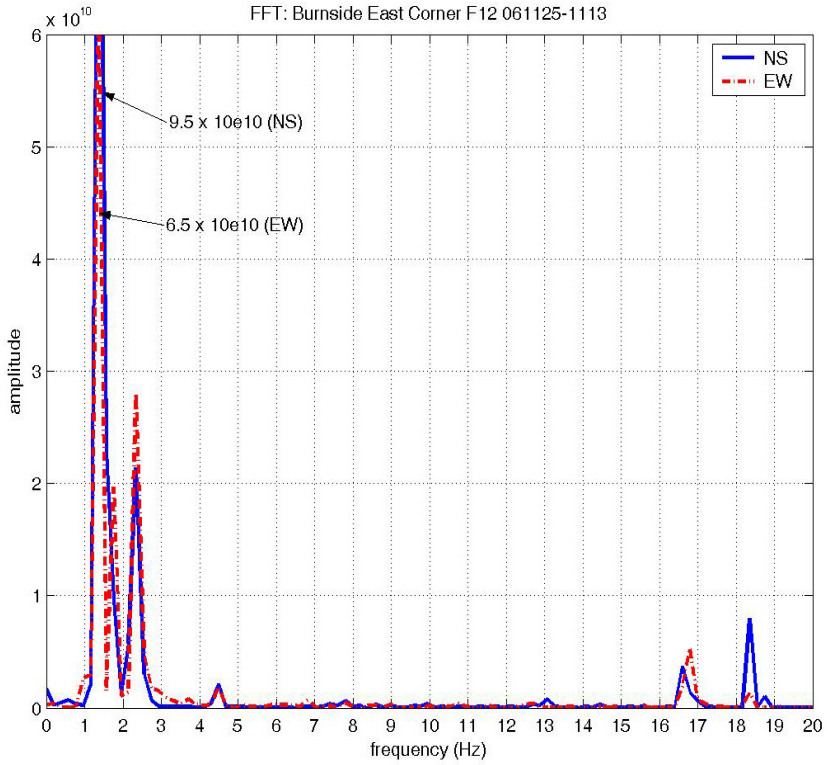

Power Spectrum Density Spectrum

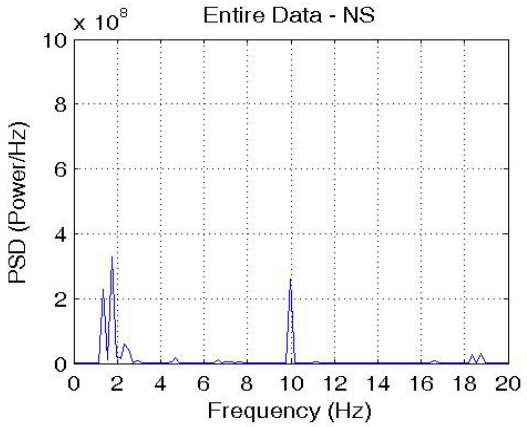

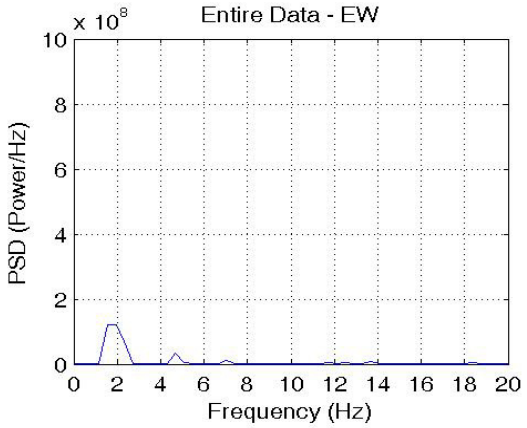

Auto-Regressive-Moving-Average Spectrum

NS component

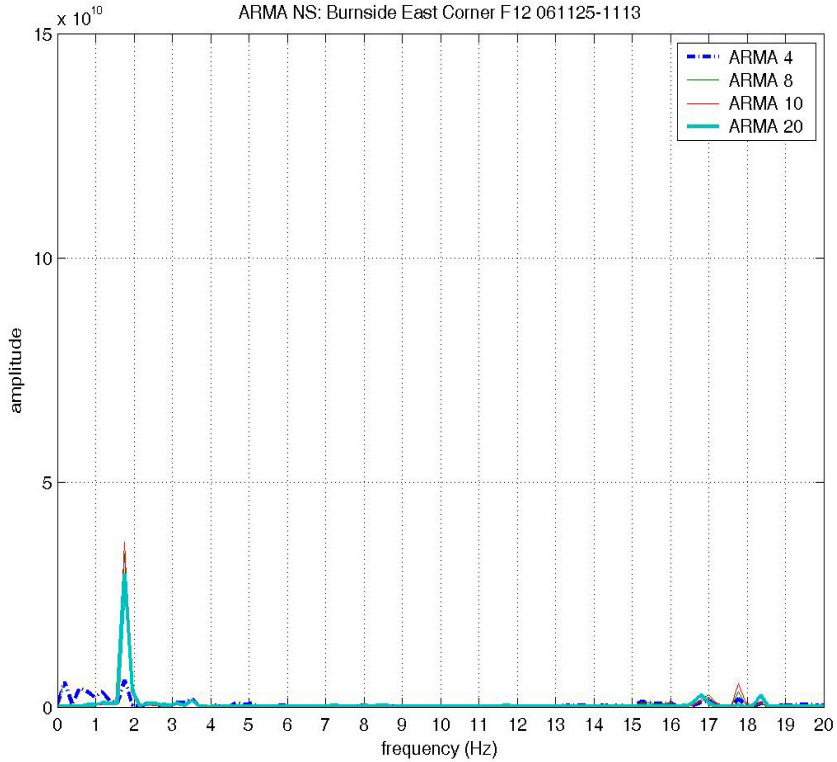

EW component